Grant agreement no. 243964

QWeCI

Quantifying Weather and Climate Impacts on Health in Developing Countries

D5.3c Climate change projection and its impact on health (malaria and RVF) for Barkedji Observatory region

Start date of project: 1st February 2010 Duration: 42 months

Lead contractor : UCAD UCAD
Coordinator of deliverable: UCAD
Evolution of deliverable

Due date : M24
Date of first draft : M38
Start of review : 10 July
Deliverable accepted : 30 July 2013

Project co-funded by the European Commission within the Seventh Framework Programme (2007-2013)		
Dissemination Level		
PU	Public	PU
PP	Restricted to other programme participants (including the Commission Services)	
RE	Restricted to a group specified by the consortium (including the Commission Services)	
CO	Confidential, only for members of the consortium (including the Commission Services)	

Introduction

Several studies were carried out on malaria vectorial transmission in many bio-geographical areas in Senegal as part of a programme targeting its epidemiology or vectors bioecology. A meticulous analysis of these studies, however, indicates that they have up to now little or no operational aiming. However with the current weight of malaria in term of morbidity and mortality, the big challenge for the scientific community and also the political decision makers is rather to find for each geographical area and each ecological context operational, methods of control in order to reduce as much as possible the burden of the disease. Regarding to the therapeutic failure with drug resistance mainly due to their anarchistic use and in front of the absence of effective vaccines as well as the emergence of vectors resistance to insecticides, a better spatial and temporal planning for prevention and control activities is essential. Such an objective needs the development for forecasting tools or further early warning system integrating various parameters having a direct or indirect impact on the transmission.

Human activities are crucial for the transmission of malaria across Africa. Environmental conditions can promote vector-borne disease transmission. Deforestation as well as cultivation of natural swamps increase solar insolation, which usually elevates local temperatures by several degrees (Githeko et al., 2000). For these reasons, larvae of An. gambiae s.l. were more frequent in pools of cultivated areas such as those found in rural areas.

On the other hand, urban malaria is considered to be an emerging problem in Africa because the populations of most large African cities have grown exponentially over the last 30 years [Donnelly et al., 2005]. Furthermore, it has been estimated that by 2030, 54% of the African population are expected to live in cities [Keiser et al., 2004 ; UNDP, 2007]. Many studies have reported evidence of malaria transmission in urban areas, and although levels are usually lower than in peri-urban and rural areas [Keiser et al., 2004 ; Robert et al., 2003], urban malaria is considered to be an emerging health problem of major importance in Africa [Donnelly et al., 2005]. In African cities, transmission is spatially heterogeneous and occurs in areas where conditions are favorable for malaria vectors [Trape and Zoulani, 1987 ; Pages et al., 2008 ; Trape and Zoulani, 1987 ; Machault et al., 1987]. Indeed, in urban settings, malaria risk heterogeneity is recorded over small distances due to the degrees of diversity of types of urbanization, density of the human population, quality of water and waste management, vector control measures, household factors, access to health care and patterns of human migration, which could import parasites from rural areas [Robert et al., 2003 ; Wang et al., 2005 ; Bogreau et al., 2006]. The occurrence of malaria in African towns has also been linked to agricultural practices [Afrane et al., 2004 ; Matthys et al., 2006 ; Klinkenberg et al., 2005 ; Robert et al., 1998], to the distance from breeding sites [Stoler et al., 2009 ; Staedke et al., 2003 ; Trape et al., 1992 ; Robert et al., 1993 ; Peterson et al., 2009] and to the vegetation cover [Peterson et al., 2009].

Recently, Gadiaga et al. (2011) have studied conditions of malaria transmission in Dakar from 2007 to 2010 through an extensive entomological survey that was conducted in 45 areas in Dakar. These authors found strong spatial and temporal heterogeneity of An. gambiae s.l. larval density, HBR (human biting rate) and malaria transmission in Dakar. They also identified the environmental factors associated with this heterogeneity. Their results aim to pave the way to set up malaria risk maps using remote sensing and Geographic Information Systems (GIS) technologies.

It is reminded that the case of study is the Ferlo which is a sahelian and sylvo-patoral area located in northern part Senegal. The usual station considered in Ferlo is Linguere. This work includes a strong component-based on modeling using the Liverpool Malaria Model (LMM), which contains two main parts (dynamics of population vectors and dynamics of malaria transmission). As it is known, Ziguinchor station which is located at the southern part of the area with high precipitation can be useful for comparison of trends in the analysis.

The Barkedji site is one of the famous Environment and Health Observatories in Senegal, which belongs to the Sahelian bio-geographic domain characterized by a short rainy season (from June to October) and a long dry season (November to May) with annual rainfall ranging from 300 to 500 mm. This Observatory located in a rural domain with a large number of temporary ponds, has been the study area of several research projects such as QWeCI and AMMA. One can notice these temporary ponds are at the same time breeding and resting habitats of many mosquitoes. The only study well documented on the malaria morbidity and mortality carried out in 1994-1995 in the village of Barkedji showed that the malaria onset is generally occurring from November to January (70%). This study further indicates that the high intensity of the transmission and the persistence of the temporary ponds remain the key factors influencing the level of malaria morbidity in this region and consequently impacting on the development of a natural malaria immunity by the indigenous population.

In Senegal, several mosquito species (*Aedes sp*. and *Culex sp*.) and livestock (Fontenille et al.1998; Diallo et al., 2000) have been found to be infected with the Rift Valley fever (RVF) virus. The epidemiological role of these mosquitoes species involved in RVF transmission cycle is complex. RVF epidemics in Senegal (Diallo et al., 2005; Ba et al, 2005; Ndione et al, 2008), do not seem to follow the same relationships as that over East Africa. During the rainy season the abundance of mosquitoes over the Ferlo is linked to the dynamic, vegetation cover and turbidity of temporary and relatively small ponds. Research has led to the development of vulnerability maps based on the dynamics of the pond size, the distances over which the infected mosquitoes seek blood meals, i.e. the flying range of mosquitoes, their aggressiveness, and the localisation of villages and cattle around ponds (Lacaux et al., 2007; Tourre et al, 2008; Ndione et al, 2008; Vignolles et al, 2009). In other words, the local ecological characteristics which influence locally the interrelationships between the vectors, parasite and hosts seem to be a big challenge for scientists. In this context, Caminade et al. (2011) studying RVF transmission have found that a dry spell followed by large rainfall event generally precedes RVF outbreaks during the late rainy season e.g. Oct-Nov.

Moreover, the rainfall intra-seasonal variability is not properly simulated by the actual state of the art climate models and scenarios of this is highly uncertain. That means mechanisms to explain links between climate and RVF are still unclear. By this way, Jones et al (2013, personal communication) almost finished coding a dynamical RVF model (two hosts – two vectors driven by daily rainfall & temperature), but the development and validation of the RVF model is still in progress. That's why this deliverable will only focus on the impact of climate on malaria (**this is a deviation from the original DoW**).

Climate change and its rapid emergence in the last decades is a major challenge to public health together with health inequity and weakening of health systems. Its effects on health will affect most of the world's population in the next decades and put the lives and well-being of billions of people at increased risk. Yet, the health impacts of climate change will not be distributed evenly and the distribution of the most severe health burdens is almost opposite to the global distribution of greenhouse gases emissions. Although the appraisal is difficult, we believe along with A. Costello and colleagues that Sub-Saharan Africa will bear the highest regional burden of climate change, with 34% of the global disability adjusted life years (DALY's) attributable to climate change, while it represents only 11% of the world's population (Costello A et al., 2009).

Despite a few scientific comments and increasing media coverage on the theme of potential health vulnerability to actual and predicted global climate change among populations in Africa, there is extremely poor detailed scientific evidence (P. Byass, 2009). Vector-borne diseases, such as malaria, and water-borne diseases, such as cholera, are constant reminders of the impact climate can have on health and thus development. They are probably the most documented infectious diseases in relation to climate change, and part of this attention seems to derive from concerns that the global disease distribution might be extended outside current endemic zones, in areas that will become wetter and warmer (Diallo et al., 2012; Dramé et al., 2012; Githeko et al, 2000; Pagès et al., 2008; Pascual et al., 2006; Peterson et al. 2009; Tanser et al., 2003; Yé et al., 2008).

The objectives of this study are:

- To evaluate and to quantify the impact of rainfall and other climatic factors (temperature, relative humidity, wind) on the dynamics of malaria and RVF vector populations;
- To quantify the climate change signal over northern Senegal using IPCC scenarios and its impact on malaria and RVF transmission and diffusion.

Methodology & datasets: Malaria

Malaria datasets (external control)

Global malaria models are difficult to validate because the current distribution of malaria is within its climate limits in many regions due to effective control measures. However, in order to attempt some validation of the different malaria models, we 1) compared the output of the malaria models for the two observed climate baseline datasets and GCM/RCM modelled baselines and 2) compared those outputs with other published malaria endemicity maps. Those malaria endemicity maps are derived from Gething et. al., 2010. Estimates of pre-intervention (1900s) malaria distribution have been published in a 1968 study (historical synthesis for four Plasmodium species) by Lysenko et al.; recent malaria endemicity estimates (2007) have been derived from the Oxford MAP project (Gething et al., 2010, Hay et al., 2009) for comparison purposes. These datasets have been digitized from the original papers.

In this report, we also use cases of malaria data particularly for recent years such as 2009, 2010, 2011 and 2012 that were available from health districts in Senegal. We put a special emphasis on sentinel sites of the PNLP (Programme National de la lute contre le Paludisme) which have been chosen in the framework of their representativeness of the malaria transmission features in different areas of Senegal. The data contains the number of malaria cases reported weekly, monthly and yearly scaled among persons of 5 years old or more but also for particularly vulnerable people (children under five years old and pregnant women) knowing that the reduction or loss of immunity increases the risk of getting malaria.

Climate Observations (control baseline runs)

In order to evaluate the respective bias-corrected baseline integrations, additional malaria integrations were conducted using two sets of gridded observed climate datasets. The first set used temperature and precipitation from the CRU dataset v3.1 (Mitchell and Jones, 2005) for a period very close to the historical integrations 1980-2009. As the CRU data were only available at monthly timescale, the VECTRI model was excluded from this analysis. The second set of integrations used the TRMM 3B42 dataset (Huffman et al., 2007) with precipitation retrievals based on microwave and precipitation radar observations, supplemented with infra-red information when the former was unavailable. The temperature information was derived from the interim reanalysis of ECMWF (Dee et

al., 2011). Both observed climate datasets [CRUTS3.1 and TRIMMERA1] were aggregated to the half degree grid scale of the CMIP5 climate data. Malaria integrations were also conducted for the modelled baseline period for each GCM [1980-2010].

Besides the clinical observed data obtained from PNLP, LMM outputs based on observed rainfall and temperature stations from CERAAS (Centre d'Etude Régionale pour l'Amélioration de l'Adaptation à la Sécheresse) will also be considered.

The CORDEX regional climate model projections for Africa (RCMs)

In this study, we also utilized an ensemble of Regional Climate model simulations performed for Africa by the Sweden's Meteorological and Hydrological Institute (SMHI) within the CORDEX project framework. All simulations were performed using the standard CORDEX domain and output specifications, which are available at:
http://cordex.dmi.dk/joomla/images/CORDEX/cordex_archive_specifications_120720.pdf
Further details about the CORDEX simulations for Africa and the SMHI RCM can also be found in Jones et al., 2011 and Nikulin et al., 2013.

SMHI has downscaled the ERA-Interim Reanalysis (1980-2010) and 8 different GCMs over the African domain, sampling both RCP4.5 and 8.5 and running in transient mode for the period 1951(1960)-2100. The employed Regional Climate Model is SMHI-RCA4. The following CMIP5 GCMs have been used to carry out the dynamical downscaling.

Institute name	GCM name	Calendar
CCCma (Canada)	CanESM2	365 days
CNRM-CERFACS (France)	CNRM-CM5	standard
MOHC (UK)	HadGEM2-ES	360 days
NCC (Norway)	NorESM1-M	365 days
ICHEC (Europe)	EC-EARTH	standard
MIROC (Japan)	MIROC5	365 days
NOAA-GFDL (USA)	GFDL-ESM2M	365 days
MPI-M (Germany)	MPI-ESM-LR	standard

SMHI has also downscaled 1 RCP2.6 GCM for 1960-2100 (EC-EARTH). All simulations cover the 1951-2100 period (historical 1951-2005 and scenario 2006-2100) but HadGEM2-ES RCP45 ends in November 2099 and RCP85 in December 2099. Note that HadGEM2-ES has the 360 day calendar, all months have 30 days.

Note that the HadGEM2-ES simulations have not been included in the malaria analysis due to a shorter available time period. We just retained 7 GCMs for the two emission scenarios rcp4.5 and rcp8.5 and the historical runs. All data have been interpolated to the common ISI-MIP grid (0.5

degree square grid). Monthly rainfall and temperature outputs for each RCM have been bias mean corrected accordingly to the ISI-MIP protocol using the CRUTS3.1monthly dataset as the reference (see ESM from Caminade et al., 2012 for further details).

The ISI-MIP global climate model projections

The CMIP5 project is collaboration among climate modellers to produce a consistent set of climate model outputs for the RCP emissions scenarios. The CMIP experimental design is described in Taylor et al., 2012. The CMIP5 output was bias-corrected by PIK (Hempel et al., 2013) for this project to ensure statistical agreement with an observational data set [the Watch Forcing Data (WFD)] over the period 1960-1999. All climate scenarios were mapped to a uniform half degree grid. There are four RCP emission scenarios: RCP2.6, RCP4.5, RCP6 and RCP8.5 representing a range of climate forcings. Climate scenarios were available for all RCPs and for the following five global climate models: HadGem2-ES; IPSL-CM5A-LR; MIROC-ESM-CHEM; GFDL-ESM2M; and NorESM1-M. The five models were selected to give a wide range of temperature and rainfall changes, rather than a representation of the likelihood of future climate changes (Warszawski et al., 2013). Climate data were available to 2100, however, malaria integrations were undertaken for three future time period (30 year averages): 2020s [2005 to 2035]; 2050s [2035-2065] and 2080s [2069-2099], with the exception of VECTRI, which instead conducted century-long integrations for each model using daily climate data. Results were mapped to a single figure for each RCP scenario for the different time periods.

Population data

For the assessment of future populations at risk of malaria used a single population projection from the new Shared Socio-economic Pathway (SSPs) set of socio-economic scenarios (Van Vuuren et al., 2012). We used the SSP2 projection which approximates to 9.5 billion people in 2055 (SSP database, 2012). SSP2 national projections for 193 countries were converted to a gridded population product by first deriving a population map for 2000 scaling the gridded GPWv3 dataset to match the national SSP totals. This map was then projected into the future using SSP national average projections to scale each grid point. A small number of countries not present in the SSP2 dataset were assigned the global-mean population growth rate over the next century. A similar methodology was used to scale population for the last century for the historical model integrations. . The reference years for the population data were as follows: current climate 2000; 2020s 2020; 2050s 2050; and 2080s used 2085 population.

.

Malaria Impact models (MIM)

LMM_RO Monthly Model (Model 1)

The model used here is a simplified version of the vector transmission potential model formulated by Jones, 2007 which uses monthly rainfall and temperature data as inputs. The number of emerging adult mosquitoes at the beginning of each month is taken to be proportional to the rain falling during the previous month. The mosquito population is then combined with the biting rate, sporogonic cycle length and survival probability calculated from monthly temperatures, together with the other parameters provided as input to the model, to derive the Reproduction Ratio, R0. If R0 >1 then malaria transmission occurs for a given month. The derivation of R0 is based on the transmission model component of the full LMM [Liverpool Malaria Model], which is a weather driven, mathematical–biological model of malaria that was originally formulated by Hoshen and Morse (2004) and has been applied at national and regional scales. The full LMM model uses daily rainfall

and temperature data as inputs. It has been successfully validated against a 20-year clinical record for Botswana (Jones and Morse, 2010). In this study we used the standard parameter settings for malaria transmission. Note that a recent modified version of the full LMM has been used to assess the impact of climate and land use scenarios on epidemic malaria risk in Africa (Ermert et al., 2012).

MARA Model (Model 2)

The MARA Seasonality model was original derived to map start and end months of the malaria transmission season for locations in Africa based on monthly long-term averages of rainfall and temperature (Craig et al., 1999). It was modified by Jones (2007) to create a very simple seasonal model of malaria transmission. The basic requirements of the model are 3 months' rainfall at a minimum value together with a catalyst month specified by another minimum rainfall value. Temperature is constrained to be greater than a threshold value plus a seasonality index calculated from the standard deviation of the monthly rainfall. The resulting output is either "ON", indicating the malaria season is in progress, or "OFF", indicating one or more of the conditions have not been met. Because of the heavily-simplified nature of the model it is recommended here for use as a guideline (e.g. for checking the output of other models), rather than a reliable indicator of malaria transmission dynamics.

VECTRI Model (Model 3)

VECTRI is a mathematical model for malaria transmission that accounts for the impact of temperature and rainfall variability on the development cycles of the malaria vector in its larval and adult stage, and also of the parasite itself. The majority of the relationships are taken from the literature for the *Anopheles gambiae* vector and the *Plasmodium falciparum* species of the parasite. Temperature affects the sporogonic and gonotrophic cycle development rates, as well as the mortality rates for adult vectors. Water temperature, closely related to air temperature impacts both the growth rate and mortality of larvae. Rainfall effects on transmission are represented by a simple physically-based model of surface pool hydrology, where low rainfall rates increase available breeding sites that decay through evaporation and infiltration, while intense rain events decrease early stage larvae through flushing (Paaijmans et al., 2007). A unique development for a regional scale malaria model is that VECTRI accounts for human population density in the calculation of biting rates. Higher population densities lead to a dilution effect resulting in lower parasite ratios (PR) in urban and peri-urban environments compared to nearby rural locations. In this respect the model is able to reproduce the reduction in Entomological inoculation rates (EIR) and PR with increasing population density that has been widely observed in field observations in Africa (Kelly-Hope et al., 2009), although the relationship is too strong in the model (Booma et al., 2011). Future population growth will therefore reduce transmission intensity in VECTRI, an impact that is not represented by the other models in the study. The model is designed for regional to continental scales at high spatial resolutions of up to 5-10km, although the integrations in this study use the same CMIP input data on the 0.5o resolution grid without interpolation. It should be emphasized that VECTRI is the only full dynamical model participating in the study operating on a daily time step and accounting for sub-seasonal variations in climate. A consequence of this is that the model is the only one that requires a representation of human migration to transport malaria parasites to new regions that may become suitable for transmission in future. In this study this is accomplished simply mixing population with a coefficient equivalent to 1% population exchange per year (the results were not sensitive to this parameter). For full details of the models mathematical framework and its evaluation see (Tompkins and Ermert, 2013).

UMEA Statistical Model (Model 4)

The malaria model is a spatial empirical-statistical model created at the Umea University (Beguin et al., 2011). The malaria model uses climate and socio-economic factors to determine the spatial distribution of endemic malaria (*falciparum*) transmission. Generalized additive logistic regression models were used to empirically estimate the relationship between endemic malaria fever transmission and climatic factors on a global scale using a global malaria dataset from Malaria Atlas Project (Gething et al., 2010, Hay et al., 2009). To allow flexible relationship and interaction between climate factors on the probability of malaria transmission areas, we tested models using thin plate splines as implemented in the *mgcv* package of the statistical software **R**.

MIASMA Model (Model 5)

The malaria module of the MIASMA model incorporates temperature effects on the survival probability and biting frequency of mosquitoes (Van Lieshout et al., 2004). The various temperature dependent relationships are aggregated into the entomological version of the equation for Ro. Due to the lack of data on several key parameters, these are set as biologically plausible constants, allowing the calculation of the critical vector density required for sustainable disease transmission (i.e. Ro >1). This threshold is lower under more suitable (warmer) climate conditions. The inverse of the critical density threshold, the 'transmission potential', is used as a relative measure of transmission intensity under different climatic conditions. The model assumes that a minimum level of monthly rainfall of 80 mm is essential for malaria transmission. The value of 80mm per month was derived by the MARA project (Mapping Malaria Risk in Africa) as a prerequisite for endemic malaria (Craig et al., 1999, MARA, 1998). In this assessment, the modelled distribution is not constrained by the current distribution of malaria vectors (as shown in Van Lieshout et al., 2004).

Methodology

A common variable metric was used across the different malaria models – climate models (RCMs and GCMs) – emission scenarios –population scenarios in order to carry out a direct inter-comparison of this super ensemble. The length of the malaria transmission season (hereafter referred as to LTS) was calculated for each malaria model based on different assumptions (due to the design of those models, see the Malaria Model Impact Model section for further details for each MIM). In order to avoid spurious result from small changes in low transmission regions, a minimum of three months continuous transmission were required in order to indicate whether the climate was suitable for malaria for a given year. In other words we defined climate suitability for malaria such as CS=1 if LTS>3months transmission. We then estimated two population outcomes using the SSP2 population projection. The population at risk of malaria (PAR) was defined as the population present in area where the climate was suitable for malaria transmission. Person months at risk were calculated at the length of the transmission season multiplied by the population living in the grid cell. The climate change attributable PAR and PMAR were estimated as the difference between future population at risk of malaria under a climate scenario compared to the future population at risk under the current climate (modelled as the GCM-specific baseline climate). It was not possible to estimate PMAR for the UMEA model which only produces annually-averaged CS output. All estimates were aggregated for different regions. [We only focus on PAR outputs in the current study.]

To estimate the various sources of uncertainties in the future scenarios we assumed a linear decomposition of the variance of the uncertainties in between three components (GCM /MIM / scenario). This is calculated for its anomalies with respect to the historical experiments. For a given time slice, the variance of the interest parameter (GCM for example) is calculated on the average

(ensemble mean) across the other parameter dimensions (so MIM & scenario) for each grid points. We then assume that:

Var_total_uncertainty=Var_GCM_uncertainty+Var_IM_uncertainty+Var_scenario_uncertainty

We then show each component separately:

GCM_relative_uncertainty= (Var_GCM_uncertainty / Var_total_uncertainty)*100 etc

Note that the linear assumption is far from being perfect e.g. it generally underestimates the total uncertainty. Table 1 summarizes the outputs available for each malaria model within the super ISI-MIP and CORDEX ensemble:

		Control Baselines		**ISI-MIP ensemble** **5 GCMs**		**CORDEX ensemble** **1RCM driven by 7GCM**	
Malaria Model	**Output variables**	CRUTS3.1 (1980-2010)	TRMM-ERAINT (1998-2010)	Historical 1980-2010 (historical merged with rcp4.5)	Scenarios (rcp2.6, 4.5, 6.0, 8.5) 2020s 2050s 2080s	Historical 1980-2010 (historical merged with rcp4.5)	Scenarios (rcp4.5, 8.5) 2020s 2050s 2080s
Vectri **(daily – dynamical)**	LTS, CS, PAR		X	X	X		
Umea **(monthly – statistical)**	CS, PAR	X	X	X	X		
LMM_ro **(monthly, steady state Ro model)**	LTS, CS, PAR	X	X	X	X	X	X
Miasma **(monthly, steady state Ro/TP**	LTS, CS, PAR	X	X	X	X	X	X

model)							
Mara **(monthly, seasonality model)**	LTS, CS, PAR	X	X	X	X	X	X

Table 1: Summary matrix of the available malaria simulations

We will start by analyzing the climate behavior, environment and geographical features of various ecological zones in Senegal such as the Senegal River Valley in the northern part, the Ferlo north-eastern zone, the coastal region (Niayes), the Groundnut Basin (Bassin arachidier), the eastern Senegal domain and "Basse Casamance" located in the southern part of the country (see Fig. 1).

Results

Results on rainfall and temperature parameters over different Senegal zones

Precipitations during the rainy season in Senegal are generated by the monsoon flow originating from the trade winds of the St. Helena high. Those trade winds bring moisture in the country in the north-eastern direction from the month of April. The duration, intensity and seasonal distribution of rainfall in a given area vary considerably from year to year, especially in regions where rainfall is less abundant. From south to north, the average duration of the rainy season ranges between 3 to 5 months, leading to a latitudinal gradient which is superimposed on an east-west gradient with more abundant rainfall occurring on the coast and in the central part of the country. In the Dakar region cumulated rainfall values range between 500 and 600 mm. The rainy season core takes place during the months of august and September with respective maxima varying from one region to another. The dry season occurs between the months of October and November and between the months of May to June. Rainfall is a key climate factor whose impacts can be read on several sectors in Senegal. Indeed, a dry spell lasting a few days or weeks during the rainy season can have dramatic impacts on the agricultural production.

Discussion of results on rainfall and temperature over different Senegal zones

Due to its extreme northern position in the country, the Senegal River Valley (Vallée du Fleuve Sénégal) which includes the Saint Louis and Matam regions is characterized by a Sahelian climate with an annual cumulative rainfall only ranging between 200 mm and 400 mm (Fig. 2). Indeed, during the rainy season, the monsoon flow coming from the anticyclone of St. Helena is causing the first precipitation in the south before reaching the central part of the country to ultimately end its journey in the northern part of Senegal. Thus rainfall decreases in magnitude and duration from south to north,

from an annual average of more than 1500 mm in the southern region to 800 mm in the central area to about 400 mm in the north. Rainfall is so low in the northern part of the country that the climate has a Sahelian or sub-Saharan behavior as it is seen in Fig. 2. Averaged monthly rainfall based on the CERAAS observation data and calculated for the period 1950-2010 shows that the northern part is marked by a rainy season starting from June-July and ending in September-early October and a dry season which is extended the rest of the year.

The annual cycle of observed rainfall shows that the rainy season usually begins in June-July. The rainfall peak is observed in August (around 100 mm) and precipitation then decreases quickly from September. The rainfall varies from one season to another; the maximum cumulated rainfall has strong year to year variations. Excepting exceptional cases such as year 2002, no rainfall is generally recorded outside the period ranging from June to October. An important decrease of annual rainfall totals during the years 1977, 1984 and 1992 with less than 200 mm recorded is shown on Fig. 4. This is confirmed by the Lamb index (standardized rainfall anomaly) highlighted on Fig. 3 which shows that almost all rainfall anomalies were negative during the period 1970-2000. For cons, the most recent years were marked by particularly positive anomalies such as the years 2005 and 2010 which were very wet. Average monthly temperatures can be very high; they can be more than 35 °C during the dry season (March, not shown). However, average annual temperatures are about 25 °C but they are linearly increasing from 1973 to 2006 (Fig. 4), with a maximum occurring in 2001 (28 °C).

The northern part of the Ferlo area has a continental behavior similar to the Sahel and its southern part similar to the Sudano-Sahelian behavior. It is represented here by the station of Linguere but it is extended over the entire region of Louga. The period from December to February is the coldest period. May and June are the warmest months as in the rest of the country. The differences that appear in terms of temperature are also found on rainfall. Rainfall decreases from south to north and from west to east. Fig. 5 represents the seasonal evolution of rainfall for the Linguere station in Louga. The first significant rains are observed in June and July generated by squall lines whose effectiveness decreases towards the west. The rainfall peak is observed in August and is slightly higher in magnitude than the one observed in Saint-Louis (100 mm) but it still remains below 150 mm. The annual rainfall totals vary from 250 mm to 500 mm (Fig. 7). The years of 1977, 1984 1992 and 2002 were particularly dry with totals not exceeding the 250 mm threshold. Precipitation significantly decreased over the Ferlo since the 1970's, with negative anomalies shown after 1970 contrasting with positive anomalies that occurred during the previous 1950-1960 period (Fig. 6). Comparing annual temperatures with those of Saint-Louis, the Ferlo is generally warmer and this can be explained by the coastal position of the Saint-Louis region which has a particular humid climate and lower temperatures. We will verify whether the observed differences in the rainfall and temperature between those regions will affect the features of the malaria transmission season analyzed later in this document.

Dakar is the western tip in the western part of Senegal. It is located at 14°N-16°N and 17°W-18°W, and it is a coastal area benefiting by its proximity to the sea and the influence of the sea breeze: low maximum temperatures and higher humidity. Fig. 8 shows that the rainfall peak occurs in august with more than 150 mm recorded. Fig. 10 also shows that the annual cumulated rainfall ranges between 300 and 500 mm. In addition, there is a strong rainfall interannual variability in this region of Senegal. Less than 200 mm was recorded in the years 1977, 1983 and 1992. This dry period contrasts with the high rainfall recorded in recent years showing an improvement of the rainfall context in Senegal. Similarly to the Linguere station, the period 1970 to the present is marked by a significant rainfall decrease excepting for a few years such as 2008 and 2010.

Annual temperature in Dakar rarely exceeds 25 °C (Fig. 10), but it keeps increasing during the period 1973 to 2006 to stabilize about 24 °C in 2006. This is the coldest part in Senegal for the reasons mentioned before. This high humidity might have an important impact on the longevity of the mosquito population and on the cycle of the vectors reproduction and parasites development.

Fig. 11 illustrates the rainfall seasonal variability in Kaolack. The climate and environmental behavior are similar for Diourbel, Fatick and Thies. Those locations are all located in the Groundnut basin (Bassin arachidier or Sine Saloum). An alternation of a long dry season (9 months) and a shorter rainy season is observed with important rainfall usually beginning in June-July and ending in early October. Like other parts of Senegal, the month of august is the wettest with a rainfall peak of 225 mm recorded in Kaolack which is far wetter than all regions considered previously. Annual total rainfall range between 400 and 700 mm, and even up to 800 mm as observed in the years 1989, 2000, 2004, 2006 and 2008 (Fig. 13). In Fig. 12, There is a rainfall decreasing trend over Kaolack occurring from the 1960s to the 2000s even if this less pronounced compared to the situation of the Ferlo and the Senegal River Valley.

In general, the groundnut basin is characterized by a tropical Sudanese climate marked by two zones:

• Saheliano-Sudanese in its northern part, where rainfall ranges between 400 and 600 mm;

• Sahelian in its southern part, where rainfall ranges is between 600 mm and 800 mm.

The coastal part from Foundiougne to Fatick is also strongly influenced by the maritime climate.

Temperatures are relatively high from April to July, with a hot and dry harmattan wind which develops and blow from the Sahara to the Sahel during the dry season. Annual temperatures are below 30 °C with a significant warming trend occurring from the 1970s to the 2000s.

The eastern region (Tambacounda) has a climate type ranging between the Sudano-Sahelian and Sudano-Guinean climate. The Azores anticyclone brings two winds which are maritime winds from

the north and the continental trade winds over the northern-east. The eastern warm and dry harmattan converges with the monsoon flow which is charged with warm and humid air over this region.

In terms of rainfall, the region is located between the isohyets 400 and 1500 mm (Fig. 16), that makes this zone among the wettest areas of the country. The maximum rainfall value is recorded in August with about 150 mm. The rainy season is extended to 4-5 months and it starts in May-June and ends in October. Temperatures have two main periods of thermal regime with the lowest temperature occurring from July to February and a period of high temperatures occurring between March and June. The relative humidity is very high during the rainy season and peaks between August and October. From January to March the relative humidity is very low with values about 10%. Figs. 15 and 16 show rainfall interannual variability over this region with positive rainfall anomalies occurring in recent years. As for the period of 50's and 60's, the anomalies are almost all positive.

In Fig. 16, high temperatures gradually increased from one year to another. This also shows a very warm year in 2001. However, intra-seasonal variations in temperature are more important as temperatures around 40 °C are commonly observed during the previous rainy season or towards the end of the season. The eastern part of Senegal is one of the hottest regions of the country.

In the southern part of the country, this part of the territory (Ziguinchor and Kolda) or “Basse-Casamance” experiences the largest rainfall in Senegal. The vegetation is characterized by a predominance of savannah. It is characterized by a Sudano-Guinean climate with 4 to 6 months of regular rain with relatively low monthly temperatures compared to the north. Indeed, this southern area is considered as the gateway generators of rain winds and is the wettest with a rainy season which starts in May and ends in November (Fig. 17). The maximum rainfall recorded in august is about 350 mm, which is equivalent to the annual accumulated rainfall often observed in the northern part of the country. For other regions, the rainfall onset is usually recorded rather since June. The wettest period occurs from July to September for all stations. In the southern zone, the rainfall stations show annual averages of 1200 mm (Fig. 19). By cons, in 1977, 1980 and 2002, the annual total rainfall was about 800 mm, which is very rare in the south. The accumulated annual rainfall represents about twice the amounts observed in the Ferlo, and five times the rainfall recorded in St. Louis which is located in the far northern part of the country. The year 2000 was the wettest with around 1800 mm of rainfall recorded with respect to the 1973-2006 period. However, the north-south rainfall gradient is still characteristic of the spatial distribution. Negative rainfall anomalies appear to be more important than in the northern part (Fig. 18).

Malaria Model validation

Malaria transmission over different zones of Senegal based on literature and PNLP observations

The risk of malaria transmission is modulated by climate including rainfall, not only by the amount and intensity of rainfall, but also by the timing e.g. whether it is the dry or rainy season. Wet years are often associated with high malaria transmission because rainfall favors the multiplication of breeding sites. Anopheles mosquitoes breed in water habitats which require the right amount of precipitation to accelerate mosquito breeding. However, it is known that Anopheles mosquitoes use different types of water bodies to breed (Nagpal et al, 1995. Robert et al, 1999.). The rainfall also affects malaria transmission in indirect ways, by increasing relative humidity and impacting on temperature, affecting where and how mosquito breeding can take place.

In all regions of the world where there is a long dry season, Anopheles populations rarely develop throughout this season. In these regions, the rate and amount of rainfall are key factors in determining the seasonal abundance and duration of anopheline species. In the Sahelian zone, drought reduced the availability of breeding sites and the intensity of malaria transmission, so that "malaria retirement" was observed (Mouchet et al., 1996). Thus, plasmodium parasite prevalence in the population declined quickly. The proposed explanation is that a large number of small rivers and once semi-permanent wetlands are now completely dry eight to ten months per year since the early 70's. This resulted in the disappearance of An. *Funestus* in northern Senegal, one of the three main vectors of malaria in tropical Africa (because the larval development of this species requires perennial or semi-perennial water bodies with abundant aquatic vegetation such as rice paddies).

Discussion on observed malaria transmission over Senegal

In the Senegal River Valley since the installations of the Diama and Manantali hydraulic dam, the irrigation schemes caused profound ecological changes mainly characterized by the creation of permanent water bodies and vegetation in wide areas. These environmental changes have led to significant changes in the malaria vectors in this area. In addition to these environmental factors, we investigated the impact of climatic factors (rainfall, humidity, temperature) on the burden of malaria. Anopheles *pharoensis* became the most abundant species (replacing the original anopheles *gambiae* species) and was subsequently heavily implicated in the transmission of malaria in the Delta River. Anopheles *funestus* which had disappeared from the river valley because of the recurrent droughts of the 1970s has recently re-colonized the area in the lower valley (Lochouarn et al., 1995). Fig. 20 shows the seasonal incidence of malaria in St. Louis, the main area in the River Valley. The malaria cases peak in October in both children and adults. 2100 malaria cases were observed, on average,in St. Louis in October.

The district of Dagana has the largest number of malaria cases (with nearly 4,500 cases in adult people), while the minimum of malaria cases was registered in the regional hospitals of St. Louis and Ndioume (less than 550 clinical cases in adults; see Fig. 21).

The sylvo-pastoral zone of the Ferlo is located at 15°17'N and 16°13'W. Due to adverse weather conditions in this region, malaria transmission mainly takes place during the rainy season. However, in areas close to temporary and lowland ponds, malaria transmission may continue after the rainy season, depending on the longevity of these ponds. Anopheles *arabiensis* and *gambiae* are rarely transmitting malaria over this region. EIR (Entomological infection rate) is highly variable depending on the location. The PIHA (number of bites received by Infected human and per year) is the lowest in the lower Ferlo valley, it passes to 100 PIHA in the upper valley (Fall, 2008). Transmission may continue until the early dry season during the years of high rainfall. Fig. 25 shows the seasonal incidence of malaria in Louga. The number of malaria cases peaks during the rainy season with a maximum of 1700 cases observed in October.

Regarding the distribution of number of cases by district, the higher number of cases was reported for the Linguere district (6600 cases within adult population and 1500 within children). The district of Dahra and CHR (Centre hospitalier Régional) in Louga have recorded less cases during the period considered. Although the dry season is marked by a few number of malaria cases, the endemic situation is perennial with high transmission occurring towards the end of the rainy season, when the anopheles vector experience more suitable climate conditions with the warming, humidity and large vegetation cover extending until October. The rainy season period corresponds to pond and vector development but also this coincides with the availabity of the plasmodim parasite (Lemasonn et al., 1997). In the typical humid savanna area, the seasonal transmission increases and can reach more than 100 PIH/year (Carnevale et al, 1984. Mouchet et al, 1993.).

Regarding the Dakar zone, it is characterized in many studies by its high urbanization level. It includes more than half of the whole urban population of Senegal. This urbanization trend is caused by an increasing input of people coming from all regions in Senegal. It is because Dakar is the administrative and economic center of the country. It often results in an illegal occupation of the space and urbanization can become uncontrolled.

This over-urbanization can reduce the drainage of the water bodies, reason why floods improve the proliferation of mosquitoes in those areas. The deficit in heath care facilities can also explain the malaria transmission in Dakar. Many studies have emphasized the consistent distribution in its facilities, services and infrastructure over the Dakar spatial domain. The lack of facilities for urban services creates an inequality in access to primary care.

On the environmental side, the liquid waste management is a key factor to consider for malaria transmission during the rainy season. In areas such as very deprived urban area, domestic water waste is usually discharged into the open near houses or drained to the beach areas. Some neighborhoods are invaded by these wastewater, others are regularly flooded during the rainy season. A survey study carried out by the Department of Sanitation in 2004 found that only 13% of households have access to sanitation and 14% sewage network are treated in a wastewater treatment plant, while 86% are dismissed without treatment to the sea and wasteland. Given all these environmental features and given the pressure on land due to consecutive evictions related to the development of new roads in Dakar, breeding sites continue to grow and allow the anopheles mosquitoes to develop. The available *arabiensis* and *melas* anopheles are commonly observed in the Dakar area. Malaria transmission generally occurs during the rainy season period as it is shown on Fig. 30 which represents the seasonal incidence of malaria in Dakar. The risk of transmission continues beyond the rainy season in areas such as those near the "Niayes" or floodplains. This transmission is very high with nearly 27000 reported malaria cases. The lag from one to two months between the observed maximum rainfall and the peak in malaria cases is a significant fact that we must try to explain. Overall, the shift from one to two months between the rainfall and malaria mortality peak seems quite logical in relation to what is known about the biology of the vector, the parasite and the host. This discrepancy is mainly due to the time required for the development of breeding sites with heavy rainfall generally followed by dry spells. The water bodies filled by rainfall are favorable for mosquito breeding followed in a few weeks by the proliferation of anopheles mosquitoes which have a strong ability to breed (up to 2000 eggs laid by a female during its life). The prevalence of falciparum gametocytes is also relatively low in the early season of malaria transmission with 16% among children in June 1995 versus 37% in November (Ndiaye et al, 1998).

Concerning the distribution of malaria cases by district, Pikine has recorded the higher number of cases. This is probably due to its suburban and crowded characteristics with floods regularly observed. Another important point is the difficulty of the population to access health care facilities which are mainly concentrated in Dakar city centre.

The main area of the groundnut basin "Bassin arachidier" is crossed by two rivers which are the Sine and the Saloum and their tributaries. The soil in some parts of the region favors the formation of flooded areas during the rainy season where anopheles breeding sites develop. The soils have various types: soil hydromorphic "Diors", and soil desk "Decks" and "Deck-Diors" which are in the lowlands and favor the formation of streams that can become favorable for mosquitoes deposits. Fig. 35 represents the seasonal incidence of malaria in the region of Kaolack. It shows that the maximum number of malaria cases is observed in October with the high proliferation of anopheles mosquitoes following the peak in rainfall. The risk of transmission is a function of rainfall with low incidence observed during the dry season. For the spatial variability, the largest regional district also Kaolack

experiences the highest number of malaria cases. By contrast, other districts have a record around 4000 cases of malaria.

In eastern part of Senegal, has alluvial valleys within the system of river basin "Falémé", the vegetation is abundant and varied given favorable for its development and the diversity of ecosystems ecological conditions. The malaria vector system is very complex in this ecological zone and consists mainly of four species: *gambiae*, *funestus*, *nili* and *arabiensis*. The involvement of *nili* anopheles in malaria transmission has recently been demonstrated for the first time in Senegal. This species provides up than 21% of the total transmission. The EIR (Entomological Inoculation Rate) is generally very variable and large in this southern area. It can be estimated at 220 PIHA in the area of Tambacounda and 270 infected bites per person during the rainy season in the Kédougou area. It is also possible to see a few cases of malaria in the dry season as water bodies persist sometimes until the dry season.

Fig. 39 illustrates the seasonal cycle of malaria cases in the region of Tambacounda. Malaria cases increase from June (corresponding to the beginning of the rainy season) to October. This increase is less pronounced in June because the breeding sites are not yet developed enough. The maximum number of malaria cases is observed in October for both children and adults. The maximum almost reaches 7000 cases. However, this region is affected by malaria throughout the year even if the degree of transmission is relatively low from February to June. Regarding the variability of the transmission across the districts (Fig. 40), the districts of Tambacounda and Goudiri are the most affected while the district of Maka Coulibantang and the Regional Hospital Tambacounda are less affected.

For the "Basse Casamance", this wettest part of the country (Kolda and Ziguinchor) is characterized by a large vegetation cover. In this environment large breeding sites can be found. The development of malaria is mainly caused by anopheles *gambiae* (predominant vector), *arabiensis* (not frequent), *funestus* and *nili* (with a lower capacity to transmit the parasite). The entomological inoculation rate is also variable in this area. It is about 13 PIHA in mangrove area and about 68 PIHA outside the mangrove area. In the latter, the intensity of transmission varies from one village to another due to local ecological features such as rice paddies. Fig. 44 shows the variation of malaria cases in Ziguinchor. The malaria transmission season is more or less different from that of other regions. This is justified by the length of the rainy season, but also by the frequency and intensity of rainfall events. For both regions, we show the occurrence of two peaks in malaria cases during the year. The first peak occurs in August (about 1500 cases) followed by a second peak in November (about 3000 clinical cases) in Ziguinchor. The first peak might be related to the early start of the rainy season over this southern region, so in July-August, breeding sites are abundant enough to favor malaria transmission. The second maximum is due to the conditions favoring the proliferation of malaria e.g

growth of the vegetation cover and occurrence of dry spells within the rainy season that impact on vector dynamics.

In addition, at the local scale, there is a great disparity in malaria transmission from one district to another. This disparity is mainly due to local ecological features such as paddy fields, near water reservoirs such as ponds, mangroves and lowland situation. The access to sanitation for households with low income and the distance of the village from the district can further explain those spatial differences.

Malaria model validation using various observation datasets

LMM simulations

Regarding the parameters of malaria as simulated by the LMM, using the University of Cologne webased information system, the trends are enough founded again. Considering the different regions, Figs. 23, 28, 33, 37, 42, and 46 correspond to LMM malaria model outputs for Saint-Louis, Linguere, Dakar, Kaolack, Tambacounda and Ziguinchor respectively. There is a significant difference in both the seasonal and the annual evolution of malaria parameters. For example, for the region of Ziguinchor, very weak values of PR (asexual parasite rate) are simulated in 1975, 1995 and 2000, and also during the period 1990-2006. Only the Tambacounda region (south-east) shows stationary variation of the PR parameter, while other regions presents strange annual variation. The gaps for maximum prevalence values (PRmax) are more important than mean and minimum value but the global trend is the same. These parameters are lower in magnitude in the northern band from Saint-Louis to Linguere but also in the region of Dakar. Based on the rainfall station data, these areas are less wet than the rest of the country.

For the EIR (Entomological Inoculation Rate) parameter, there is also a large temporal and spatial disparity. It ranges between 3 to 5 months depending on the regions from the north, center and southern part of the country. This is consistent with observations. The period of existence is so remarkable from June to December, but particularly from October to December where it can reach 100 infective bites per human per night in October in the south and southeast regions. However, for the northern area (Saint-Louis), EIR does not often exceed 5 infective bites per human night even during the period of high transmission. EIR simulated values are close to zero in Saint Louis for many years throughout the simulation period. Figs. 23, 28 and 33 show discontinuity of the EIR at the interannual time scale. This finding is somewhat contradictory with the observations because this parameter is usually directly related to the transmission of malaria and remains really high in all over Senegal in the observations.

The figures 23, 28, 33, 37, 42, and 46 show LMM model outputs for St. Louis, Linguère, Dakar, Kaolack, Tambacounda and Ziguinchor respectively. As an example for the region of Ziguinchor, there is a very pronounced drop the parasite ratio in 1975, 1995 and 2000, while a sharp decrease was observed during the period 1990-2006. Only the Tambacounda region (south-east) shows a more or less stationary variation of the PR parameter (asexual parasite rate), while other regions are experiencing a change in PR saw. Gaps in its PRmax interannual changes are more important than PRm PRmin but they know all simultaneous trends. These parameters are lower in the northern band from St. Louis Linguère but also for the region of Dakar. On the rainfall level also, these areas are less rainfall than the rest of the country as we finished saying earlier.

For the parameter "cases per 100 people per day," simulated by the LMM, a logical trend is also observed through Figs. 24, 29, 34, 38, 43 and 47. It is seen that the size of the parameter increases from the north to the south being 0.2 (in Saint-Louis) to 3.5 in Ziguinchor. So, it follows the latitudinal gradient on rainfall in Senegal but also the ecological and environmental reality. As it is noted with the observations in the different health districts, the development of malaria in the end of the rainy season is again found with the DMC. However, the difference in the number of cases before and during the transmission season is greater with simulations than observation. The DMC shows a very weak occurrence of malaria outside the period SON (September, October and November). But taking into account others factors that affect outbreaks of shown by observations, it seems to be logical because the model mainly consider rain and temperature only as inputs. So the occurrence of malaria observed during the dry season is due to mainly by parameters not integrated into the LMM system.

Multi-Malaria model ensemble

MIASMA is the best malaria model during the pre-intervention period (1900s see Fig 48a versus Fig 48j) while the MARA model captures the recent distribution of P. *falciparum* for the 2000s. The LMM_ro model simulates the epidemic belt too far south with respect to the observations. Note that the MAP reference dataset (baseline for the 2000s) can be questionable for Senegal (especially the location of the epidemic belt which is defined for extreme low prevalence (1 per thousand) ratio in children < 10y.)

There is a general decrease in observed malaria endemicity over Senegal (south-east especially, see Fig 48c) that might be related to the warming and drying trend experienced over the region during the 20th century (consistent with the observed disappearance of A. *funestus* in the late 1990s early 2000s, see Mouchet et al., 1998). The GCM/RCM driven runs reproduce fairly well the control runs (e.g. the malaria model runs driven by climate observations) (Figure 47&50). Therefore, bias corrections of the GCMs/RCMs inputs are correct.

The simulated decrease in the south-west of Senegal (Fig 48i-48l-48f) is consistent with the observed changes (but smaller in magnitude). The observed regional increase in malaria endemicity along the western coasts (from Dakar to Banjul) is partly captured by the different malaria model simulations.

These results seems to confirm LMM simulations for Ziguinchor (even for Tambacounda) where very pronounced drop of PR (asexual parasite rate) in 1975, 1995 and 2000 is noticed, while the sharp decrease was observed during the period 1990-2006. In fact, Tambacounda region (south-east) shows also a more or less stationary variation of the parameter PR while other regions are experiencing a change in PR.

Impact of Intervention versus the effect of climate on malaria transmission over Senegal

Recent data from the PNLP (National Program for Malaria control in Senegal) are displayed in Figs. 22, 27 and 32. They can provide an indication of the impact of Intervention versus the effect of climate on malaria transmission over Senegal. Number of suspected cases, number of tested cases, number of confirmed cases (positive test) and number of negative test are investigated. This recent database has been created in order to update the malaria context in Senegal. This data is also classified by age group. The PNLP reminds that the former malaria data was not a very good representative of the situation. The introduction of TDR (Test de Diagnostique Rapide e.g. rapid diagnostic test) in 2007 showed significant differences between this dataset and the reality of malaria morbidity in Senegal. Despite the political struggles, the evolution was almost stationary within morbidity following data until the year of 2007. However, with the systematization of the TDR after 2007 it has been a quick decline in malaria cases has been highlighted, showing a result that is more consistent with good initiatives within combating against malaria, particularly in Senegal. The TDR are widespread in 2009, the reference year for the new database data of PNLP. The sentinel sites where these data come from are chosen following various behavior as endemic disease. They are enough representatives for different areas which can give really results trough malaria transmission in Senegal. These sites are focus in Saint-Louis, Matam, Tambacounda and Dakar Kedougou and are a number of four districts by region.

Figs. 22, 27, 32 and 41 show that, considering the last four years (2009, 2010, 2011 and 2012); there are nevertheless a significant number of cases of malaria in the four regions taken as examples (Saint Louis, Louga, Dakar and Tambacounda). The number of malaria cases recorded in 2010 is greater with exception observed for Saint-Louis. This is consistent with observations in previous figures showing positive anomalies of rainfall in Ferlo, and all Senegal regions. It is therefore a particularly

wet year with positive anomaly in Senegal. By cons it is in 2009 when it is recorded the lowest number of cases of malaria in areas cited as examples. However, the year of 2009 was more or less rainy with a positive anomaly of precipitations. Another thing is that the peaks of malaria are found again and again in October. For the peak of malaria observed in November 2009 and 2010 in the suburb zone (Pikine, Dakar), it is often explained by recurrent floods with significant consequences even during two or three months after the end of the rainfall season. It is observed that the transmission is more important in Pikine (urban area) than Linguere (rural area), yet health facilities are more accessible to Dakar but it should be noted that transmission is more favorable there for many reasons.

It is also observed that after 2009 which is the reference year within the updated database of PNLP corresponding to the use of TRD (Rapid Diagnostic Test) for malaria diagnostic and ACT (Artemisinine-based Combination Therapy) for treatment, an important decrease in malaria transmission was observed over the different sentinel sites in Senegal. The sentinel sites are chosen according to their representativeness of malaria transmission over Senegal regions and there 4 are sentinel sites by region. It's important to know that the updated database of PNLP does not cover all health districts of the country regions nowadays. The only regions where there are at first sentinel sites are Saint-Louis, Matam, Louga, Dakar, Tambacounda but the sites are being extended at least to others regions such as Kaolack and Ziginchor.

Future projections, uncertainties & Malaria Models behaviour and sensitivity to climate change

A general decrease in the simulated length of the malaria transmission season is generally shown in the ISI-MIP and CORDEX super ensemble over Senegal (fig 51 & fig 52). Large differences are highlighted between the ISI-MIP & CORDEX patterns. The decrease is more pronounced over the northern part of Senegal in the CORDEX RCM based ensemble while this is more restricted to the central and south-eastern part of the country in the ISI-MIP GCM based ensemble.

Uncertainties at the northern border are mainly driven by the GCMs for ISI-MIP, but uncertainties are mainly ruled by the impact models (fig 53), the scenario contribution to the super ensemble uncertainty is small. For CORDEX, the RCM rule the total uncertainties during the 2020s, then the uncertainty related to the RCM decreases, but it is still governing uncertainty in the northern part and over the western coasts of Senegal. Impact model uncertainty is still important in the south in the CORDEX ensemble.

A general decrease is simulated in the simulated length of the transmission season (LTS) for the future over Senegal whatever time period & scenario considered (fig 55). A stronger decreasing trend is simulated for the far future e.g. 2080s and for the most extreme emission scenario e.g. rcp85. The decrease in LTS as simulated by the lmm_LMM_ro & VECTRI might be related to a temperature

effect for those models (see Fig 56). Temperatures are getting warm enough (above 28°C) to impact on the adult mosquito survival scheme (above 28-30°C adult mosquitoes die in the model which causes the decrease in LTS over this region) for those two malaria models. This is consistent with the observed disappearance of An. *funestus* over northern Senegal that followed the 1980s drought. The malaria epidemic fringe is shifted southward for most malaria models (fig 57 & fig 58). Future climate becomes suitable for malaria transmission for MARA (Fig 59-60-61). Opposite behaviour is shown for the two most realistic dynamical malaria models such as VECTRI and LMM_ro (northern Senegal becomes unsuitable for malaria transmission in the model's world).

Population at risk increases (mainly driven by the linear increase in population not the changes in LTS) excepting during the 2080s where climate becomes so unsuitable in northern Senegal that no more additional person at risk are shown.

Discussion & perspectives

In this report, it is processed and analyzed in terms of spatial and temporal variability, some climate and malaria parameters. Using 2001-2009 observations from PNLP (National Program for control of malaria in Senegal) and LMM simulations, the main findings are the latitudinal gradient north-south found again trough different areas of Senegal. A strong inter-annual variability of rainfall is observed in the different Senegal regions. In analysis, we have taken into account the different regions of malaria with their behaviors not associated only with climate but also environmental and social conditions. The evolution of malaria has the same trend as precipitations for each area considered with a time delay of 1 or 2 months between the maximum on rain and malaria outbreaks. The high malaria transmission is found in the wetter area such as the southern part such as "Basse Casamance" but also in the urban area such as Dakar suburbs in case of floods occurrence synonyms of water body's development. In Ferlo the existence in terms of frequency and sustainability is due the several and big temporal ponds near habitations.

Results summary

The first results obtained from observations and simulations data over the Senegal observatory in the Ferlo region, confirm that the risk of malaria transmission is mainly linked with climate parameters such as rainfall, temperature and relative humidity. A lag of one to two months between the maximum in malaria cases and the rainfall peak is often observed. Malaria data from the PNLP (National Program for control of malaria in Senegal) was used here for validation and to allow us to identify the different health districts. The database contains detailed information on public health facilities all over Senegal. From the PNLP database through specified sentinel sites, epidemiological features with various potential transmissions have been identified in this report.

A general decrease in the simulated length of the transmission season (LTS) is simulated by different malaria models for the future over Senegal whatever time period & scenario considered. A stronger decreasing trend is simulated for the 2080s and the most extreme emission scenario (rcp85). The decrease in LTS shown by the LMM_ro & VECTRI malaria models is mainly related to a temperature effect for those models. Temperatures are getting warm enough (above 28°C) to impact on the adult mosquito survival scheme (above 28-30°C adult mosquitoes die in the model this causes a decrease in the simulated length of the malaria transmission season). The simulated malaria epidemic fringe is shifted southward for most malaria models in the future with respect to the current climate control runs.

Effects of climate versus intervention in Senegal

It is also observed that after 2009 which is the reference year within the updated database of PNLP corresponding to the use of TRD (Rapid Diagnostic Test) for malaria diagnostic and ACT (Artemisinine-based Combination Therapy) for treatment, an important decreasing is observed in the malaria evolution over the different sentinel sites in Senegal. The sentinel sites are chosen according to their representativeness of malaria transmission over Senegal regions and there 4 are sentinel sites by region. It's important to know that the updated database of PNLP does not cover now all health districts of the country regions. The only regions where there are at first sentinel sites are Saint-Louis, Matam, Louga, Dakar, Tambacounda but the sites are being extended at least to others regions such as Kaolack and Ziginchor.

We did not take local demographic and socioeconomic circumstances into account nor make provision for the effect of malaria control on transmission explicitly in malaria models used in this work. The inability of global circulation models to accurately predict the current climate from retrospective data has led to a debate about their application also. As global climate dynamics increases and models are increasingly able to handle this complexity, projections of the probable response of the climate system to any scenario are likely to improve and the model will constitute a valid baseline for assessment.

The resurgence of highland malaria cannot necessarily be attributed to recent climate change. Malaria is a complex disease that is affected by a range of factors in addition to climate—a recent analysis of four highland sites in Africa where large increases in malaria cases noted showed no large climatic change during resurgence or the last century. Some of these cases were attributed to factors such as drug resistance, breakdown of control programs, and land-use change.

However, climate provides the framework within which transmission is possible and other factors (except those that determine the availability of breeding sites—irrigation, construction of dams, or

removal of potential breeding sites) can affect malaria transmission only in spatio-temporal zones that are climatically suitable.

QWECI recognized the need to improve understanding of how climate-related and other ecological factors affect the spread and severity of malaria. We believe that transmission maps generated by malaria models (well improved during QWECI) could form an integral component of this strategy. Malaria models shown in this report had achieved a good accuracy and are validated against empirical data. This work is an important first step towards a model of intensity of transmission and constitutes a valid baseline against which interventions can be planned and climate change projections evaluated.

The recent PNLP database taking into account number of suspected cases of malaria, number of tested cases, number of confirmed cases (positive tests), number of negative tests allow us to better understand the difference noticed sometime between observations and simulations results. However, the seasonal and spatial trends are the same by observations and modeling. Nevertheless, for the vector and parasite parameters simulated by malaria models, it would be interesting to have deep comparison of observational data from IPD (Pastor Institute of Dakar) collected during QWECI project.

References

Afrane YA, Klinkenberg E, Drechsel P, Owusu-Daaku K, Garms R, Kruppa T: Does irrigated urban agriculture influence the transmission of malaria in the city of Kumasi, Ghana? *Acta Trop* 2004, **89**:125-134.

Alonso, D., M.J. Bouma, and M. Pascual, 2011: Epidemic malaria and warmer temperatures in recent decades in an east african highland. *Proc Biol Sci,* **278(1712)**, 1661-9

Armstrong BG. "Fixed factors that modify the effects of time-varying factors: applying the case-only approach". *Epidemiology* 2003; **14**:467-472.

Ayala D., Fontaine M.C., Cohuet A., Fontenille D., Vitalis R., Simard F., 2011. Chromosomal inversions, natural selection and adaptation in the malaria vector Anopheles funestus. Mol. Biol. Evol. **28(1)**:745-58.

Ba Y, Diallo D, Kebe CMF, Dia I, Diallo M., 2005, Aspects of bioecology of two Rift Valley Fever virus vectors in Senegal (West Africa): Aedes vexans and Culex poicilipes (Diptera: Culicidae), *J Med Entomol*, **42** : 739-750.

Barnett TP. Comparison of near-surface air temperature variability in 11 coupled global climate models. *J Climate* 1999; **12**:511-518.

BASU, R. "High ambient temperature and mortality: a review of epidemiologic studies from 2001 to 2008" *Environmental Health* 2009, 8:40

Beguin, A., et al., 2011, The opposing effects of climate change and socio-economic development on the global distribution of malaria. *Global Environmental Change*, **21**(4): p. 1209-1214.

Bogreau H, Renaud F, Bouchiba H, Durand P, Assi SB, Henry MC, Garnotel E, Pradines B, Fusai T, Wade B, Adehossi E, Parola P, Kamil MA, Puijalon O, Rogier C: Genetic diversity and structure of African Plasmodium falciparum populations in urban and rural areas. *Am J Trop Med Hyg* 2006, **74**:953-959.

Bouma, M.J., et al., 2011, Global malaria maps and climate change: a focus on East African highlands. *Trends in Parasitology*, **27**(10): p. 421-2.

Byass, P. "Climate change and population health in Africa: where are the scientists?" *Global Health Action* 2009. DOI: **10**.3402/gha.v2i0.2065.

Caminade C. and L. Terray, 2010. 20th century Sahel rainfall variability as simulated by the ARPEGE AGCM and future changes. Climate Dynamics, 35(1), 75-94

Caminade C., J.M. Medlock, S. leach, K.M. McIntyre, M. Baylis, A.P. Morse, 2012. Suitability of European climate for the Asian tiger mosquito Aedes Albopictus: recent trends and future scenario. Journal of the Royal Society Interface. 9(75): 2708-2717.

Caminade C., J.A. Ndione, C.M.F. Kebe, A. E. Jones, S. Danuor, S. Tay, Y.M. Tourre, J.P. Lacaux, J.B. Duchemin, I. Jeanne, A.P. Morse, 2011. Mapping Rift Valley Fever and Malaria risk over West Africa using climatic indicators. Atm. Sc. Lett., 12: 96-103.

Chaves, L.F. and C.J. Koenraadt, 2010. Climate change and highland malaria: Fresh air for a hot debate. *Q Rev Biol,* 13 **85(1)**, 27-55.

Confalonieri, U., et al., 2007. *Human health*, in *Climate Change 2007: Impacts, Adaptation and Vulnerability. Contribution of Working Group II to the Fourth Assessment Report of the Intergovernmental Panel on Climate Change*, M.L. Parry, et al., Editors. 2007, Cambridge University Press: Cambridge,UK. p. 391-431.

Costello A, Abbas M, Allen A, Ball S, Bell S, Bellamy R, Friel S, Groce N, Johnson A, Kett M, Lee M, Levy C, Maslin M, McCoy D, McGuire B, Montgomery H, Napier D, Pagel C, Patel J, de Oliveira JA, Redclift N, Rees H, Rogger D, Scott J, Stephenson J, Twigg J, Wolff J, Patterson C. "Managing the health effects of climate change: Lancet and University College London Institute for Global Health Commission". *Lancet* 2009; 373: 1693733.

Craig, M.H., R.W. Snow, and D. Le Sueur, 1999. A climate based distribution model of malaria transmission in Sub-Saharan Africa. *Parasitology Today*, **15**(3): p. 104-105.

Dee, D. P et al., 2011. The ERA-Interim reanalysis: configuration and performance of the data assimilation system. Q.J.R. Meteorol. Soc., **137**: 553–597. doi: 10.1002/qj.828

Diallo M., Lochouarn L., Ba K., Sall A. A., Mondo M., Girault L., Mathiot C., 2000, First isolation of the Rift Valley fever virus from *Culex poicilipes* (Diptera: Culicidae) in Nature, *Am. J. Trop. Med. Hyg.*, **62**: 702-704

Diallo M., Nabeth P., Bâ, K., Sall A. A., Bâ Y., Mondo M., Girault L, Mohameden O. Abdalahi, Mathiot C,, 2005, Mosquitoes vectors of the 1998-1999 outbreak of Rift Valley Fever and other arboviruses (Bagaza, Sanar, Wesselsbron and West Nile) in Mauritania and Senegal, *Medical and Veterinary Entomology*, **19**, 119-126.

Diallo A., Ndam N.T., Moussiliou A., Dos Santos S., Ndonky A., Borderon M., Oliveau S., Lalou R., Le Hesran JY. "Asymptomatic Carriage of Plasmodium in Urban Dakar: The Risk of Malaria Should Not Be Underestimated". *PLoS ONE* 2012; **7**(2).

Dondorp et al. 2010. Artemisinin resistance: current status and scenarios for containment. Nat Rev. MicroBiol. **8**:272-280.

Donnelly MJ, McCall PJ, Lengeler C, Bates I, D'Alessandro U, Barnish G, Konradsen F, Klinkenberg E, Townson H, Trape JF, Hastings IM, Mutero C: Malaria and urbanization in sub-Saharan Africa. *Malar J* 2005, 4:12.

Drame P, Machault T V, Diallo A, Cornelie S, Poinsignon A, Lalou R, Mbacke S., Dos Santos S., Rogier C., Pages F., Le Hesran JY and Remous F. "IgG responses to the gSG6-P1 salivary peptide for evaluating human exposure to Anopheles bites in urban areas of Dakar region, Senegal". Malaria Journal, 2012; 11(1):72.

Druyan L., 2010. Studies of 21st century precipitation trends over West Africa. Int. J. Climatol. **31:** 1415-1424

Edlund S., Davis M., Douglas J.V., A. Kershenbaum, N. Waraporn, J. Lessler and J.H. Kaufman 2012. A global model of malaria climate sensitivity: comparing malaria response to historic climate data based on simulation and officially reported malaria incidence. Malaria Journal, 11:331

Ermert V., Fink A., Jones A.E., Morse A.P., 2011. Development of the Liverpool Malaria Model part I – refining the parameter settings and mathematical formulation of basic processes based on a literature review. Malaria Journal 10:35.

Ermert, V., et al., 2012. The Impact of Regional Climate Change on Malaria Risk due to Greenhouse Forcing and Land-Use Changes in Tropical Africa. *Environmental Health Perspective*, **120**(1): p. 77-84.

Feachem, R.G., 2011. The global fund: Getting the reforms right. *The Lancet*, **378(9805)**, 1764-1765.

Fontenille D., Traoré-Lamizana M., Diallo M., Thonnon J., Digoutte J.P., Zeller H.G., 1998, New vector of Rift Valley fever in West Africa, Emerg. Infect. Dis., **4**: 289-293.

Gething, P.W et al., 2010. *Climate change and the global malaria recession* Nature, 2010. **465**: p. 342-347.

Githeko AK, Lindsay SW, CONFALONIERI UE, PATZ JA. "Climate change and vector-borne diseases: a regional analysis". *Bull World Health Organ* 2000; **78**: 113647.

Gosling SN, Mcgregor GR and Paldy A. "Climate change and heat-related mortality in six cities. Part 1: model construction and validation", *Int J Biometeorol* 2007; **51**:525–540.

Hay, S.I., Rogers D.J., S.E. Randolph, D.I. Stern, J. Cox, G.D. Shanks and R.W. Snow, 2002. Hot topic or hot air? Climate change and malaria resurgence in East African highlands. Trends in Parasitology 18(12):530-534.

Hay S.I, Cox J, Rogers DJ, Randolph SE, Stern DI, Shanks GD, Myers MF, Snow RW. Climate change and the resurgence of malaria in the East African highlands. *Nature.* 2002 Feb 21; 415(6874):905-9.

Hay, S.I. and Snow R.W., 2006. The malaria atlas project: developing global maps of malaria risk. Plos Med 3:e473, doi:10.1371/journal.pmed.0030473

Hay, S.I., et al., 2009. *A world malaria map: Plasmodium falciparum endemicity in 2007.* PLoS Med., **6**(3): p. e1000048.

Hempel, S., et al., 2013. A trend-preserving bias correction – the ISI-MIP approach. *Earth System Dynamics*, in press.

Hoshen, M. B., and A. P. Morse, 2004. A weather-driven model of malaria transmission. *Malaria J.*, **3**, 32, doi:10.1186/1475-2875-3-32.

Huffman, G.J., et al., 2007. The TRMM Multisatellite Precipitation Analysis (TMPA): Quasi-global, multiyear, combined-sensor precipitation estimates at fine scales. *Journal of Hydrometeorology* **8**: p. 38-55.

Jones, A., 2007. *Seasonal ensemble prediction of malaria in Africa*, University of Liverpool: Liverpool. PhD Thesis.

Jones, A. and A.P. Morse, 2010. Application and validation of a seasonal ensemble prediction system using a dynamic malaria model. Journal of Climate, **23**: p. 4202–4215.

Jones C, F.Giorgi and G.Asrar, 2011. The Coordinated Regional Downscaling Experiment: CORDEX, An international downscaling link to CMIP5: *CLIVAR Exchanges*, No. 56, Vol 16, No.2 pages 34-40.

Keiser J, Utzinger J, Caldas de Castro M, Smith TA, Tanner M, Singer BH: Urbanization in sub-saharan Africa and implication for malaria control. *Am J Trop Med Hyg* 2004, **71**:118-127.

Kelly-Hope, L. and F.E. McKenzie, 2009. The multiplicity of malaria transmission: a review of entomological inoculation rate measurements and methods across sub-Saharan Africa. *Malaria Journal*, **8**(1): p. 19.

Kinney PL, O'Neill MS, Bell ML and Schwartz J. "Approaches for estimating effects of climate change on heat-related deaths: challenges and opportunities", environmental sciences & policy 2008; 87-96.

Klinkenberg E, McCall PJ, Hastings IM, Wilson MD, Amerasinghe FP, Donnelly MJ: Malaria and irrigated crops, Accra, Ghana. Emerg Infect Dis 2005, **11**:1290-1293.

Lacaux J.P., Tourre Y. M., Vignolles C., Ndione J.A., Lafaye M., 2007. Ranking Ponds from High-Resolution Remote Sensing: Application to Rift Valley Fever Epidemics in the Ferlo Region (Senegal), *Remote Sensing of Environment*, **106**, 66-74.

Le Sueur D. F. Binka, C. Lengeler, D. De Savigny, R.W. Snow, T. Teusher and Y.T. Touree, 1997. An Atlas of malaria in Africa. Africa Health **19**:23-24.

Lysenko A.J & Semasko I.N., 1968. in Itogi Nauki [in russian]: Medicinskaja Geografijia (ed Lebedew, A.W.) 25-146 (Academy of Sciences, Moscow).

Machault V, Gadiaga L, Vignolles C, Jarjaval F, Bouzid S, Sokhna C, Lacaux JP, Trape JF, Rogier C, Pages F: Highly focused anopheline breeding sites and malaria transmission in Dakar. *Malar J 2009*, **8**:138.

MacLeod D.A, C. Caminade, A.P. Morse, 2012. Useful decadal climate prediction at regional scales? A look at the ENSEMBLES stream 2 decadal hindcasts. *Env. Res. Lett* 7 044012 doi:10.1088/1748-9326/7/4/044012

Maharaj R. et al. 2012. The feasibility of malaria elimination in South Africa. Malaria journal, **11**:423

Matthys B, N'Goran EK, Kone M, Koudou BG, Vounatsou P, Cisse G,Tschannen AB, Tanner M, Utzinger J: Urban agricultural land use and characterization of mosquito larval habitats in a medium-sized town of Cote d'Ivoire. *J Vector Ecol 2006*, **31**:319-333.

MARA, 1998. Towards an Atlas of Malaria Risk in Africa. First Technical Report of the MARA/ARMA collaboration, MARA/ARMA: Durban.

P. Martens, R.S. Kovats, S. Nijhof, M.T.J. Livermore, D.J. Bradley, J. Cox, A.J. McMichael, 1999. Climate change and future population at risk of malaria. Global Environmental Changes 9(1):S89-S107.

MAP, Oxford, 2010a. The spatial limits of Plasmodium vivax malaria transmission map in 2010 globally: [http://www.map.ox.ac.uk/browse-resources/transmission-limits/Pv_limits/world/]

MAP, Oxford, 2010b. Dominant vectors map in 2010 globally: [http://www.map.ox.ac.uk/browse-resources/multiple-vectors/dominant_malaria_vectors/world/]

Medina-Ramon M, Zanobetti A, Cavanagh DP, and Schwartz J. "Extreme Temperatures and Mortality: Assessing Effect Modification by Personal Characteristics and Specific Cause of Death in a Multi-City Case-Only Analysis", *Environmental Health Perspectives 2006*; 114(**9**): 1331-1336.

Mitchell, T.D. and P.D. Jones, 2005. An improved method of constructing a database of monthly climate observations and associated high-resolution grids. *International Journal of Climatology* **25**: p. 693-712.

Mouchet J., Laventure S., Blanchy S., Fioramonti R., Rakotonjanabelo A., Rabarison P., Sircoulon J., Roux, J., 1997. The reconquest of the Madagascar highlands by malaria. Bull. Soc. Pathol. Exot. **90(3)**:162-8

Mouchet, J., S. Manuin, S. Sircoulon, S. Laventure, O. Faye, A.W. Onapa, P. Carnavale, J. Julvez, and D. Fontenille, 1998: Evolution of malaria for the past 40 years: impact of climate and human factors. *Journal of the American Mosquito Control Association*, **14,** 121-130.

Nabarro DN, Tayler EM. The roll back malaria campaign. *Science* 1998; **280**: 2067-2068.

Nájera, J. A., Kouznetsov, R. L., and C. Delacollette, 1998. *Malaria epidemics: Detection and control, forecasting and prevention*. WHO/MAL/98.1084. World Health Organization, Geneva, Switzerland. [http://www.who.int/malaria/docs/najera_epidemics/naj_toc.htm]

Ndione J-A., Besancenot J-P., Lacaux J-P., Sabatier P., 2003, Environnement et épidémiologie de la fièvre de la vallée du Rift (FVR) dans le bassin inférieur du fleuve Sénégal, *Environnement, Risques et Santé*, **2(3)**, 176-182.

Ndione J. A., Diop M., Lacaux J.P., Gaye A.T., 2008. Variabilité intra-saisonnière de la Pluviométrie et émergence de la fièvre de la vallée du rift (FVR) dans la vallée du fleuve Sénégal : nouvelles considérations, *Climatologie*, vol. **5**, 83-97

Nikulin G et al., 2013. Precipitation Climatology in An Ensemble of CORDEX-Africa Regional Climate Simulations. Accepted for publication in Journal of Climate doi: http://dx.doi.org/10.1175/JCLI-D-11-00375.1

Omumbo, J., B. Lyon, S. Waweru, S. Connor, and M. Thomson, 2011. Raised temperatures over the kericho tea 51 estates: Revisiting the climate in the east african highlands malaria debate. *Malaria Journal*, **10(1)**:12.

Paaijmans, K.P., et al., 2007. Unexpected high losses of Anopheles gambiae larvae due to rainfall. PLOSONE, **2**(11): p. e1146

Pages F, Texier G, Pradines B, Gadiaga L, Machault V, Jarjaval F, Penhoat K, Berger F, Trape JF, Rogier C, Sokhna C: Malaria transmission in Dakar: a two-year survey. *Malar J* 2008, 7:178.

Parry, M. L., Rozenzweig, C., Iglesias, A., Livermore, M. & Fisher, G. "Effects of climate change on global food production under SRES emissions and socioeconomic scenarios". *Glob. Environ. Change* 2004; **14**, 53–-67.

Pascual M, Ahumuda JA, Chaves LF, Rodo X, BOUMA M. "Malaria resurgence in the East African highlands: temperature trends revisited". *Proc Natl Acad Sci* 2006; **103**: 5829-34.

Patz Patz JA, Hulme M, Rosenzweig C, Mitchell TD, Goldberg RA, Githeko AK, Lele S, McMichael AJ, Le Sueur D.. Climate change: regional warming and malaria resurgence. *Nature.* 2002 Dec 12;**420**(6916):627-8; discussion 628

Peterson AT. "Shifting suitability for malaria vectors across Africa with warming climates". *BMC Infect Dis* 2009; **9**: 59.

Peterson I, Borrell LN, El-Sadr W, Teklehaimanot A: A temporal-spatial analysis of malaria transmission in Adama, Ethiopia. Am J Trop Med Hyg 2009, 81:944-949.
Rey G., Fouillet A., Jougla E. et Hemon D. « Vagues de chaleur, fluctuations ordinaires de températures et mortalité en France depuis 1971 ». *Population* 2007 ; 62(**3**): 533-563.

Robert V, Le Goff G, Toto JC, Mulder L, Fondjo E, Manga L, Carnevale P: Anthropophilic mosquitoes and malaria transmission at Edea, Cameroon. *Trop Med Parasitol* 1993, 44:14-18.

Robert V, Awono-Ambene P, Thioulouse J: Ecology of larval mosquitoes, with special reference to Anopheles arabiensis (Diptera: Culcidae) in market-garden wells in urban Dakar, Senegal. *J Med Entomol* 1998, **35**:948-955.

Robert V, Macintyre K, Keating J, Trape JF, Duchemin JB, M W, Beier JC: Malaria transmission in urban sub-saharan Africa. *Am J Trop Med Hyg* 2003, **68**:169-176.

Ross R., 1911. The Prevention of Malaria. 2nd edition London: Murray 1911.

Sachs JD, 2001. A new global commitment to disease control in Africa. Nat. Med **7**:521-523.

Sachs JD, 2002. A new global effort to control malaria. Department of Economics discussion paper #:0203-11. New York Columbia University Department of Economics.

SAKAP, 2008. Evaluation of Malaria Health Education Interventions using knowledge, attitudes and practices (KAP) in South Africa. Brief Report available online : [http://www.mrc.ac.za/malaria/SAKAP.pdf]

Schar, C., Pier LV., Daniel L., Christoph F., Christian H., Mark A. L., and Christof A. "The role of increasing temperature variability in European summer heatwaves". Nature 2004; 427, 332–-336.

Schwartz J. "Who is sensitive to extremes of temperature? A case-only analysis". *Epidemiology* 2005; **16**:67–72.

SSP Database, 2012: https://secure.iiasa.ac.at/web-apps/ene/SspDb.

Staedke SG, Nottingham EW, Cox J, Kamya MR, Rosenthal PJ, Dorsey G: Short report: proximity to mosquito breeding sites as a risk factor for clinical malaria episodes in an urban cohort of Ugandan children. *Am J Trop Med Hyg* 2003, **69**:244-246.

Stoler J, Weeks JR, Getis A, Hill AG: Distance threshold for the effect of urban agriculture on elevated self-reported malaria prevalence in Accra, Ghana. *Am J Trop Med Hyg* 2009, **80**:547-554.

Tanser FC, Sharp B, Le Sueur D. "Potential effect of climate change on malaria transmission in Africa". *Lancet* 2003; 362: 1792-8.

Taylor, K.E., R.J. Stouffer, and G.A. Meehl, 2012. An overview of CMIP5 and the experiment design, *Bulletin American Meteorological Society*. **93**: p. 485–498.

The World Health Organisation. *The World Health Report* 2002 (WHO, Geneva, 2002).

The World Health Organisation. Climate change and human health - Risks and responses.2003 (WHO, Geneva, 2003), 322p.

Tourre Y.M., Lacaux J-P., Vignolles C., Ndione J. A., Lafaye M., 2008. Mapping of Zones Potentially Occupied by Mosquitoes (ZPOMs) Aedes vexans and Culex poicipiles, the Main Vectors of Rift Valley Fever in Senegal, *Geospatial Health*, **3**(**1**), 69-79.

Trape JF, Lefebvre-Zante E, Legros F, Ndiaye G, Bouganali H, Druilhe P, Salem G: Vector density gradients and the epidemiology of urban malaria in Dakar, Senegal. *Am J Trop Med Hyg* 1992, **47**:181-189.

Tompkins, A.M. and V. Ermert, 2013, A regional-scale, high resolution dynamical malaria model that accounts for population density, climate and surface hydrology. *Malaria Journal* (in review).

UNPD: World Urbanization Prospects: the 2007 revision population database. 2007.

Van Lieshout, M., et al., 2004. Climate change and malaria: analysis of the SRES climate and socioeconomic scenarios, *Global Environmental Change*. **14**(1): p. 87-99.

Van Vuuren, D.P., et al., 2012. A proposal for a new scenario framework to support research and assessment in different climate research communities. *Global Environmental Change*, **22**(1): p. 21-35.

Vignolles C., Lacaux J-P., Tourre Y.M., Bigeard G., Ndione J. A., Lafaye M., 2009. Rift Valley Fever in a zone potentially occupied by Aedes vexans in Senegal: dynamics and risk mapping, Geospatial Health, 3 (**2**), 211-220.

Wang SJ, Lengeler C, Smith TA, Vounatsou P, Cisse G, Diallo DA, Akogbeto M, Mtasiwa D, Teklehaimanot A, Tanner M: Rapid urban malaria appraisal (RUMA) in sub-Saharan Africa. *Malar J* 2005, 4:40.

Warszawski, L. et al., 2013. Research Design of the Intersectoral Impact Model Intercomparison Project (ISI-MIP). Proceedings of the National Academy of Sciences (USA) in review.

WHO. A global strategy for malaria control. Geneva: World Health Organization, 1993.

WHO, 1974. Malaria control in countries where time-limited eradication is impracticable at present. Report of a WHO Interregional conference. Geneva, World Health Organization.

Wilhelmi OV and Hayden MH. "Connecting people and place: a new framework for reducing urban vulnerability to extreme heat" *Environment Research Letter* 2010; doi:10.1088/1748-9326/5/1/014021.

Yé Y, Sankoh OA, Kouyaté B, Sauerborn R. Environmental factors and malaria transmission risk: modeling the risk in a holoendemic area of Burkina Faso. Surrey, UK: Ashgate; 2008.

List of figures

Fig. 46: Ziguinchor : Interannual variability of the average rate of asexual parasites (PRa in% black curve, left axis) and the minimum rate (PRmin in% blue curve, left axis) and maximum (PRmax, in% red curve, left axis) of asexual parasites. Seasonal characteristics of malaria (right axis): Monthly entomological inoculation rate (color palette). The months of maximum transmission are marked with «X".

Fig. 47: Annual cycle of malaria incidence (for 100 people) simulated by the DMC for Ziguinchor station.

Fig. 48: Observed and simulated malaria distribution for three malaria models (lmm_r0, mara and miasma).

Fig. 49: Estimation of current malaria distribution and validation (Tier II validation) ISI-MIP – 5 malaria models.

Fig. 50: Estimation of current malaria distribution and validation (Tier II validation) CORDEX – 3 malaria models.

Fig.51: The effect of climate scenarios on future malaria distribution: changes in length of the malaria season (ISI-MIP ensemble).

Fig. 52: The effect of climate scenarios on future malaria distribution: changes in length of the malaria season (CORDEX ensemble).

Fig. 53: Assessment of relative contribution of malaria model (IM), climate model (GCM), and emissions scenario (RCP) to final estimates of future malaria distribution under climate change. This is carried out for the ISI-MIP super ensemble.

Fig. 54: Assessment of relative contribution of malaria model (IM), climate model (RCM), and emissions scenario (RCP) to final estimates of future malaria distribution under climate change. This is carried out for the CORDEX super ensemble.

Fig. 55: Sensitivity of the simulated changes in the length of the malaria season to climate change for a) the ISI-MIP and b) the CORDEX ensemble over Senegal (10.5N-17N / 18W-11W).

Fig. 56: Sensitivity of the simulated changes in the length of the malaria season to mean annual rainfall and temperature for the ISI-MIP ensemble over Senegal.

Fig. 57: Sensitivity of the simulated malaria epidemic belt to climate change for a) the ISI-MIP and b) the CORDEX ensemble.

Fig. 58: Sensitivity of the simulated malaria epidemic belt to climate change for a) the ISI-MIP and b) the CORDEX ensemble.

Fig. 59: Simulated changes in climate suitability for malaria transmission (CS) for a) the ISI-MIP and b) the CORDEX noresm1 experiment.

Fig. 60: Simulated changes in climate suitability for malaria transmission (CS) for a) the ISI-MIP and b) the CORDEX gfdl_esm2m experiment.

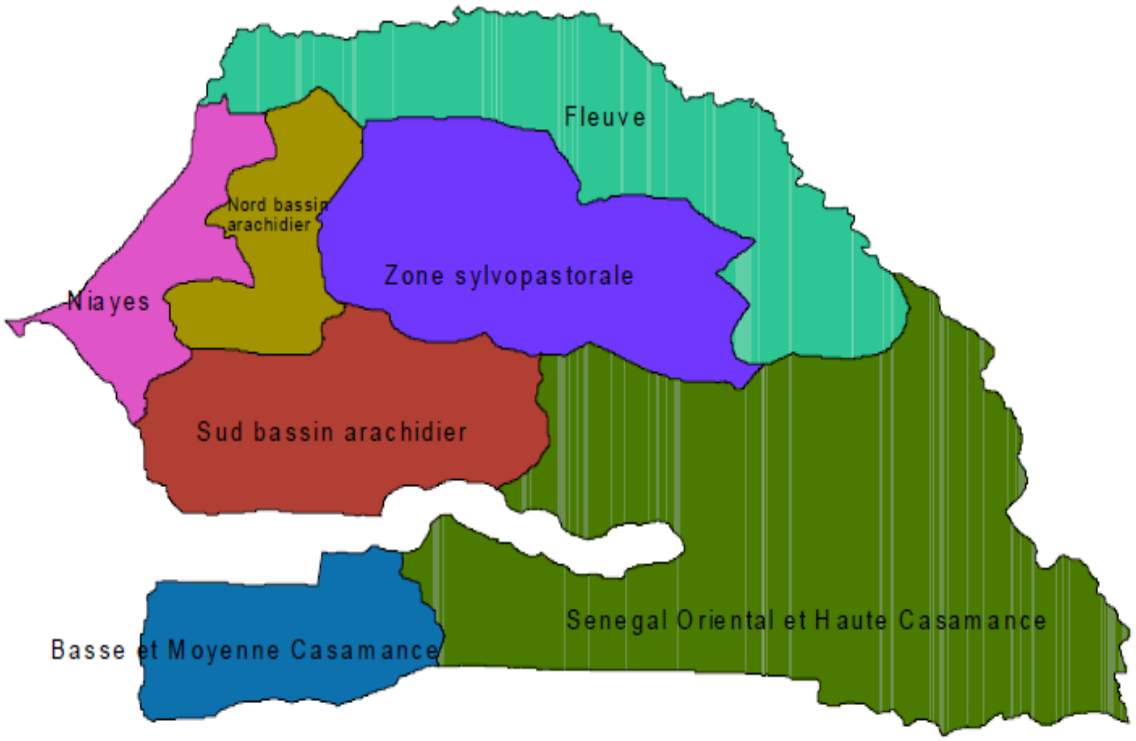

Fig. 1: Different ecological zones of Senegal

« Vallée du Fleuve Senegal in the northern part »: Example of Saint-Louis

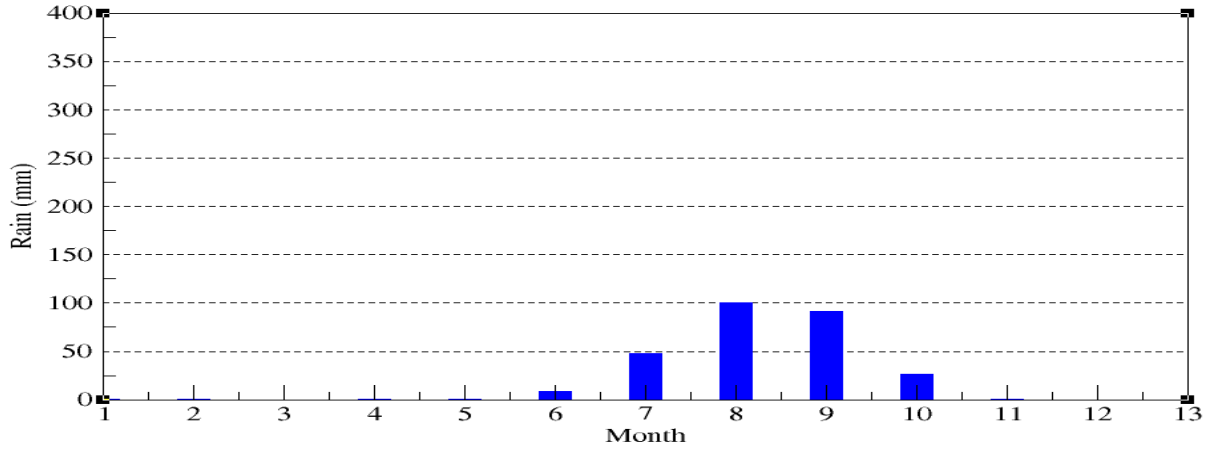

Fig. 2: Annual cycle of rainfall over Saint-Louis (1950-2010)

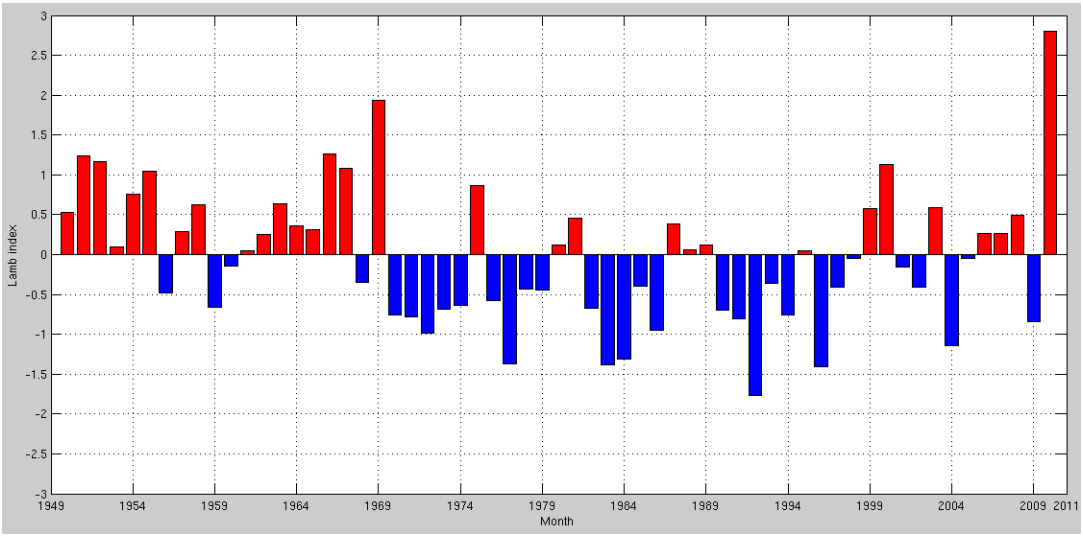

Fig 3: Lamb index of rainfall in Saint-Louis (1950-2010)

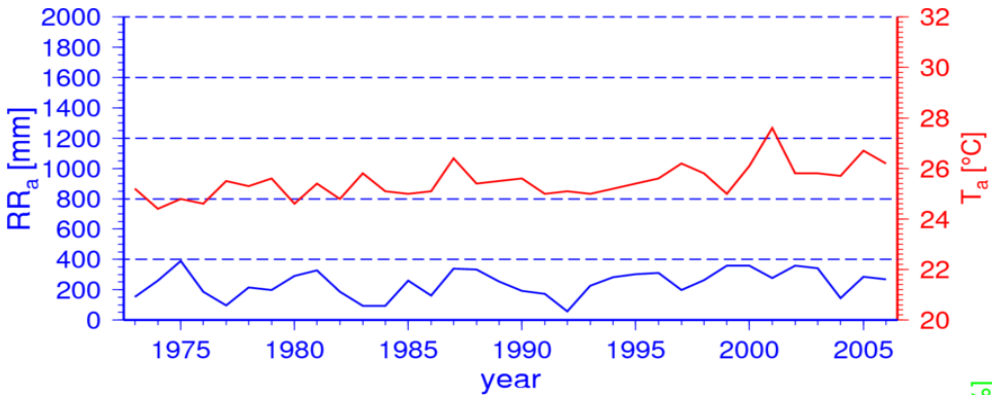

Fig. 4: Interannual variability of rainfall and temperatures observed in Saint-Louis, 1973-2006

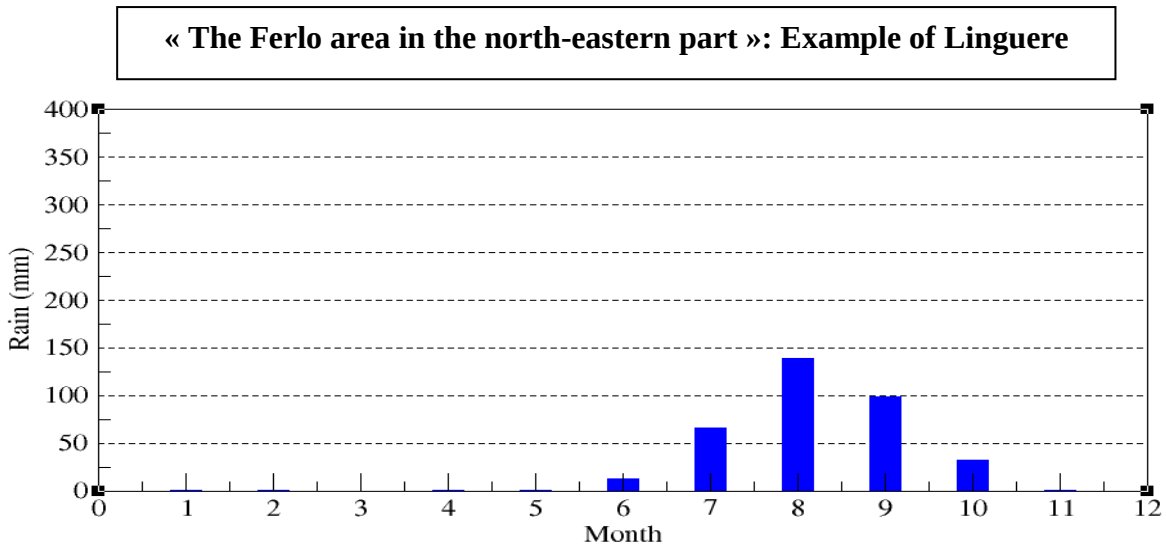

Fig. 5 : Annual cycle of rainfall over Linguere (1950-2010)

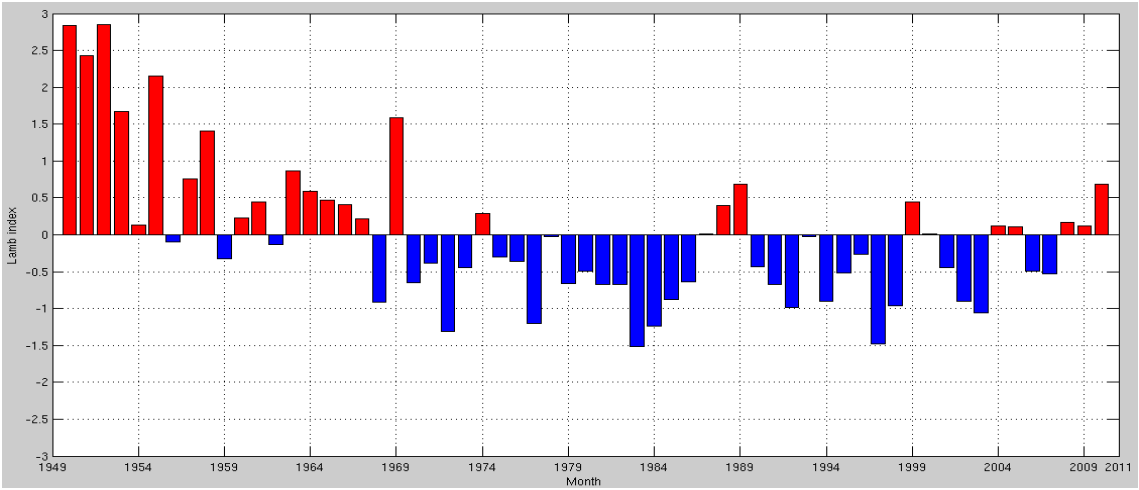

Fig. 6 : Lamb index of rainfall in Linguere (1950-2010)

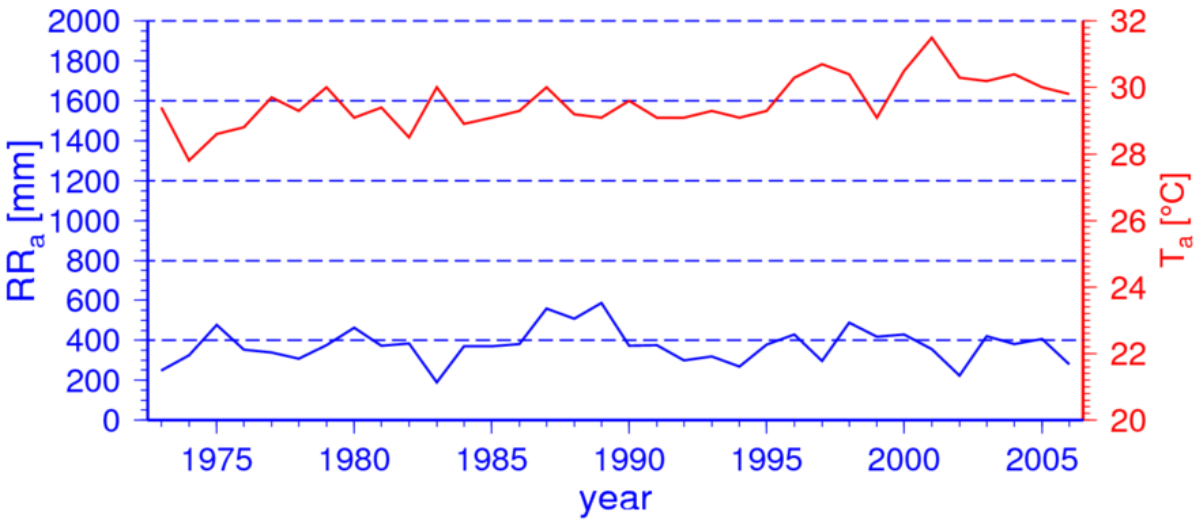

Fig. 7: Interannual variability of rainfall and temperature observed in Linguere (1973-2006)

In the Coast : Dakar zone

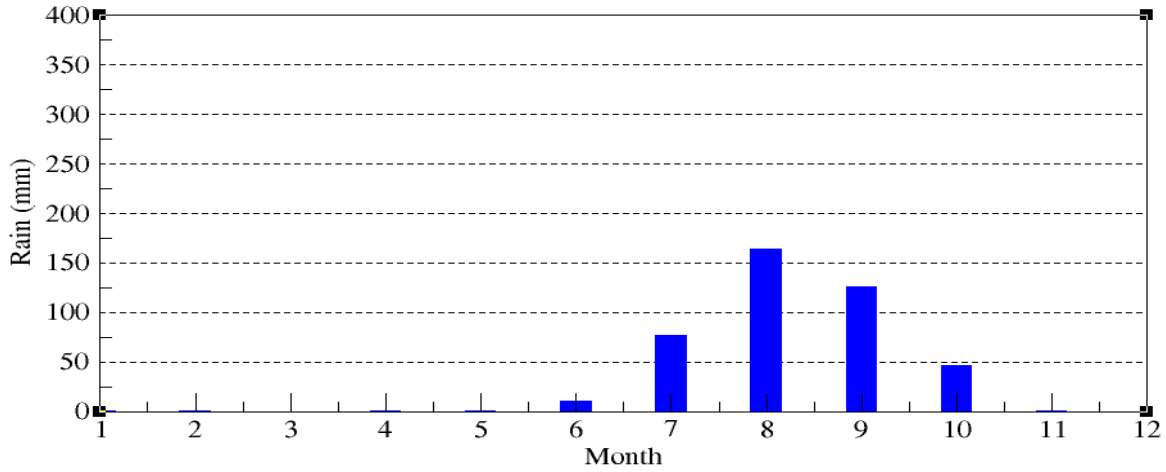

Fig. 8: Annual cycle of rainfall over Dakar (1950-2010)

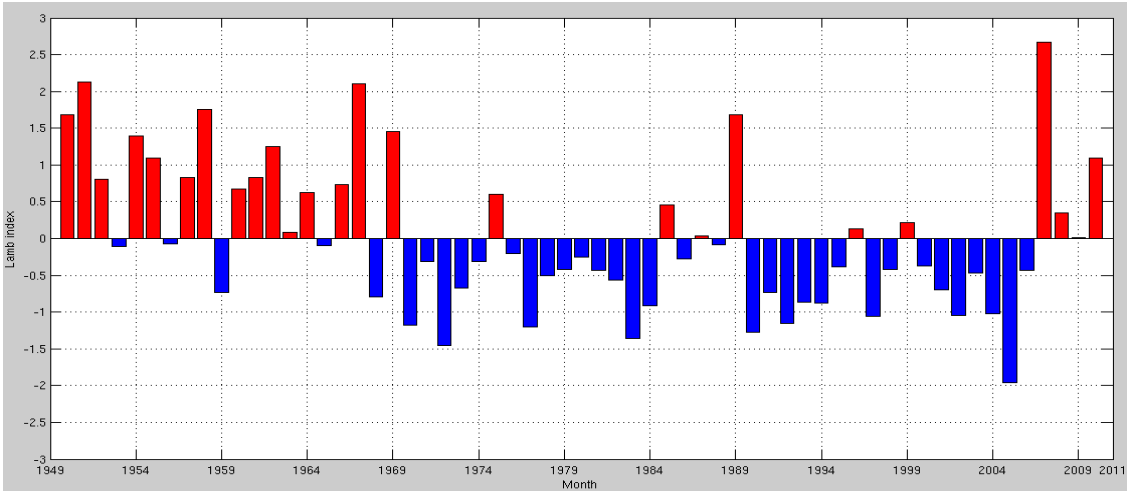

Fig. 9: Lamb index of rainfall in Dakar (1950-2010)

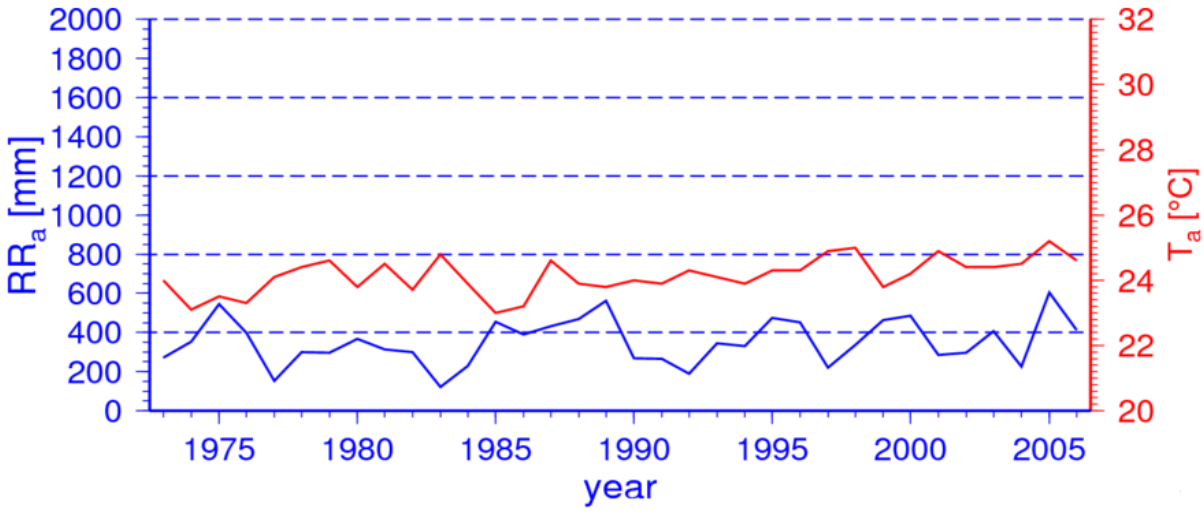

Fig. 10: Interannual variability of rainfall and temperatures observed in Dakar (1973-2006)

« Bassin Arachidier » : Example of Kaolack

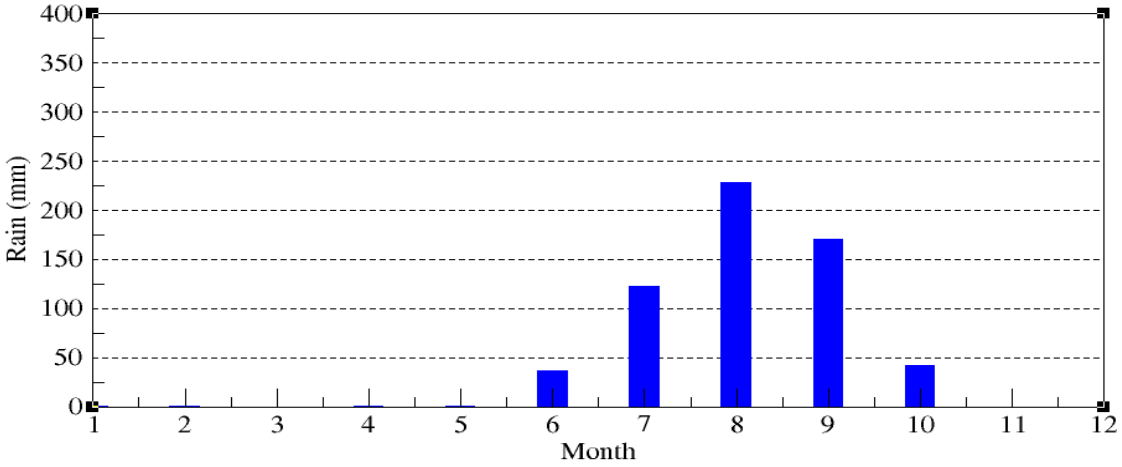

Fig. 11: Annual cycle of rainfall over Kaolack (1950-2010)

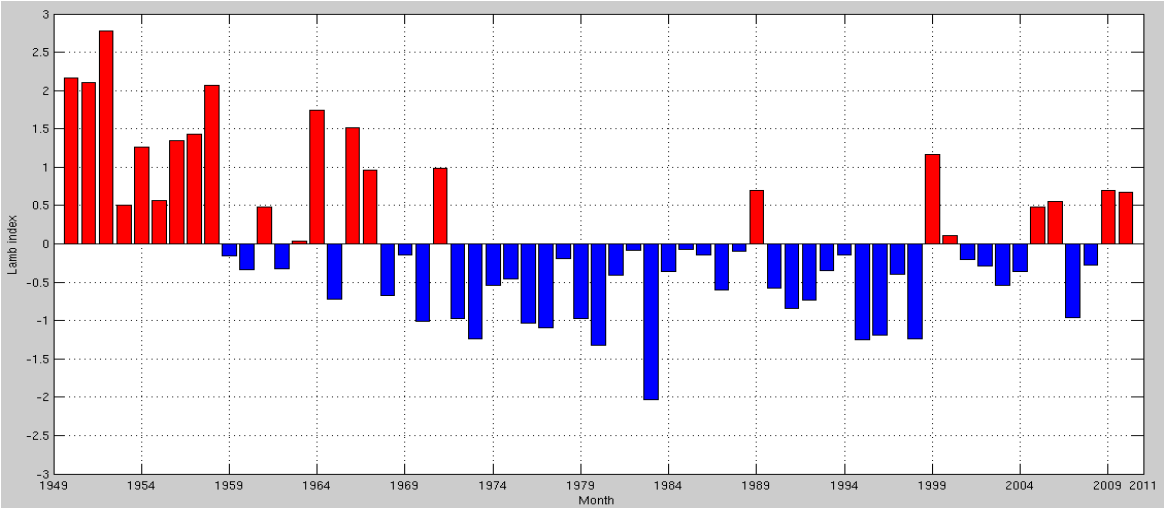

Fig. 12: Lamb index of rainfall in Kaolack (1950-2010)

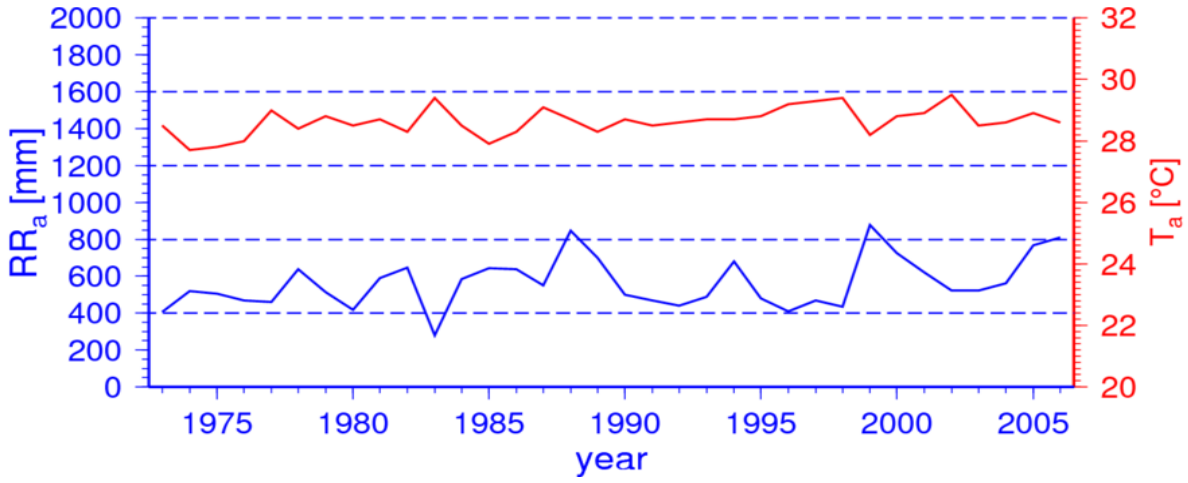

Fig. 13: Interannual variability of rainfall and temperatures observed in Kaolack (1973-2006)

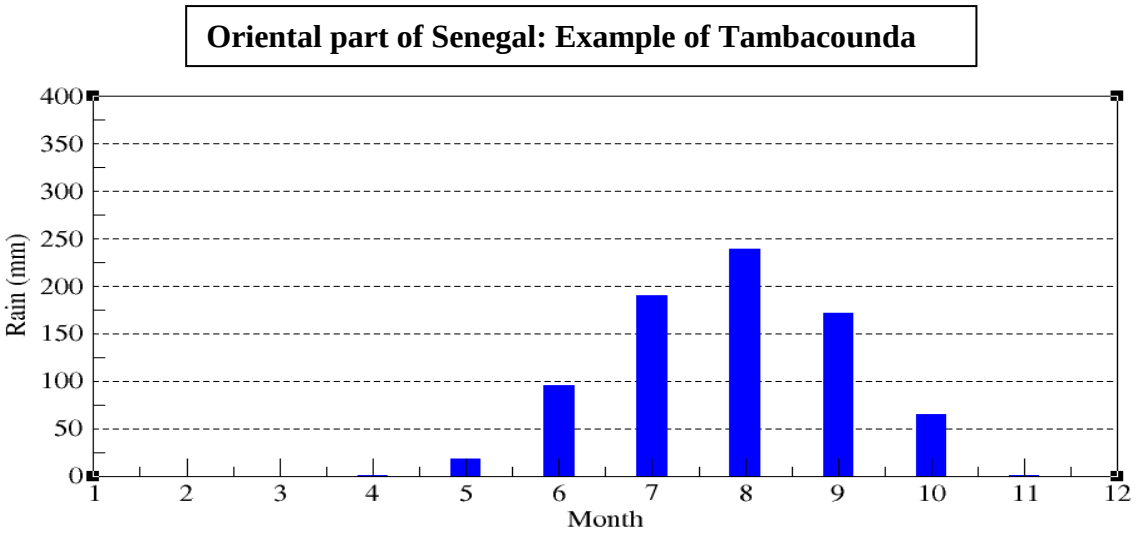

Fig. 14: Annual cycle of rainfall over Tambacounda (1950-2010)

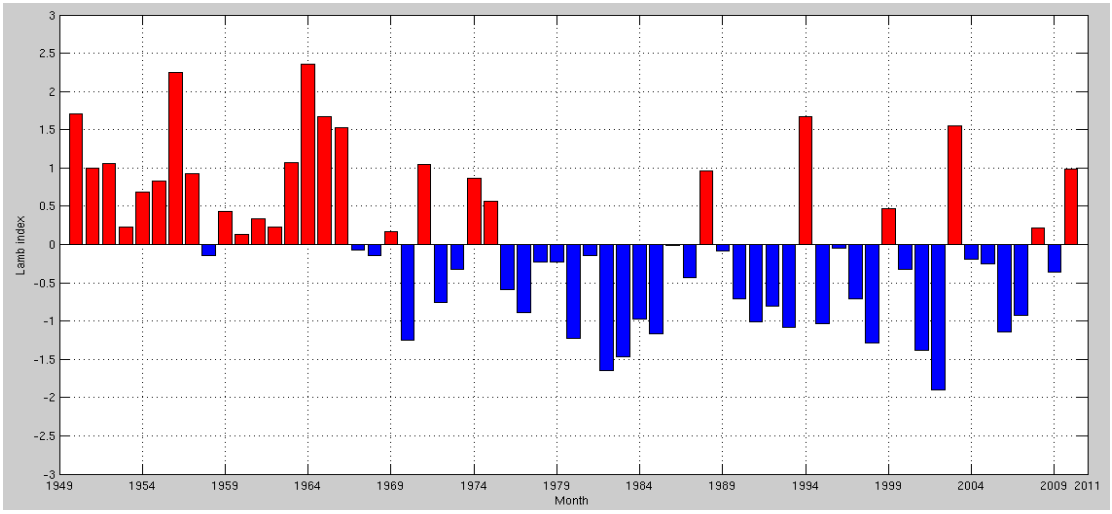

Fig. 15: Lamb index of rainfall in Tambacounda (1950-2010)

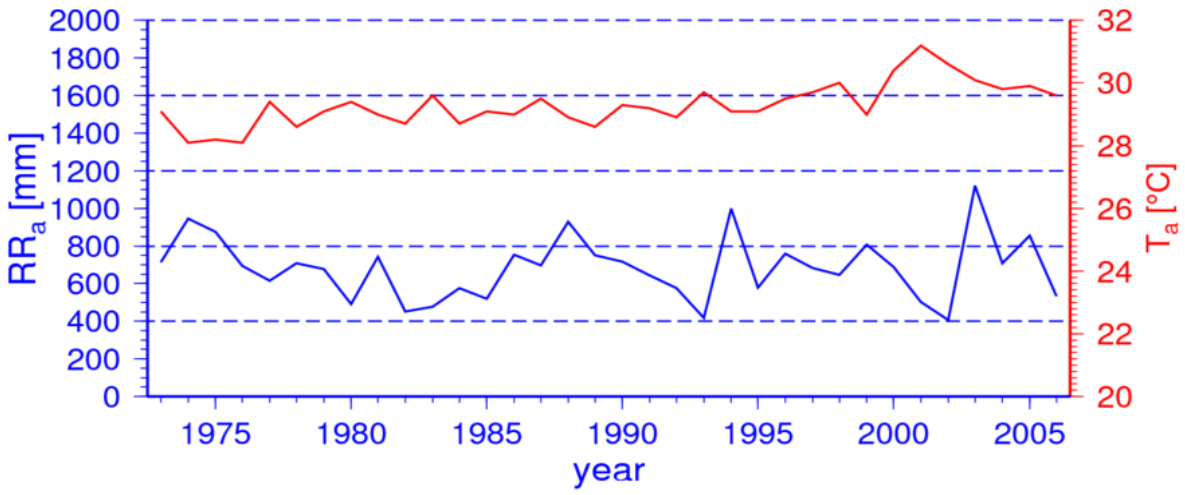

Fig. 16: Interannual variability of rainfall and temperatures observed in Tambacounda (1973-2006)

« Basse-Casamance »: Example of Ziguinchor

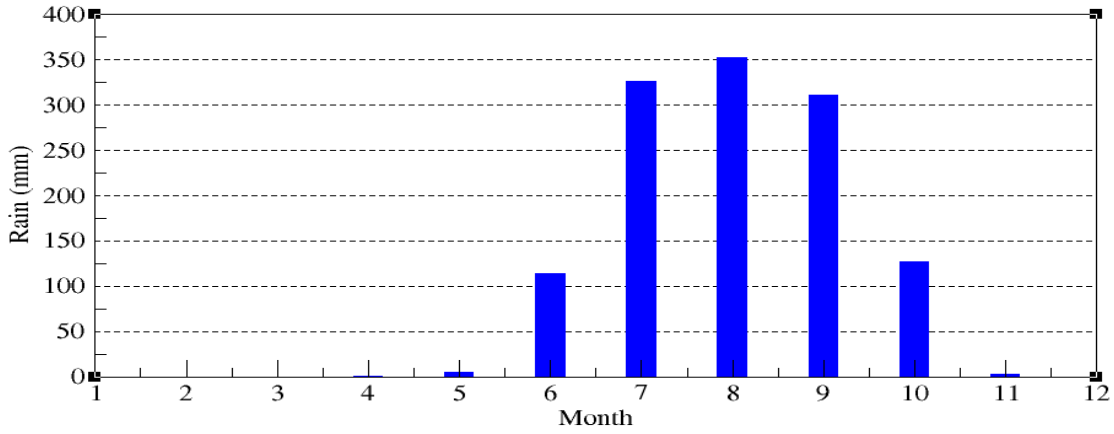

Fig. 17: Annual cycle of rainfall over Ziguinchor (1950-2010)

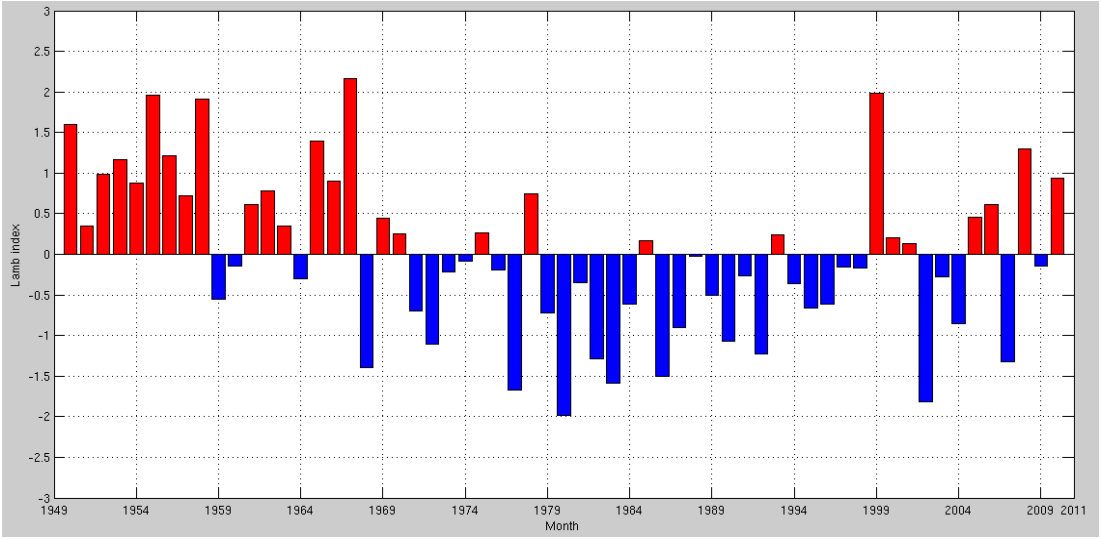

Fig. 18 : Lamb index of rainfall in Ziguinchor (1950-2010)

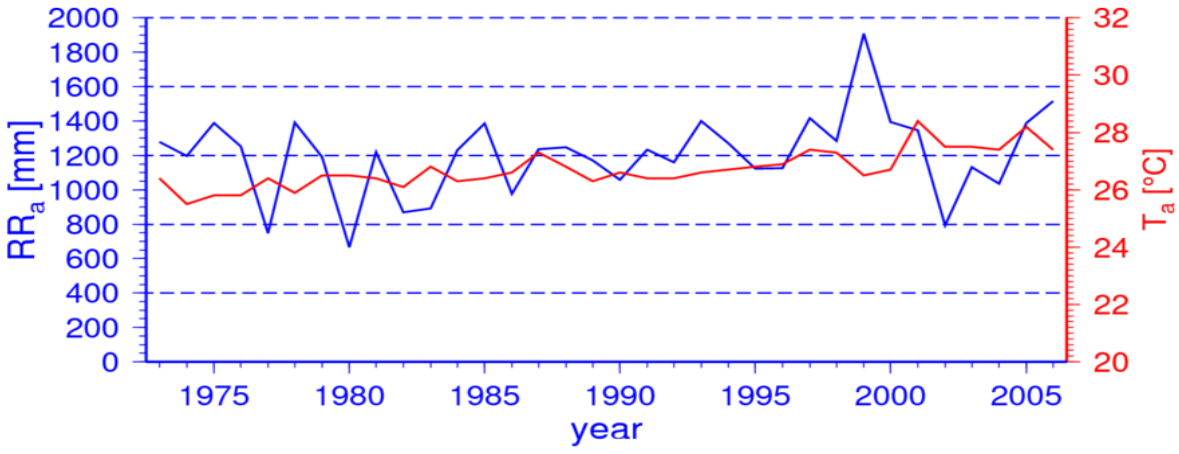

Fig 19: Interannual variability of rainfall and temperatures observed in Tambacounda (1973-2006)

« Vallée du Fleuve Senegal in the northern part »: Example of Saint-Louis

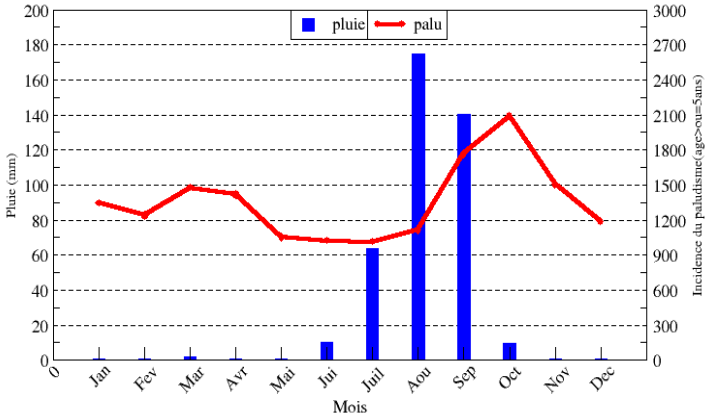

Fig. 20: Annual cycle of malaria outbreaks observed Saint-Louis (2000-2009)

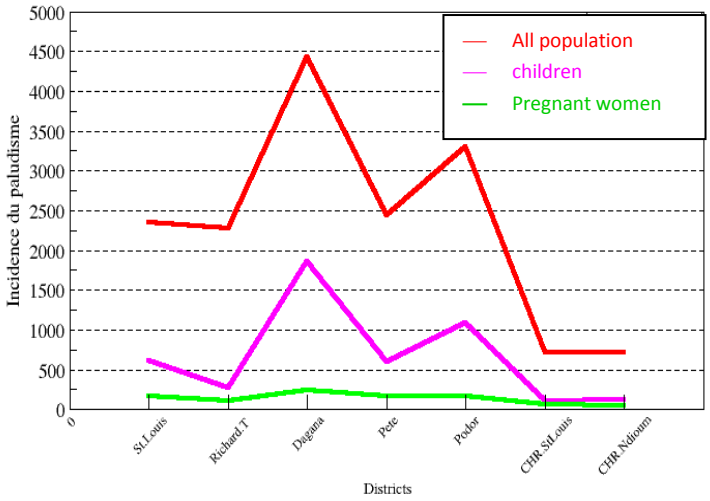

Fig. 21: Distribution of malaria incidence in different health districts of Saint-Louis area.

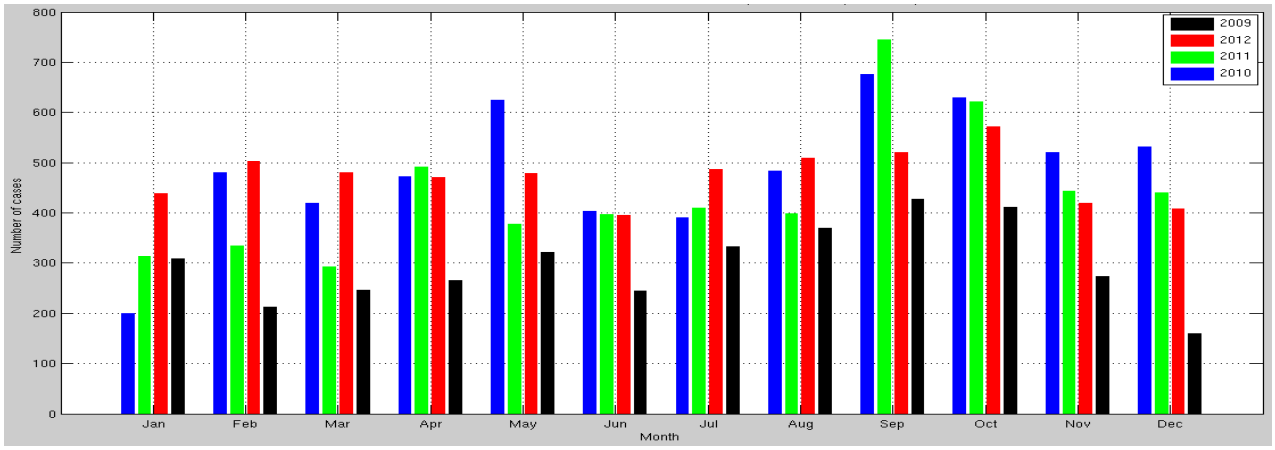

Fig. 22: Sentinel site of Podor, Saint-Louis: cases of malaria in Niandane post (2009-2012)

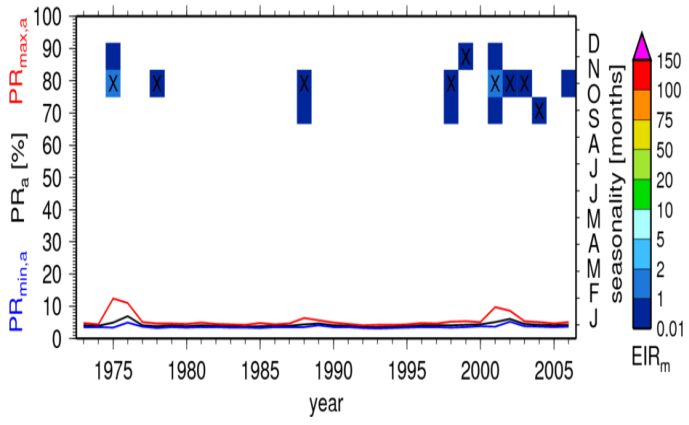

Fig. 23 : Saint-Louis: Interannual variability of the average rate of asexual parasites (PRa in% black curve, left axis) and the minimum rate (PRmin in% blue curve, left axis) and maximum (PRmax, in% red curve, left axis) of asexual parasites. Seasonal characteristics of malaria (right axis): Monthly entomological inoculation rate (color palette). The months of maximum transmission are marked with «X".

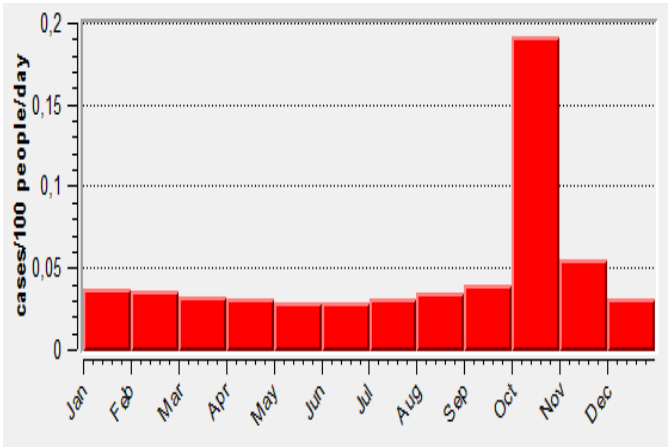

Fig. 24: Annual cycle of malaria incidence (for 100 people) simulated by the DMC for Saint-Louis station.

« The Ferlo area in the north-eastern part »: Example of Louga

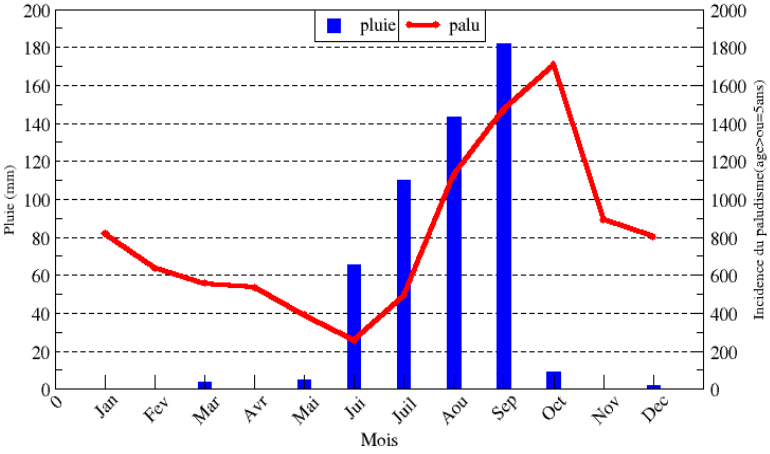

Fig. 25: Annual cycle of malaria outbreaks observed in Louga area (2000-2009).

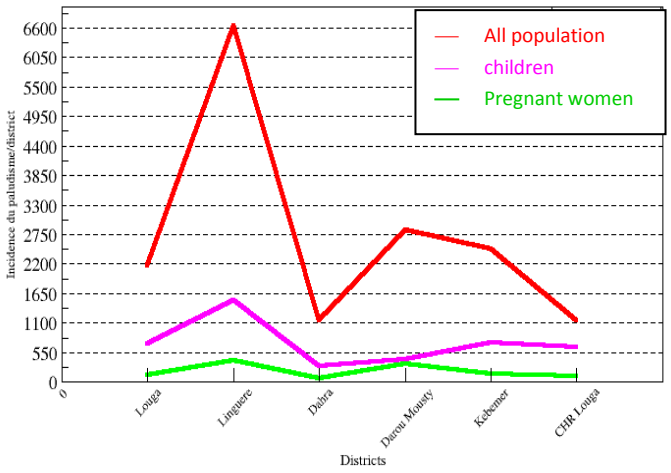

Fig. 26: Distribution of malaria incidence in different health districts of Louga area (2000-2009).

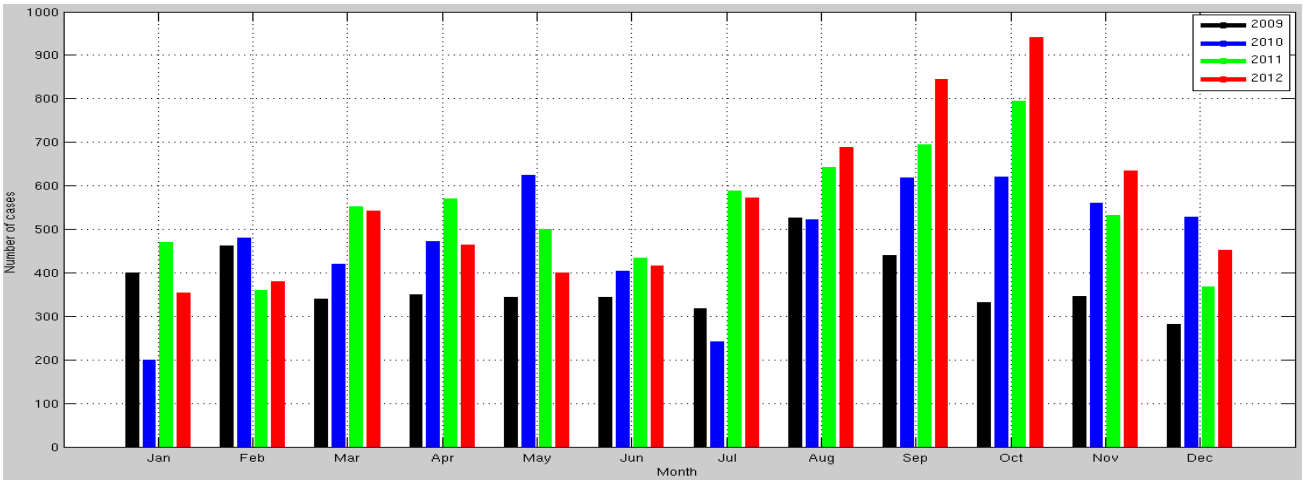

Fig. 27: Sentinel site of Linguere, Louga: cases of malaria in Barkedji post (2009-2012)

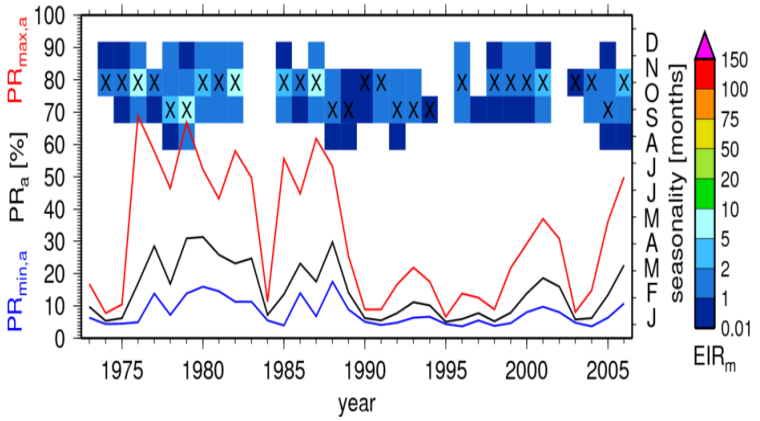

Fig. 28 : Louga: Interannual variability of the average rate of asexual parasites (PRa in% black curve, left axis) and the minimum rate (PRmin in% blue curve, left axis) and maximum (PRmax, in% red curve, left axis) of asexual parasites. Seasonal characteristics of malaria (right axis): Monthly entomological inoculation rate (color palette). The months of maximum transmission are marked with «X".

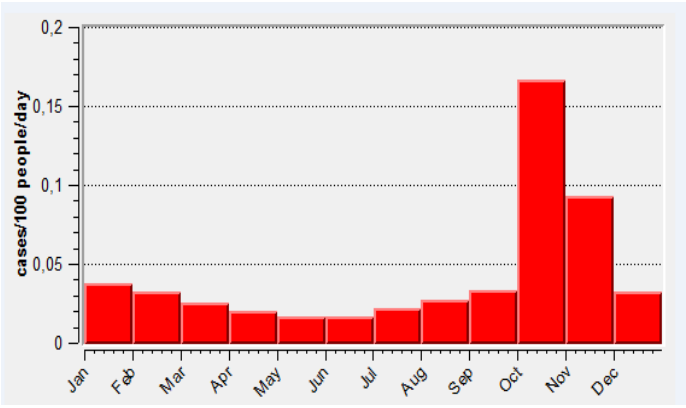

Fig. 29: Annual cycle of malaria incidence (for 100 people) simulated by the DMC for Louga station.

In the Coast part: Dakar zone

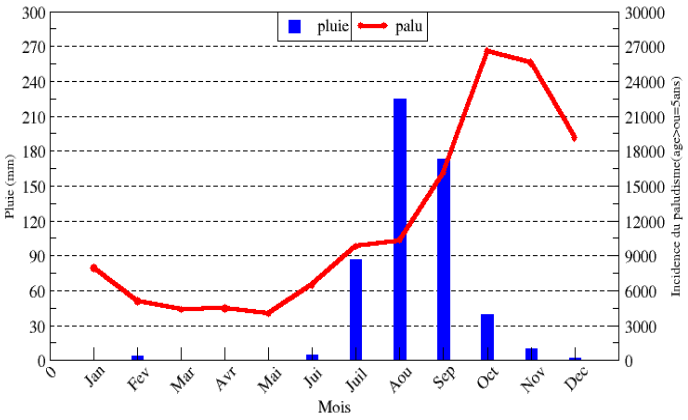

Fig. 30: Annual cycle of malaria outbreaks observed in Dakar area (20(2009).

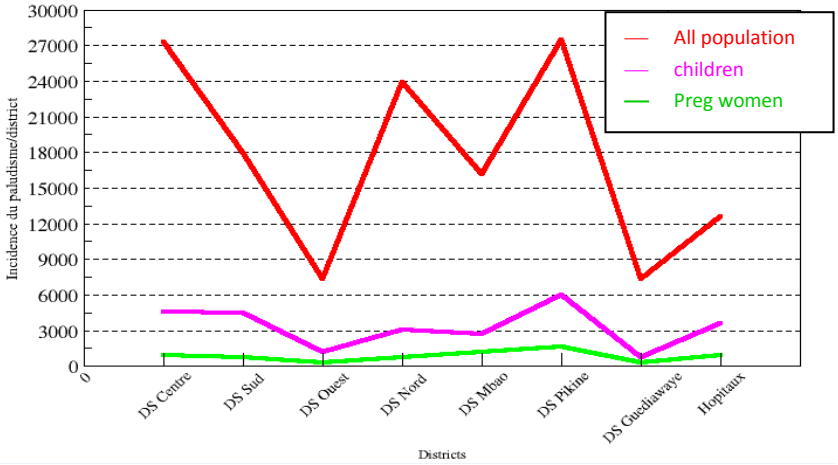

Fig. 31: Distribution of malaria incidence in different health districts of Dakar area (2000-2009).

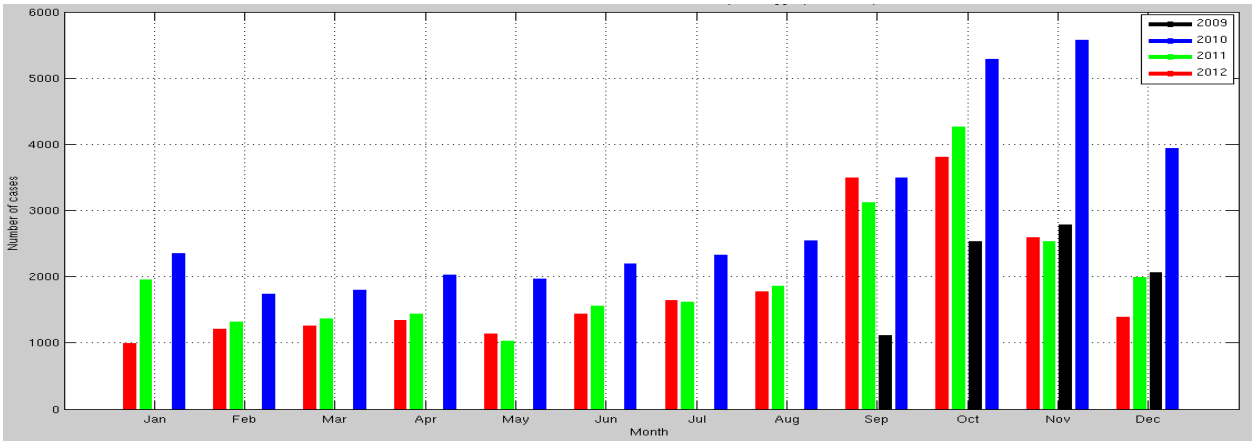

Fig. 32: Sentinel site of Pikine, Dakar: cases of malaria in Deggo post (2009-2012)

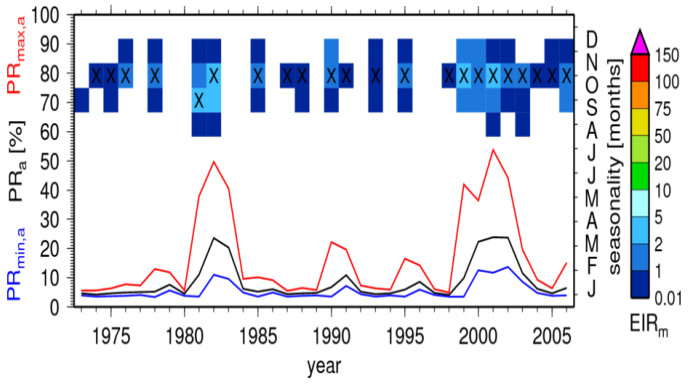

Fig. 33 : Dakar: Interannual variability of the average rate of asexual parasites (PRa in% black curve, left axis) and the minimum rate (PRmin in% blue curve, left axis) and maximum (PRmax, in% red curve, left axis) of asexual parasites. Seasonal characteristics of malaria (right axis): Monthly entomological inoculation rate (color palette). The months of maximum transmission are marked with «X".

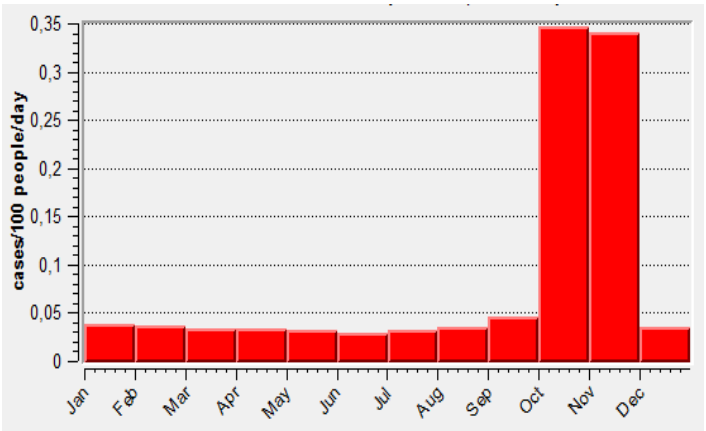

Fig. 34: Annual cycle of malaria incidence (for 100 people) simulated by the DMC for Dakar station.

« Bassin Arachidier » : Example of Kaolack

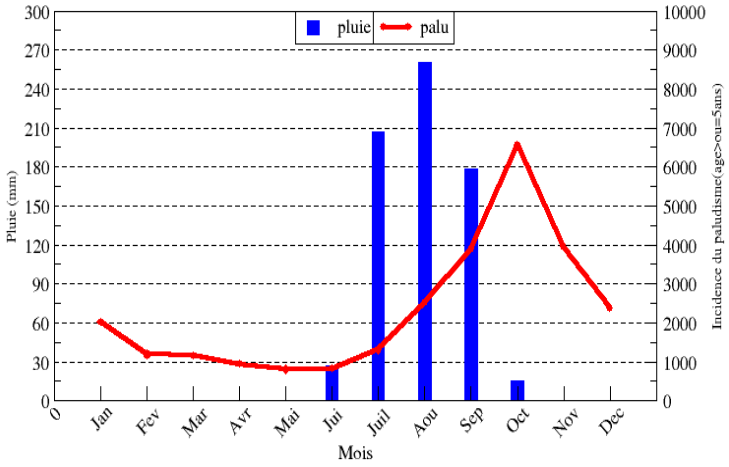

Fig. 35: Annual cycle of malaria outbreaks observed in Kaolack area (2000-2009).

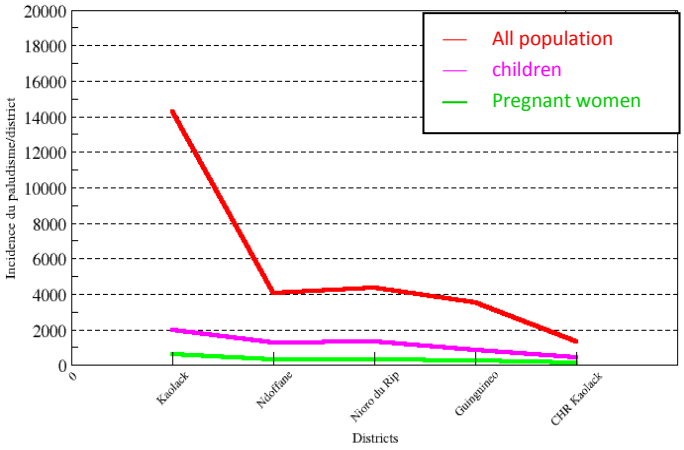

Fig. 36: Distribution of malaria incidence in different health districts of Kaolack (2000-2009).

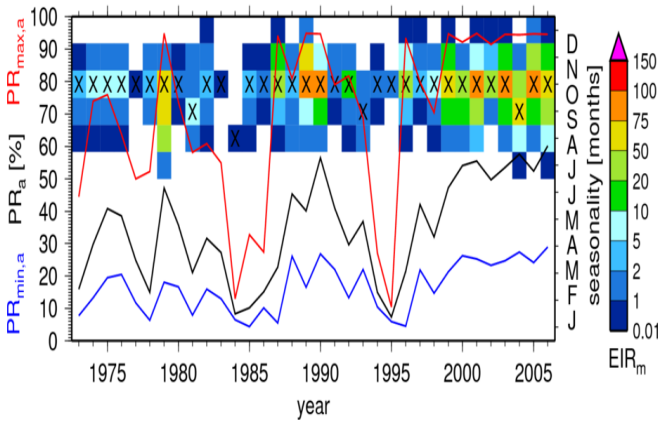

Fig. 37 : Kaolack : Interannual variability of the average rate of asexual parasites (PRa in% black curve, left axis) and the minimum rate (PRmin in% blue curve, left axis) and maximum (PRmax, in% red curve, left axis) of asexual parasites. Seasonal characteristics of malaria (right axis): Monthly entomological inoculation rate (color palette). The months of maximum transmission are marked with «X".

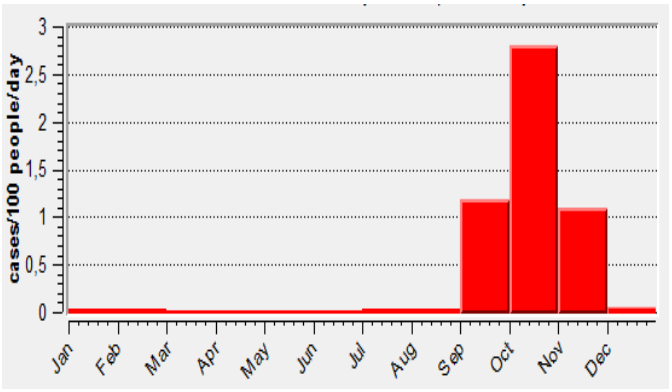

Fig. 38: Annual cycle of malaria incidence (for 100 people) simulated by the DMC for Kaolack station.

Oriental part of Senegal: Example of Tambacounda

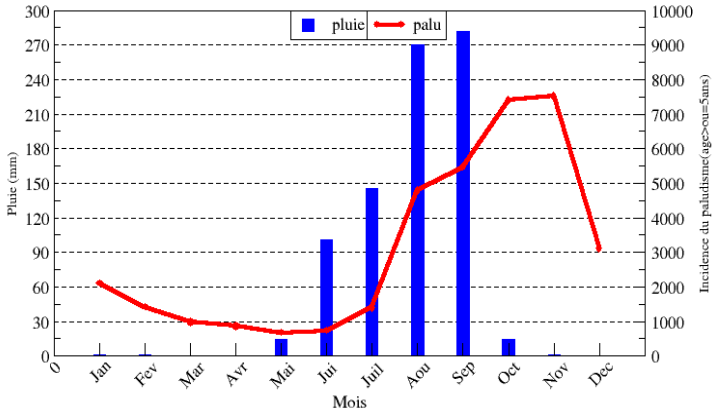

Fig. 39 : Annual cycle of malaria outbreaks observed in Tamba area (2000-2009).

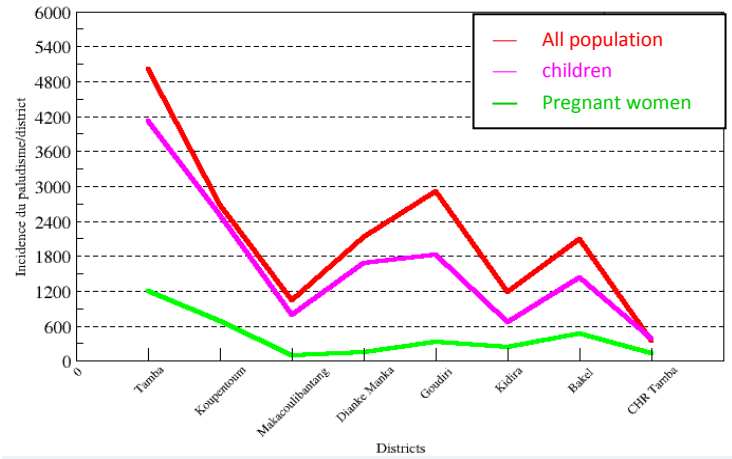

Fig. 40: Distribution of malaria incidence in different health districts of Tambacounda (2000-2009).

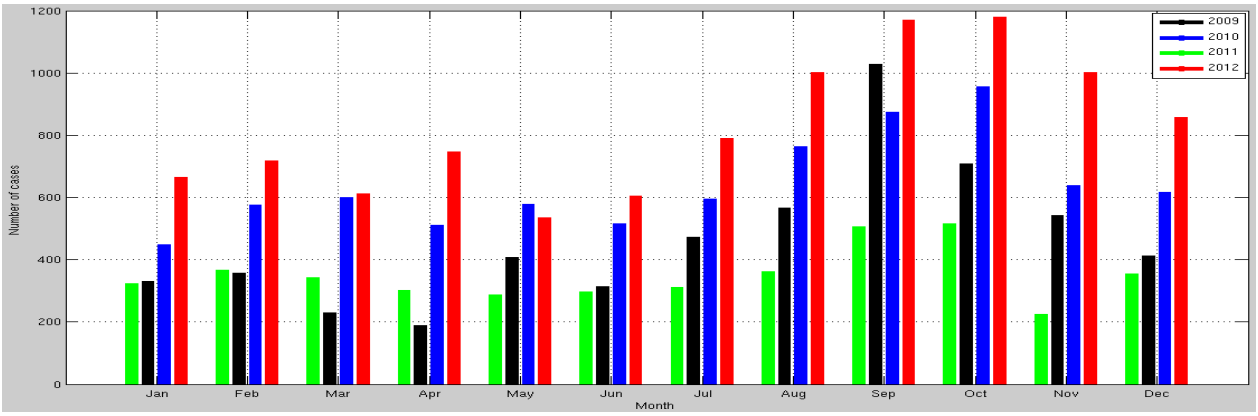

Fig. 41: Sentinel site of Bakel, Tambacounda: cases of malaria in Gabou post (2009-2012)

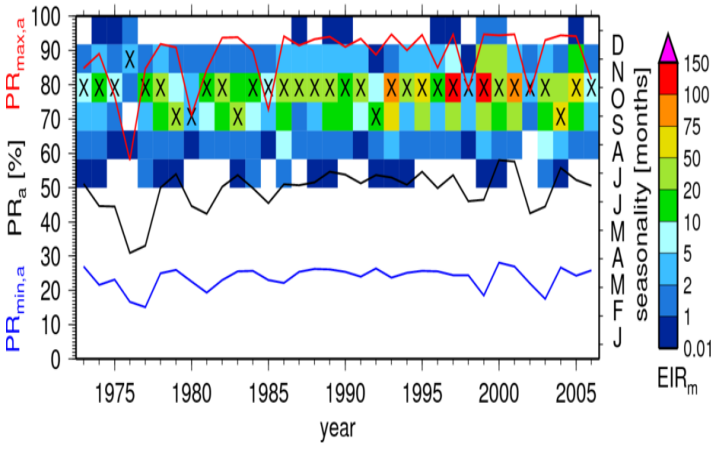

Fig. 42 : Tambacounda : Interannual variability of the average rate of asexual parasites (PRa in% black curve, left axis) and the minimum rate (PRmin in% blue curve, left axis) and maximum (PRmax, in% red curve, left axis) of asexual parasites. Seasonal characteristics of malaria (right axis): Monthly entomological inoculation rate (color palette). The months of maximum transmission are marked with «X".

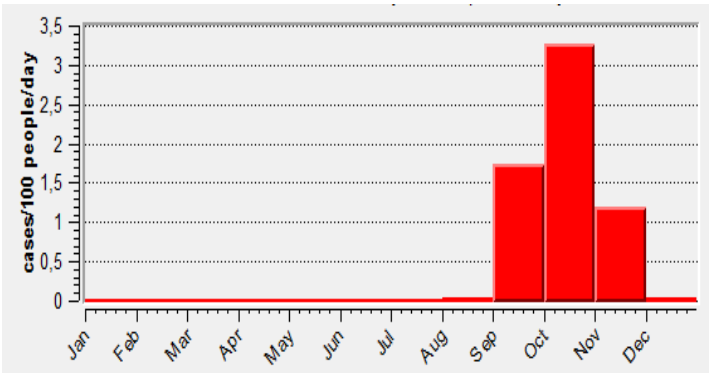

Fig. 43: Annual cycle of malaria incidence (for 100 people) simulated by the DMC for Tamba station (2000-2009).

« Basse-Casamance »: Example of Ziguinchor

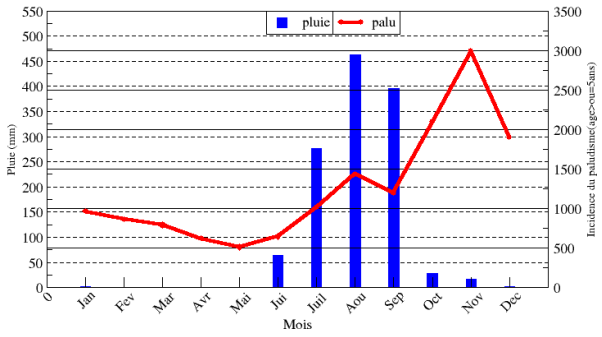

Fig. 44: Annual cycle of malaria outbreaks observed in Ziguichor area (2000-2009).

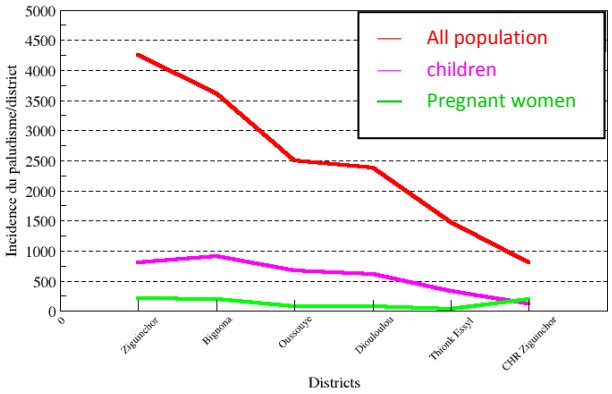

Fig. 45: Distribution of malaria incidence in different health districts of Ziguinchor (2000-2009).

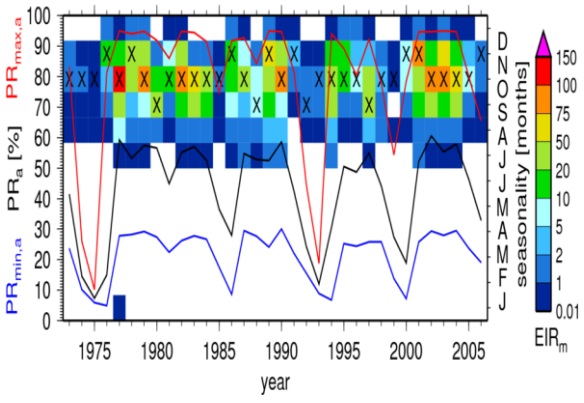

Fig. 46: Ziguinchor : Interannual variability of the average rate of asexual parasites (PRa in% black curve, left axis) and the minimum rate (PRmin in% blue curve, left axis) and maximum (PRmax, in% red curve, left axis) of asexual parasites. Seasonal characteristics of malaria (right axis): Monthly entomological inoculation rate (color palette). The months of maximum transmission are marked with «X".

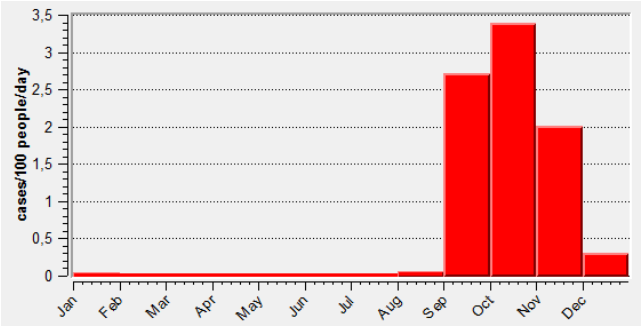

Fig. 47: Annual cycle of malaria incidence (for 100 people) simulated by the DMC for Ziguinchor station.

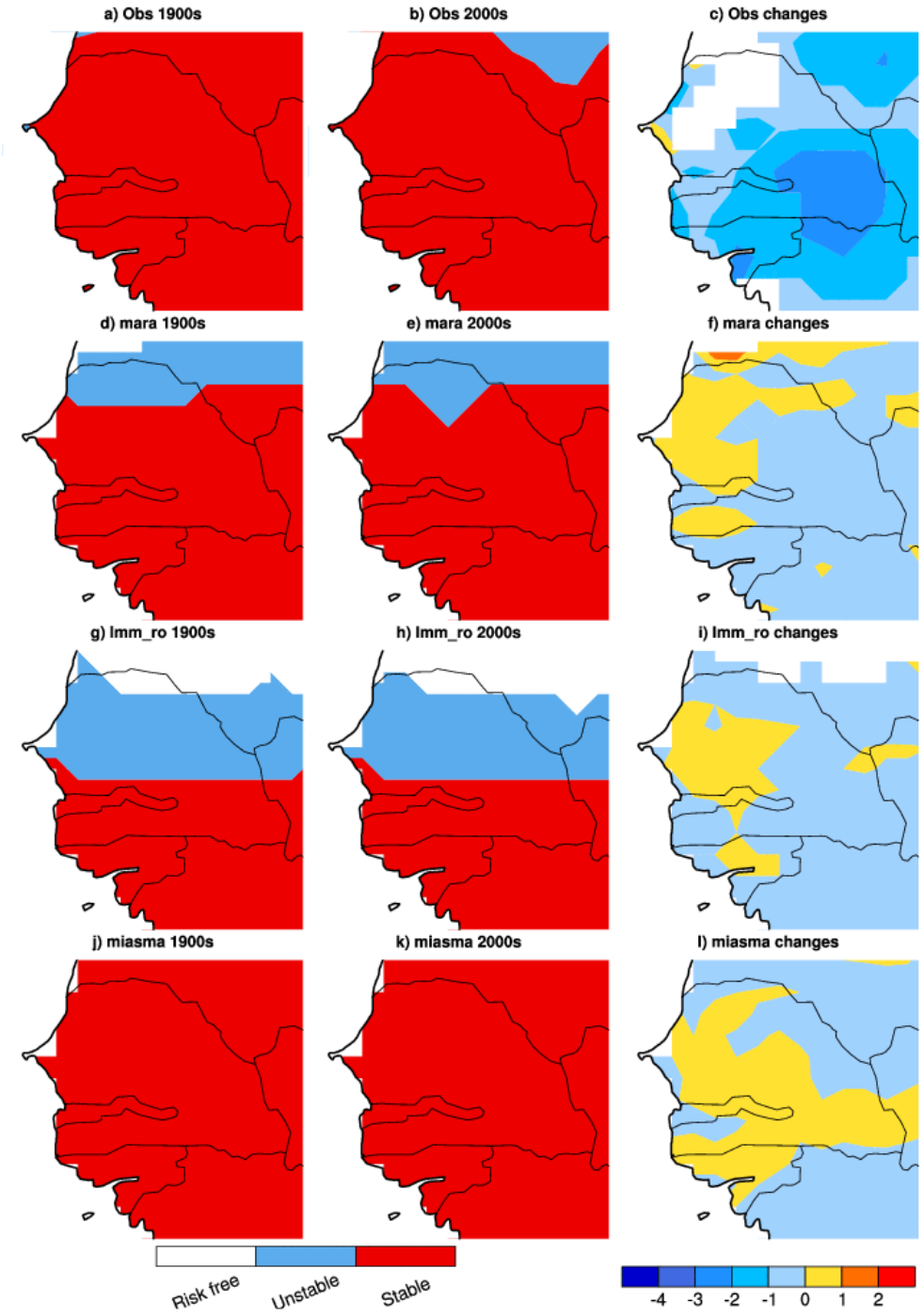

Fig. 48: Left: Observed and simulated malaria distribution (three categories, risk free in white, unstable/epidemic in blue, stable/endemic in red) for three malaria models. For the observation (a, b) all endemic sub-categories (hypoendemic, mesoendemic, hyperendemic and holoendemic) have been included in the stable category. The 1900s data (a) is based on the Lysenko et al., 1968 study, the 2000s (b) based on the Gething et al., 2010 paper. For the simulations unstable malaria is defined for a length of the transmission season (lts) ranging between 1 and 3 months, suitable is defined for lts above 3 months (this is carried out based on the CRUTS3.1 control runs for the period 1901-1910 and 2000-2009).
Right: Change in endemicity class between 1900s and 2000s for the observations (a). For the simulations (g,i,l) changes in the length of the malaria transmission season (in months).

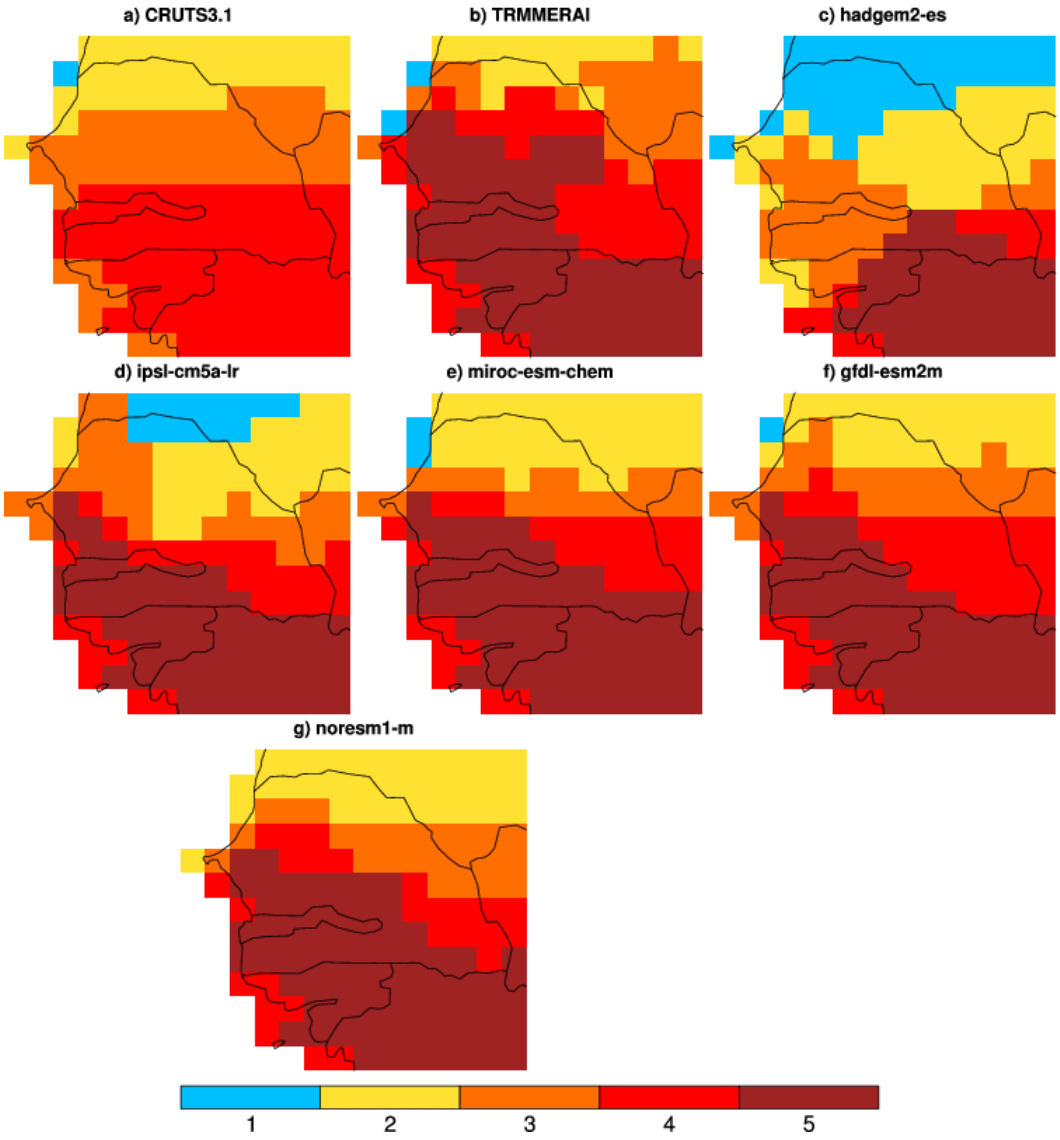

Fig. 49: Estimation of current malaria distribution and validation (Tier II validation) ISI-MIP – 5 malaria models.
The different colours show the number of malaria models which agree on the suitability of climate for malaria. This is carried out for two observation baseline (CRUTS3.1 over the period 1980-2009 & TRMMERAI over the period 1999-2010) and the historical experiments over the period 1980-2010 for the five different ISI-MIP GCMs. Note that for the CRUTS3.1 baseline, only four malaria models were used (lmm, miasma, mara & umu-who).

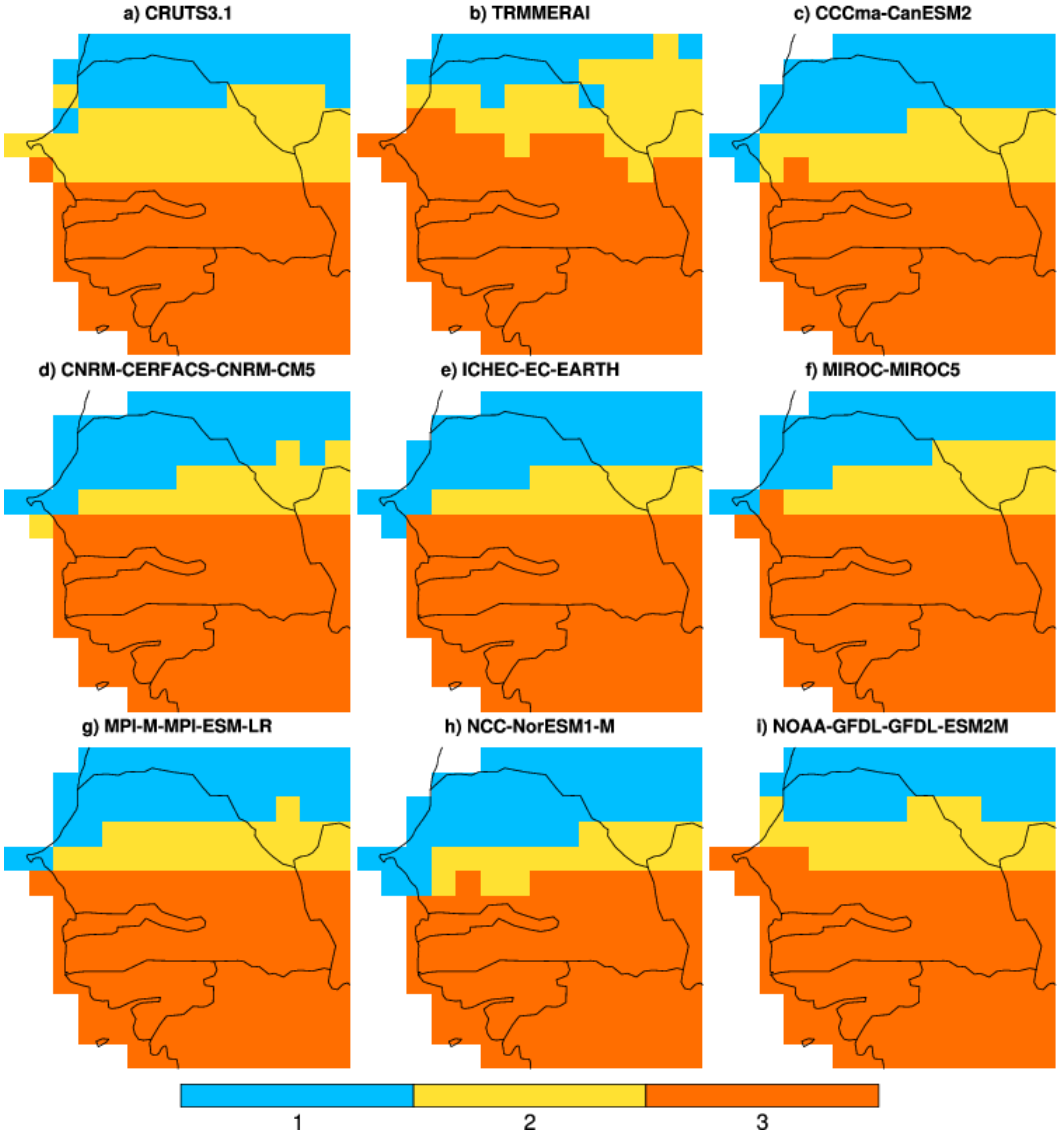

Fig. 50: Estimation of current malaria distribution and validation (Tier II validation) CORDEX – 3 malaria models. The different colours show the number of malaria models which agree on the suitability of climate for malaria. This is carried out for two observation baseline (CRUTS3.1 over the period 1980-2009 & TRMMERAI over the period 1999-2010) and the historical experiments over the period 1980-2010 for the seven different CORDEX RCMs.

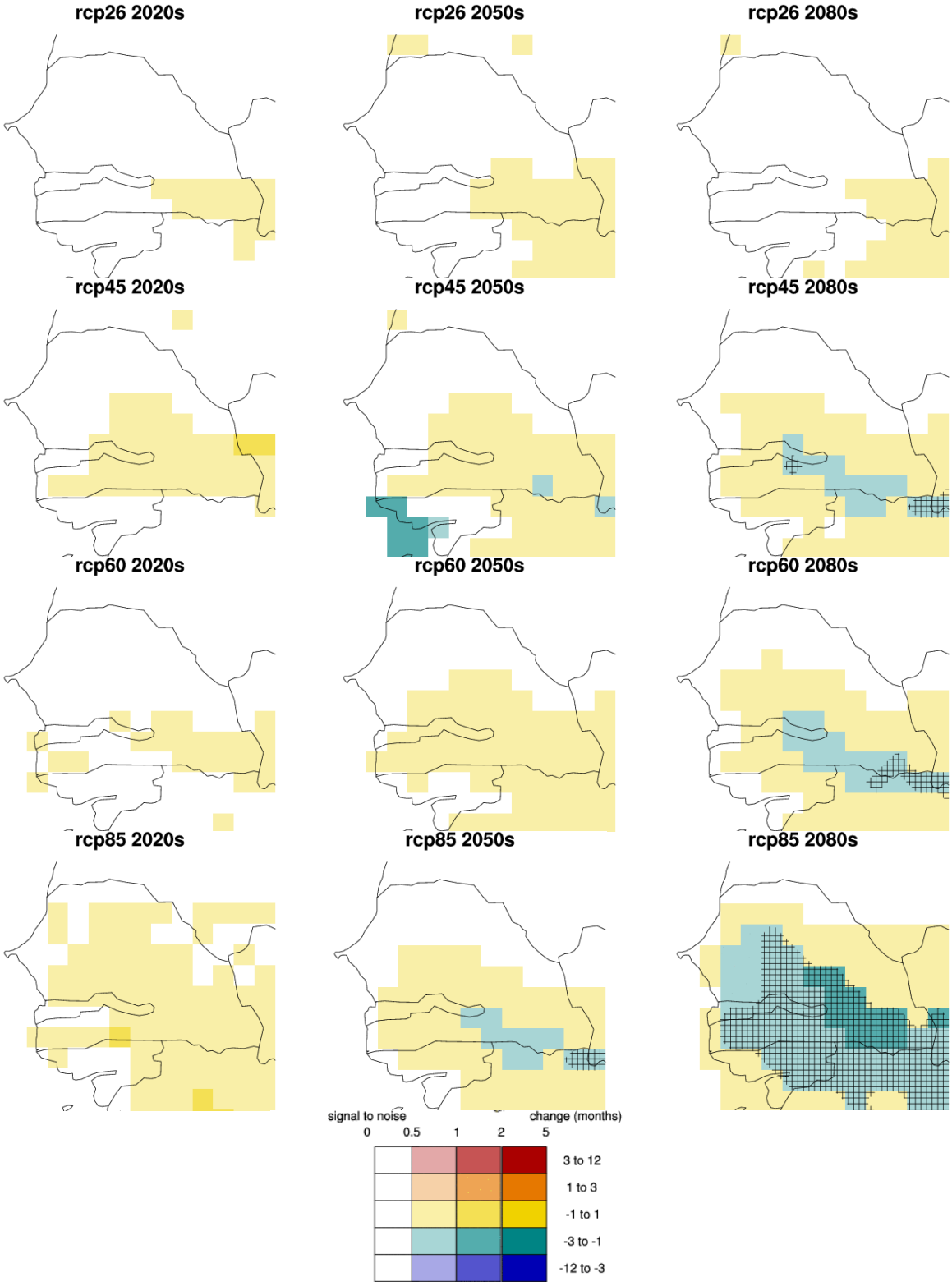

Fig.51: The effect of climate scenarios on future malaria distribution: changes in length of the malaria season (ISI-MIP ensemble). Each map shows the results for a different emission scenario (RCP). The different hues represent change in the length of the transmission season for the mean of CMIP5 sub-ensemble (with respect to the 1980-2010 historical mean. The different saturations represent signal-to-noise (μ/Sigma) across the super ensemble (the noise is defined as one standard deviation within the multi-GCM and multi-malaria ensemble). The stippled area shows the multi-malaria multi GCM agreement (60% of the models agree on the sign of changes if the simulated absolute changes are above one month of malaria transmission).

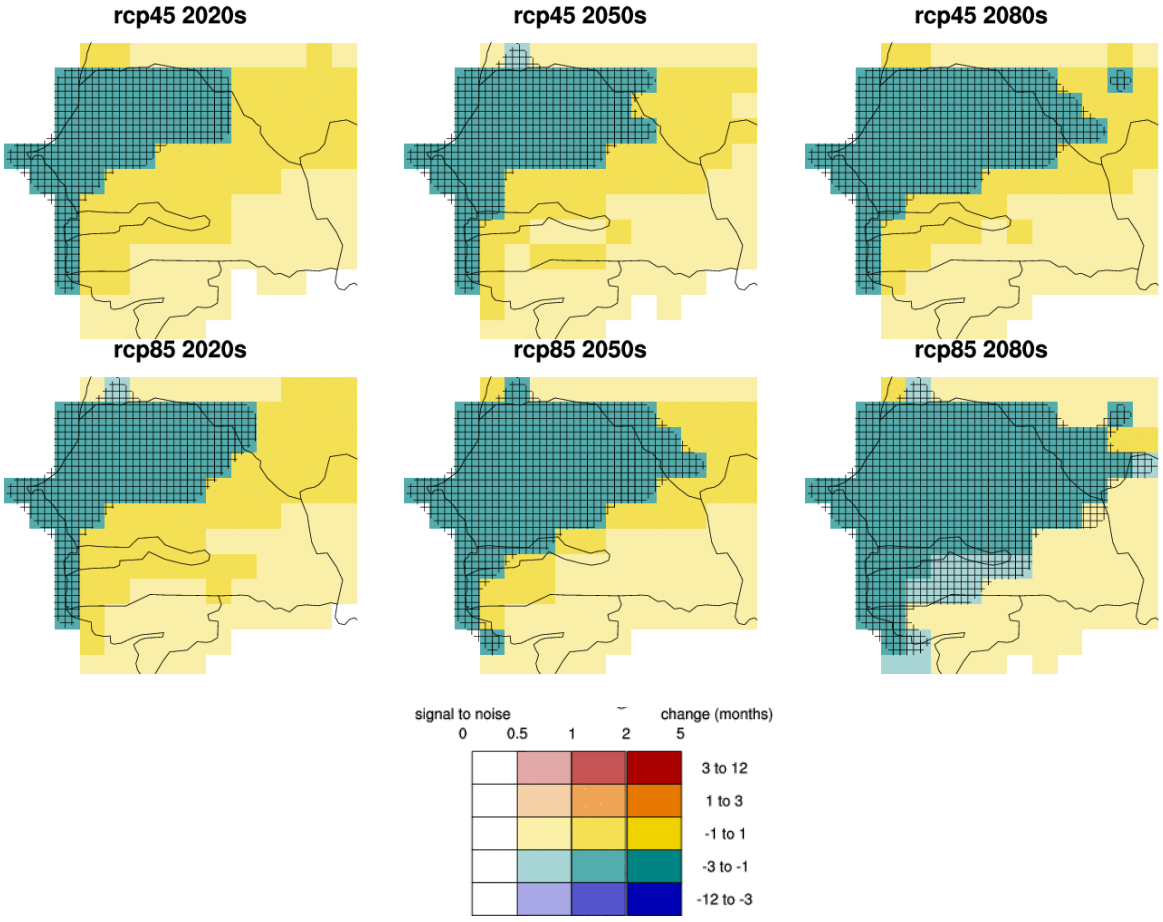

Fig. 52: The effect of climate scenarios on future malaria distribution: changes in length of the malaria season (CORDEX ensemble). Each map shows the results for a different emission scenario (RCP). The different hues represent change in the length of the transmission season for the mean of CMIP5 sub-ensemble (with respect to the 1980-2010 historical mean. The different saturations represent signal-to-noise (μ/Sigma) across the super ensemble (the noise is defined as one standard deviation within the multi-GCM and multi-malaria ensemble). The stippled area shws the multi-malaria multi GCM agreement (60% of the models agree n the sign of changes i the simulated absolute changes are above one month of malaria transmission).

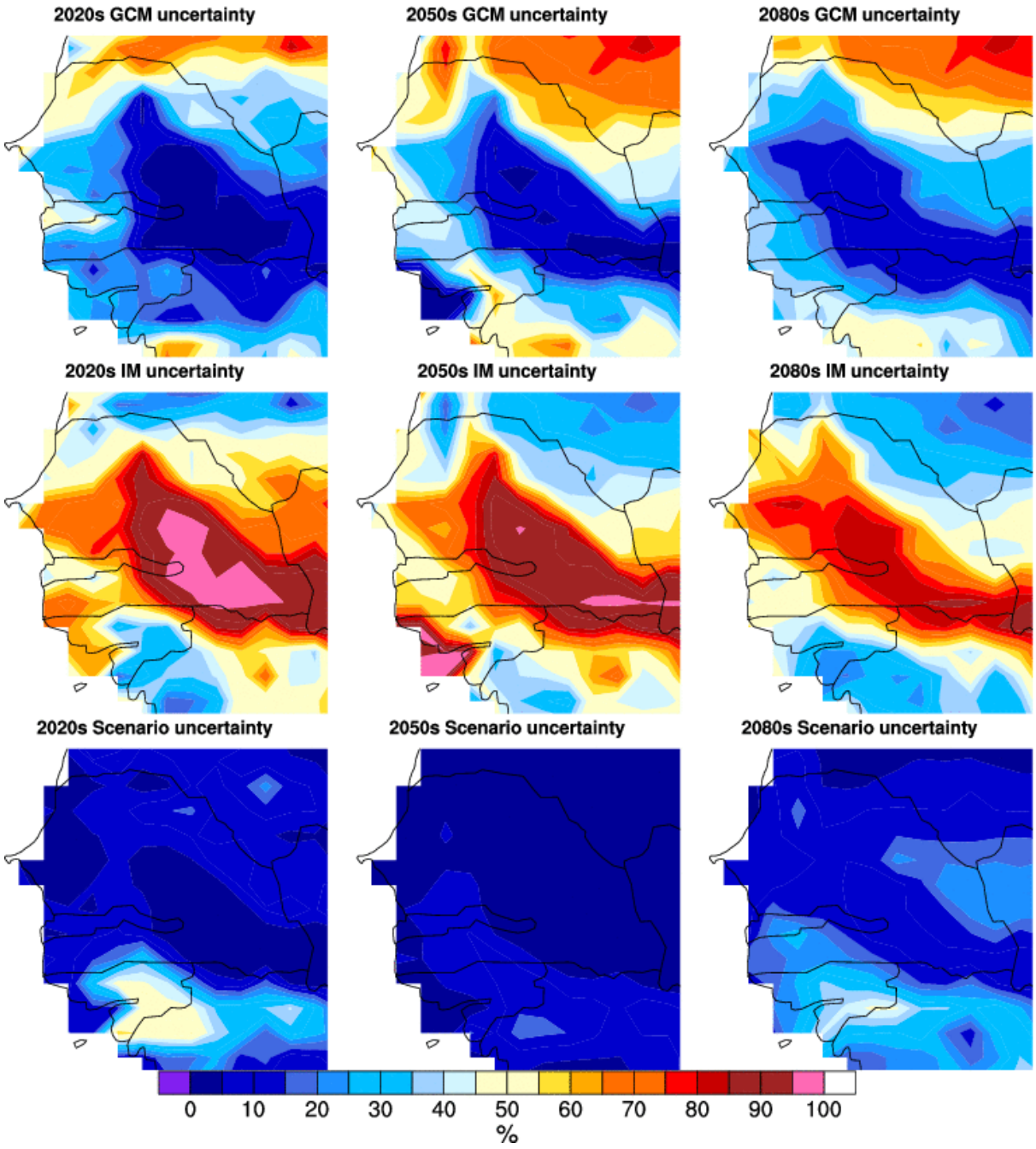

Fig. 53: Assessment of relative contribution of malaria model (IM), climate model (GCM), and emissions scenario (RCP) to final estimates of future malaria distribution under climate change. This is carried out for the ISI-MIP super ensemble.

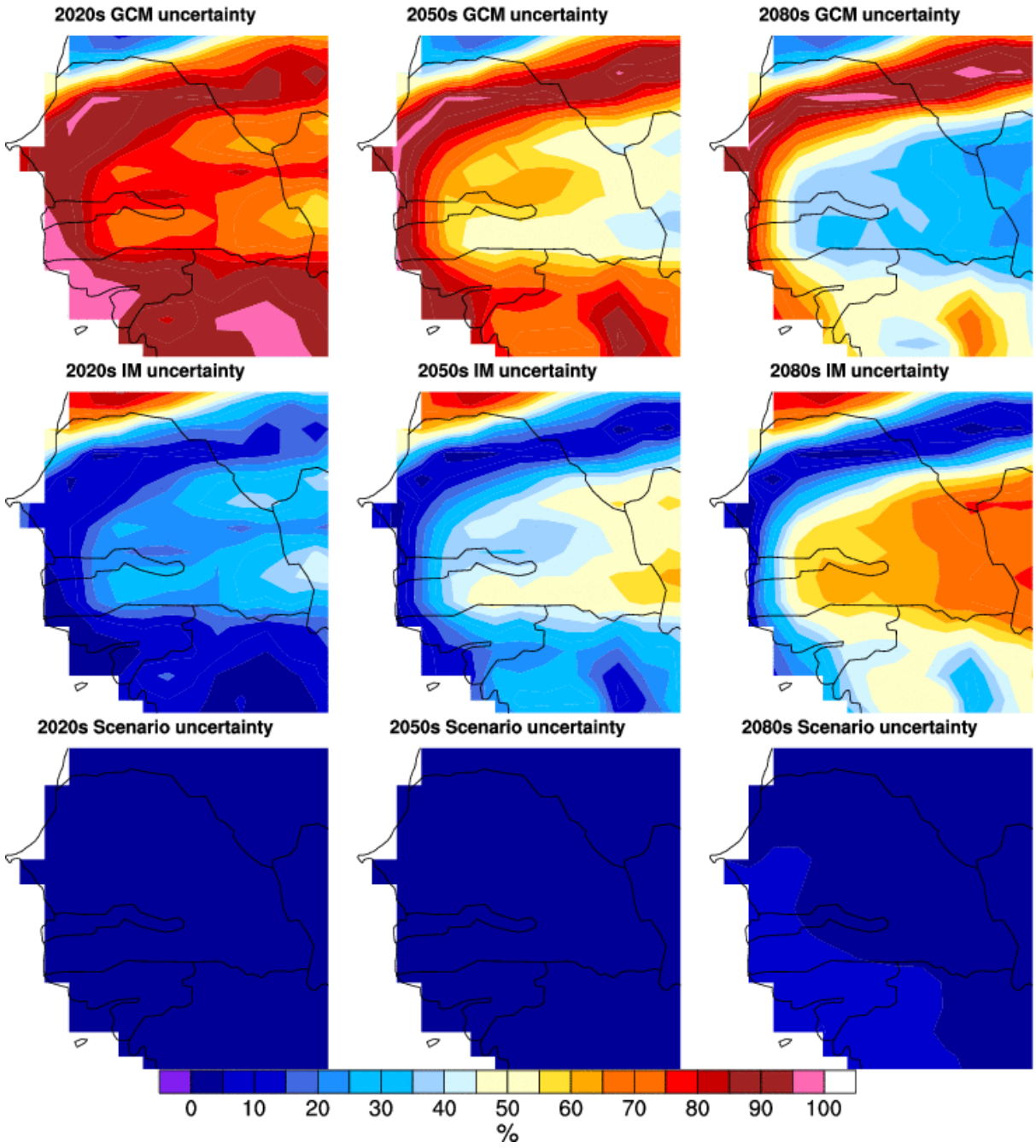

Fig. 54: Assessment of relative contribution of malaria model (IM), climate model (RCM), and emissions scenario (RCP) to final estimates of future malaria distribution under climate change. This is carried out for the CORDEX super ensemble.

a) ISI-MIP

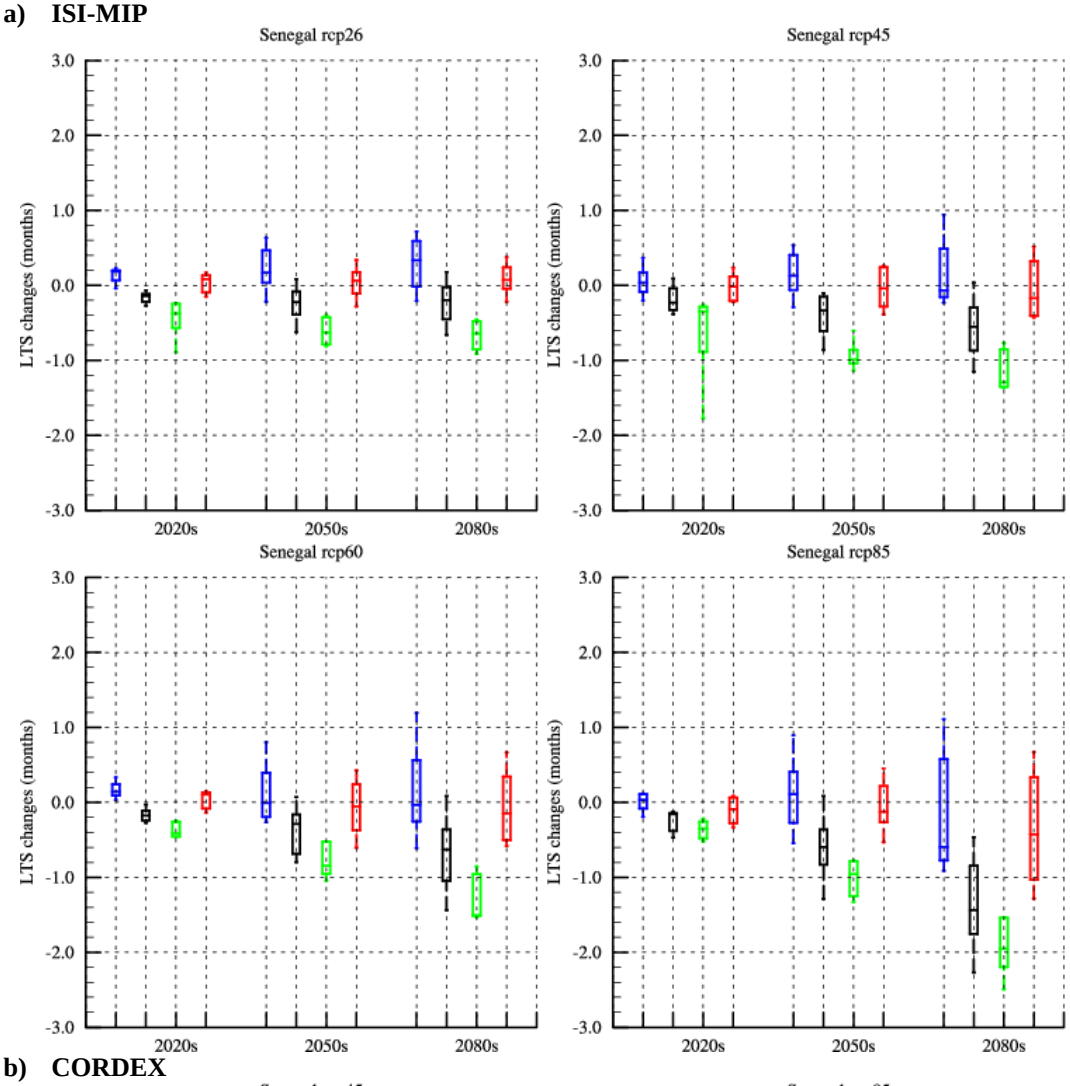

b) CORDEX

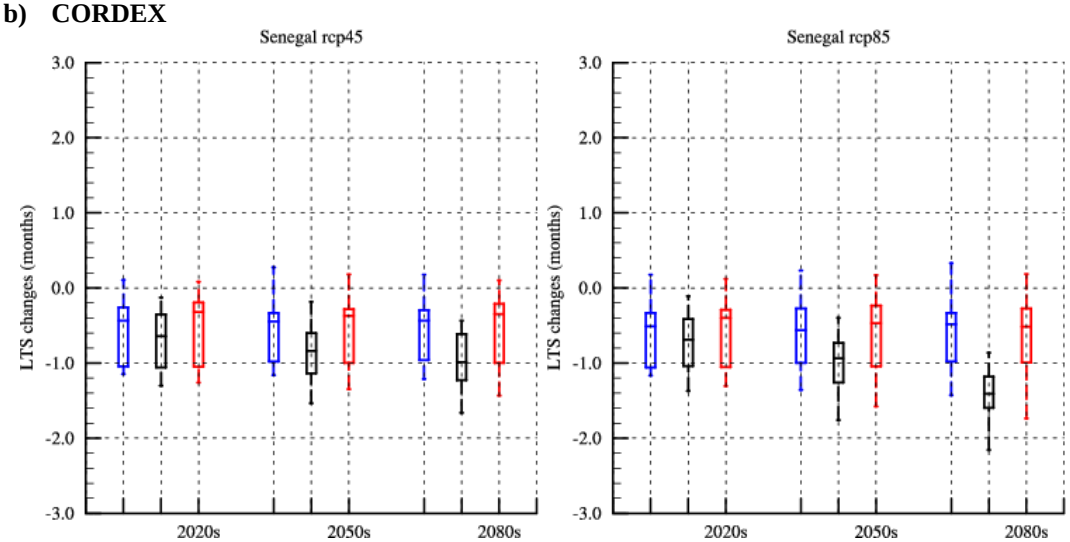

MARA, LMM_ro, Vectri & MIASMA

Fig. 55: Sensitivity of the simulated changes in the length of the malaria season to climate change for a) the ISI-MIP and b) the CORDEX ensemble over Senegal (10.5N-17N / 18W-11W). The boxplots depicts the minimum, 25th percentile, median, 75th percentile and the maximum across the driving climate models distribution. Blue: MARA, black: LMM_ro, green: Vectri, red: MIASMA

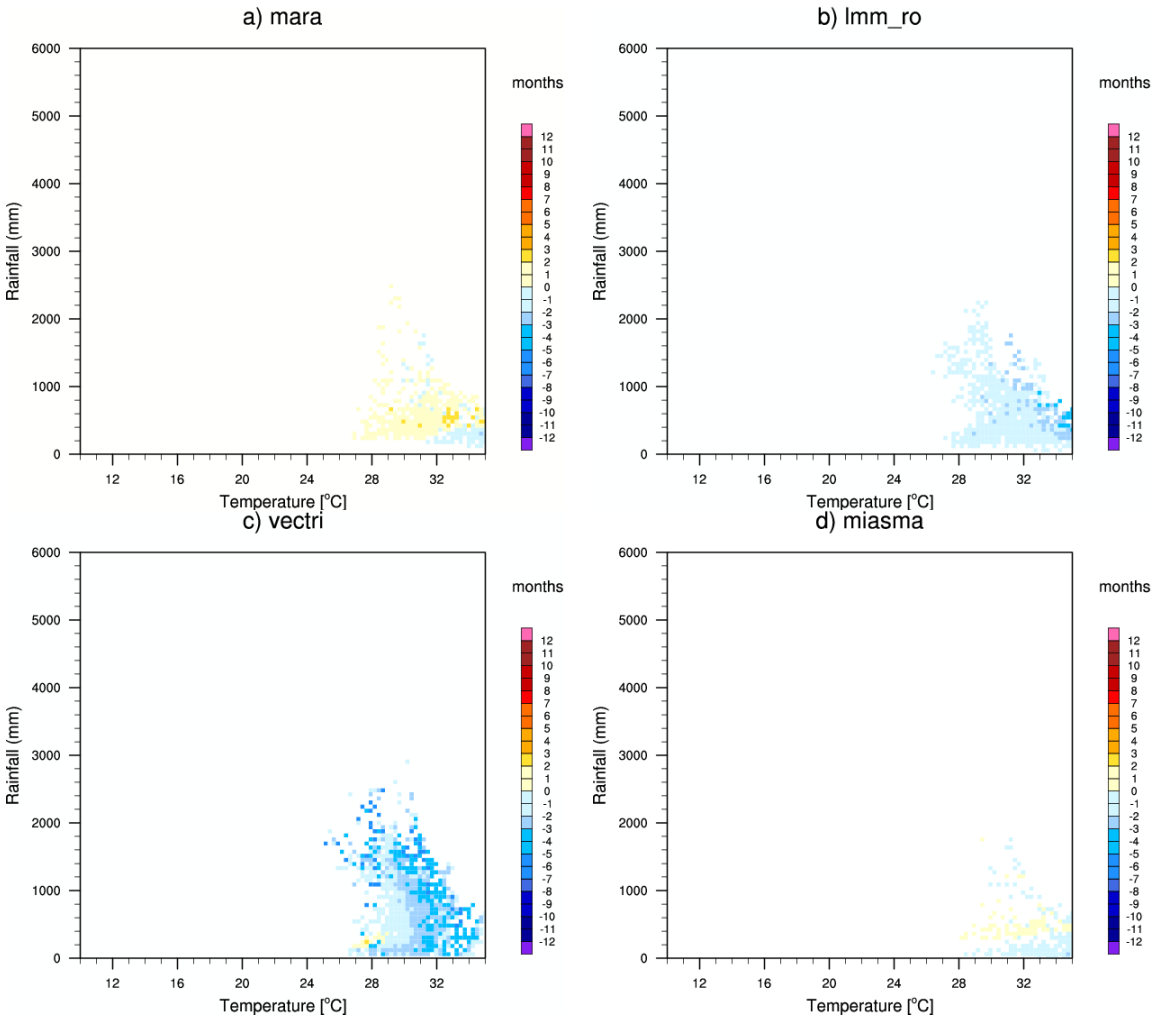

Fig. 56: Sensitivity of the simulated changes in the length of the malaria season to mean annual rainfall and temperature for the ISI-MIP ensemble over Senegal. Mean changes in the length of the transmission season are calculated for all emission scenarios, GCMs and time slices. If the simulated absolute changes are above one month, then they are plotted versus mean future annual rainfall (mm – Y axis) and temperature (°C – X axis). Results are similar for the CORDEX ensemble (not shown).

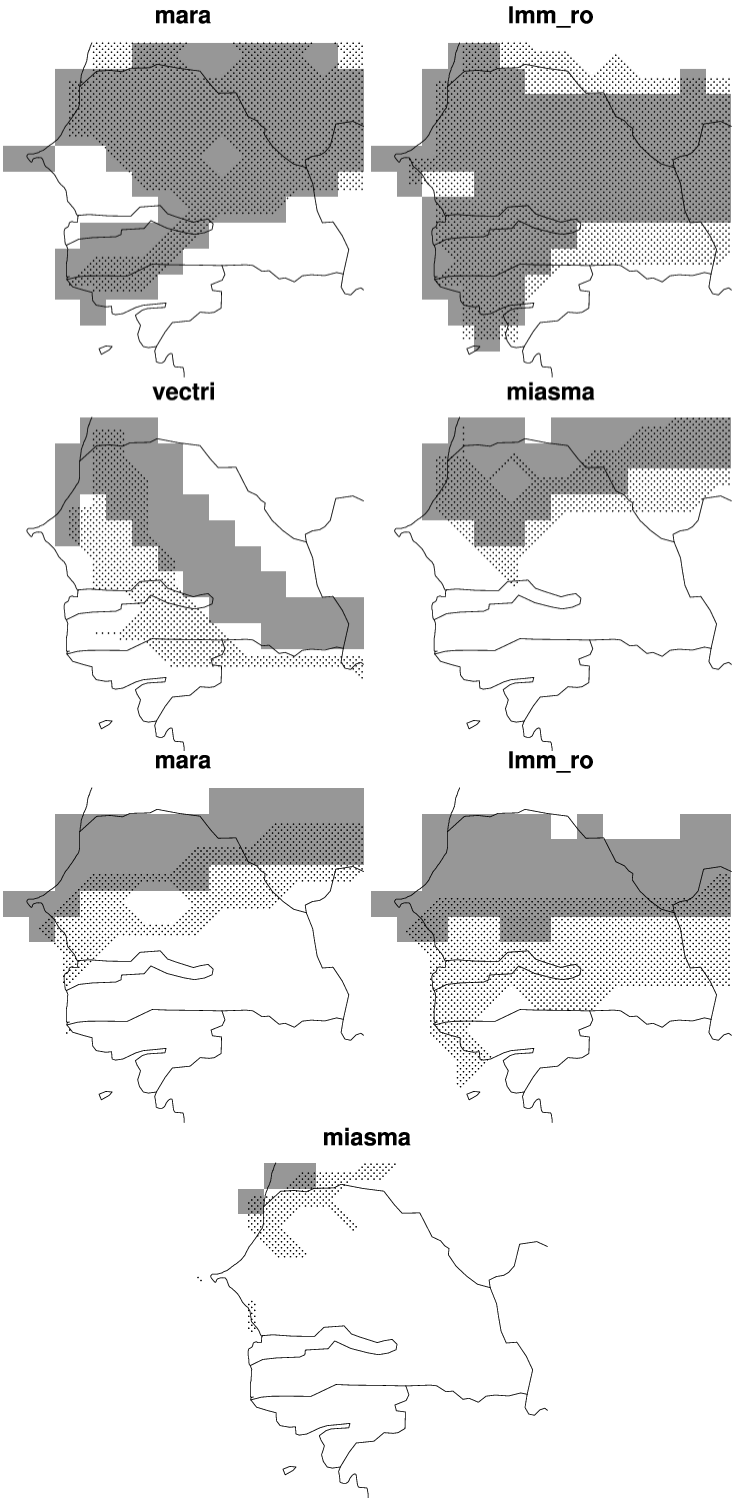

Fig. 57: Sensitivity of the simulated malaria epidemic belt to climate change for a) the ISI-MIP and b) the CORDEX ensemble. The gray shading depicts the location of the epidemic belt (for a short malaria transmission season e.g. 1 month<=LTS<3 months) based on the multi-model ensemble mean for the historical experiments (1980-2010 average). The dotted area depicts the epidemic fringe location based on the rcp4.5 emission scenario for the 2080s.

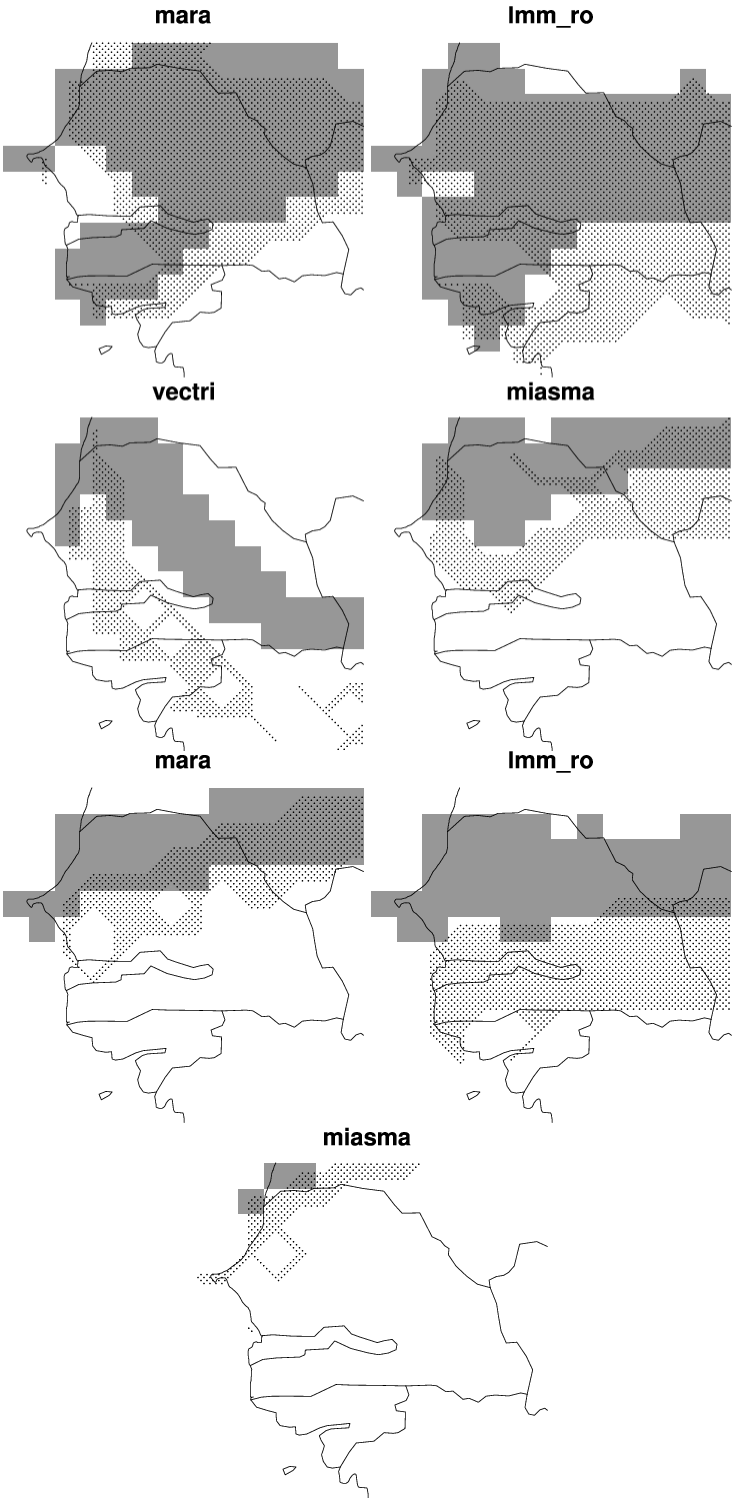

Fig. 58: Sensitivity of the simulated malaria epidemic belt to climate change for a) the ISI-MIP and b) the CORDEX ensemble. The gray shading depicts the location of the epidemic belt (for a short malaria transmission season e.g. 1 month<=LTS<3 months) based on the multi-model ensemble mean for the historical experiments (1980-2010 average). The dotted area depicts the epidemic fringe location based on the rcp8.5 emission scenario for the 2080s.

a) ISI-MIP (noresm1)

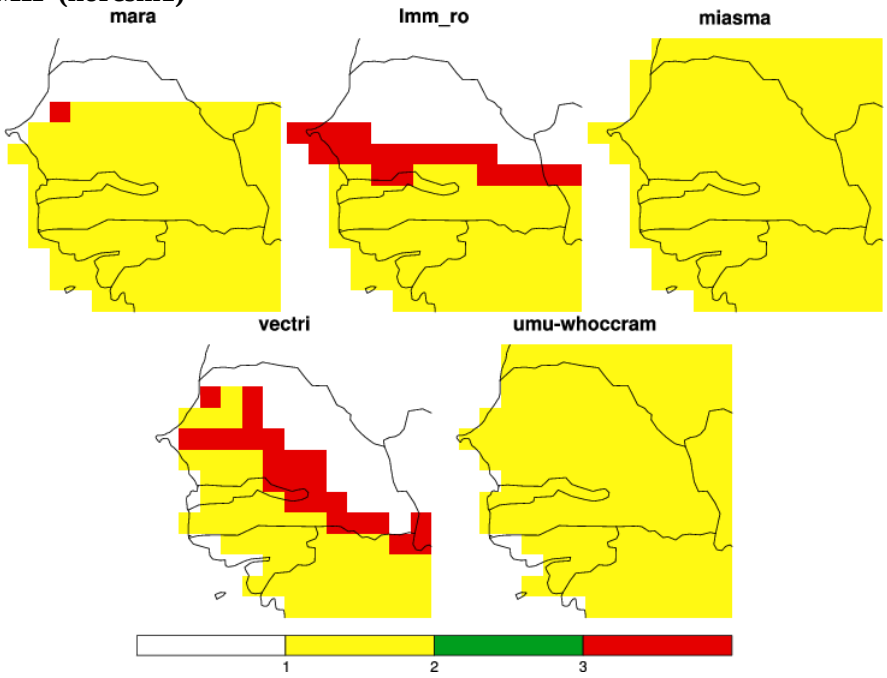

b) CORDEX (noresm1)

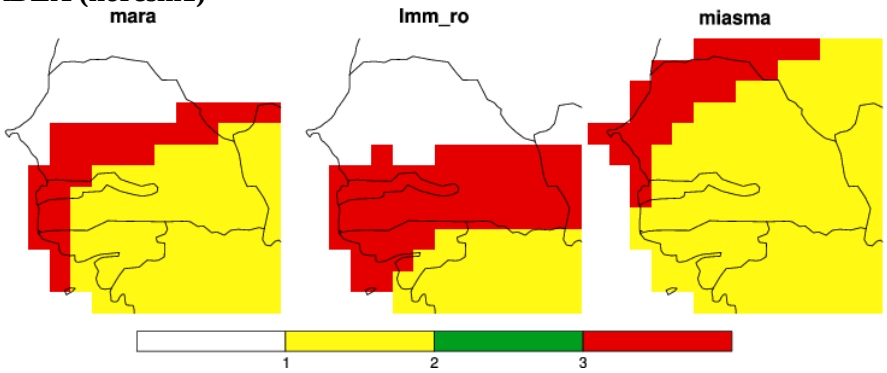

Future climate is still suitable for malaria transmission
Future climate becomes unsuitable for malaria transmission
Future climate becomes suitable for malaria transmission

Fig. 59: Simulated changes in climate suitability for malaria transmission (CS) for a) the ISI-MIP and b) the CORDEX noresm1 experiment. Changes are calculated for the most extreme emission scenario (rcp85) for the 2080s with respect to the historical run (1980-2010). White areas depict regions where future climate is still unsuitable for malaria, yellow where it is still suitable, red where it becomes unsuitable and green where it becomes suitable.

a) ISI-MIP (gfdl_esm2m)

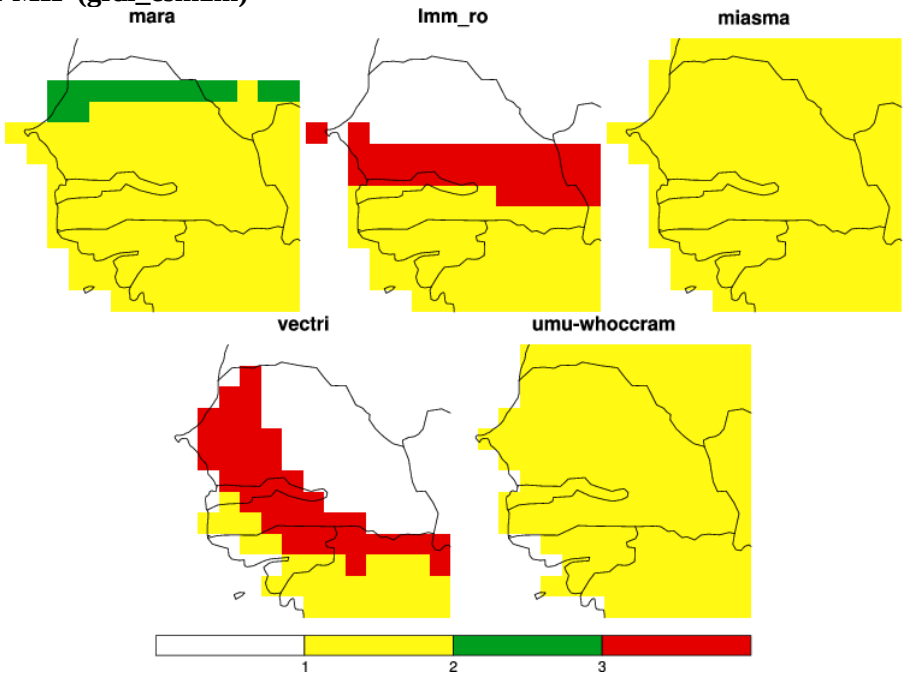

b) CORDEX (gfdl_esm2m)

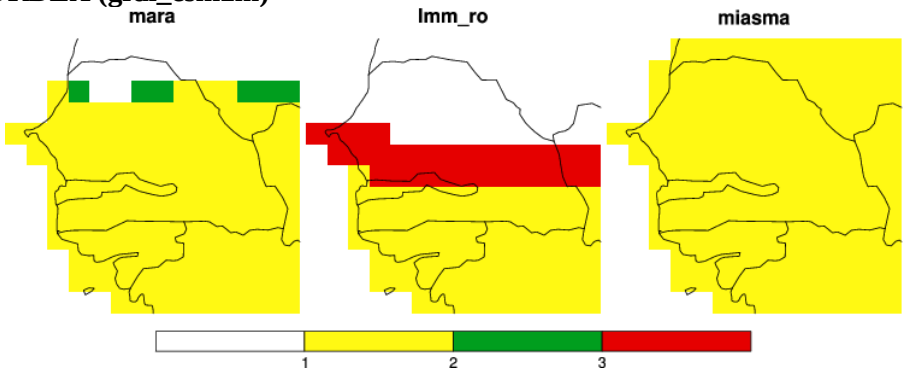

Future climate is still suitable for malaria transmission
Future climate becomes unsuitable for malaria transmission
Future climate becomes suitable for malaria transmission

Fig. 60: Simulated changes in climate suitability for malaria transmission (CS) for a) the ISI-MIP and b) the CORDEX gfdl_esm2m experiment. Changes are calculated for the most extreme emission scenario (rcp85) for the 2080s with respect to the historical run (1980-2010). White areas depict regions where future climate is still unsuitable for malaria, yellow where it is still suitable, red where it becomes unsuitable and green where it becomes suitable.

a) ISI-MIP (miroc5)

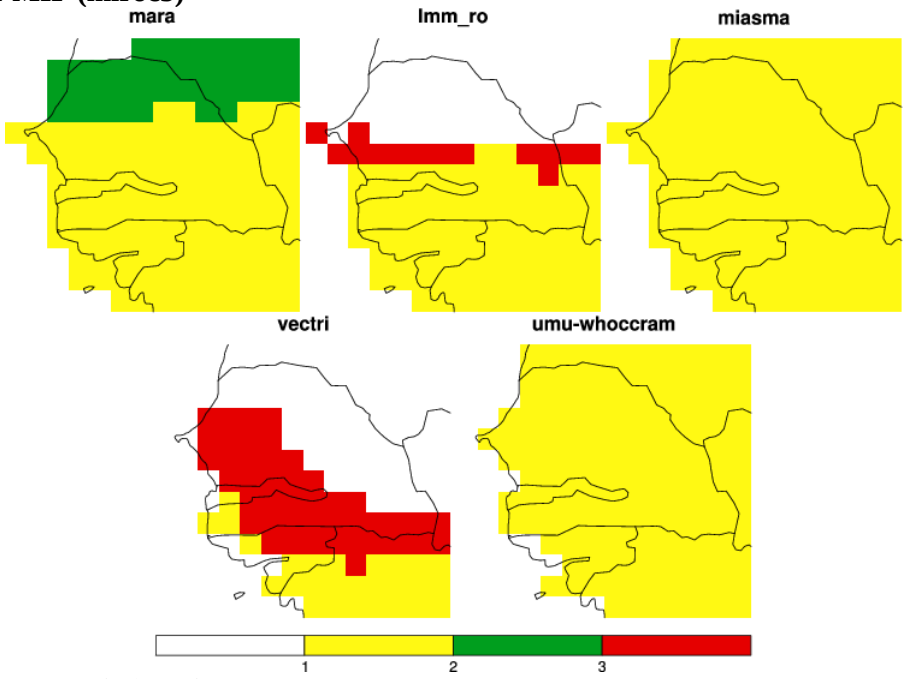

b) CORDEX (miroc5)

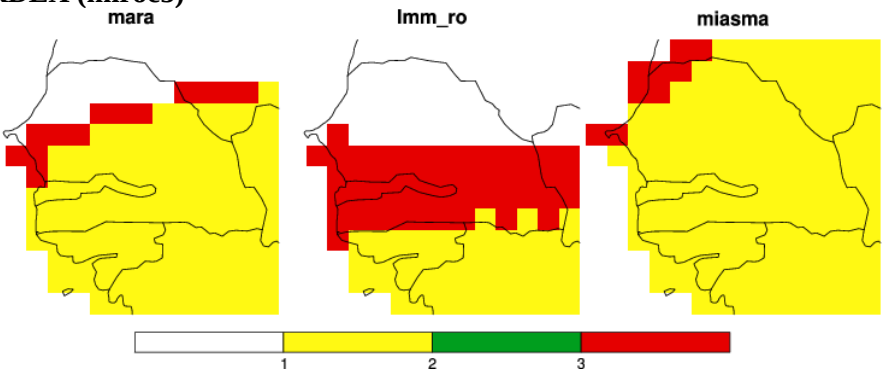

Future climate is still suitable for malaria transmission
Future climate becomes unsuitable for malaria transmission
Future climate becomes suitable for malaria transmission

Fig. 61: Simulated changes in climate suitability for malaria transmission (CS) for a) the ISI-MIP and b) the CORDEX miroc5 experiment. Changes are calculated for the most extreme emission scenario (rcp85) for the 2080s with respect to the historical run (1980-2010). White areas depict regions where future climate is still unsuitable for malaria, yellow where it is still suitable, red where it becomes unsuitable and green where it becomes suitable.

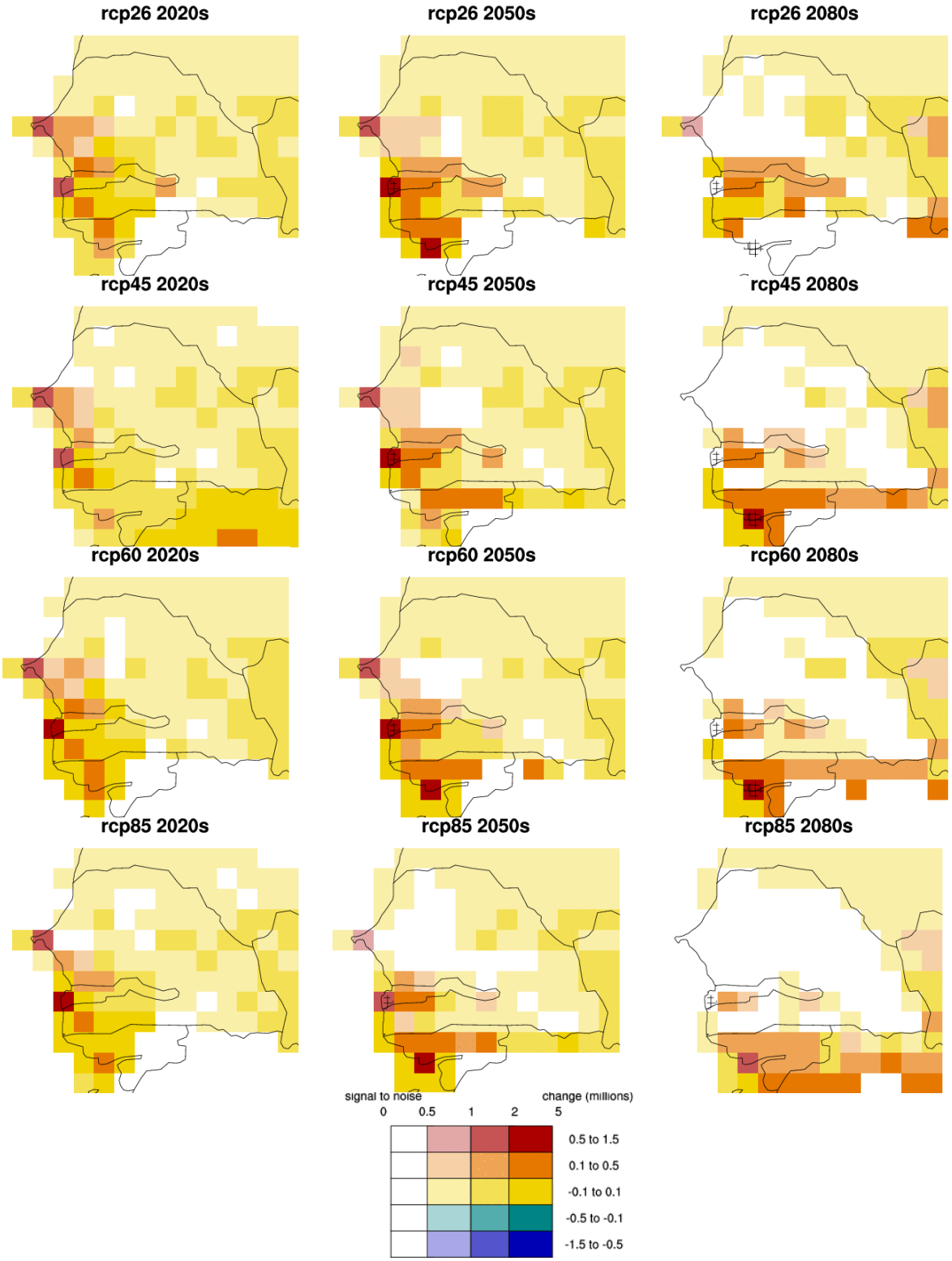

Fig. 62: The effect of climate scenarios on future population at risk of Malaria: changes in additional people at risk of malaria (ISI-MIP ensemble). Each map shows the results for a different emission scenario (RCP). The different hues represent change in the length of the transmission season for the mean of CMIP5 sub-ensemble (with respect to the 1980-2010 historical mean. The different saturations represent signal-to-noise (μ/Sigma) across the super ensemble (the noise is defined as one standard deviation within the multi-GCM and multi-malaria ensemble). The stippled area shows the multi-malaria multi GCM agreement (60% of the models agree on the sign of changes).

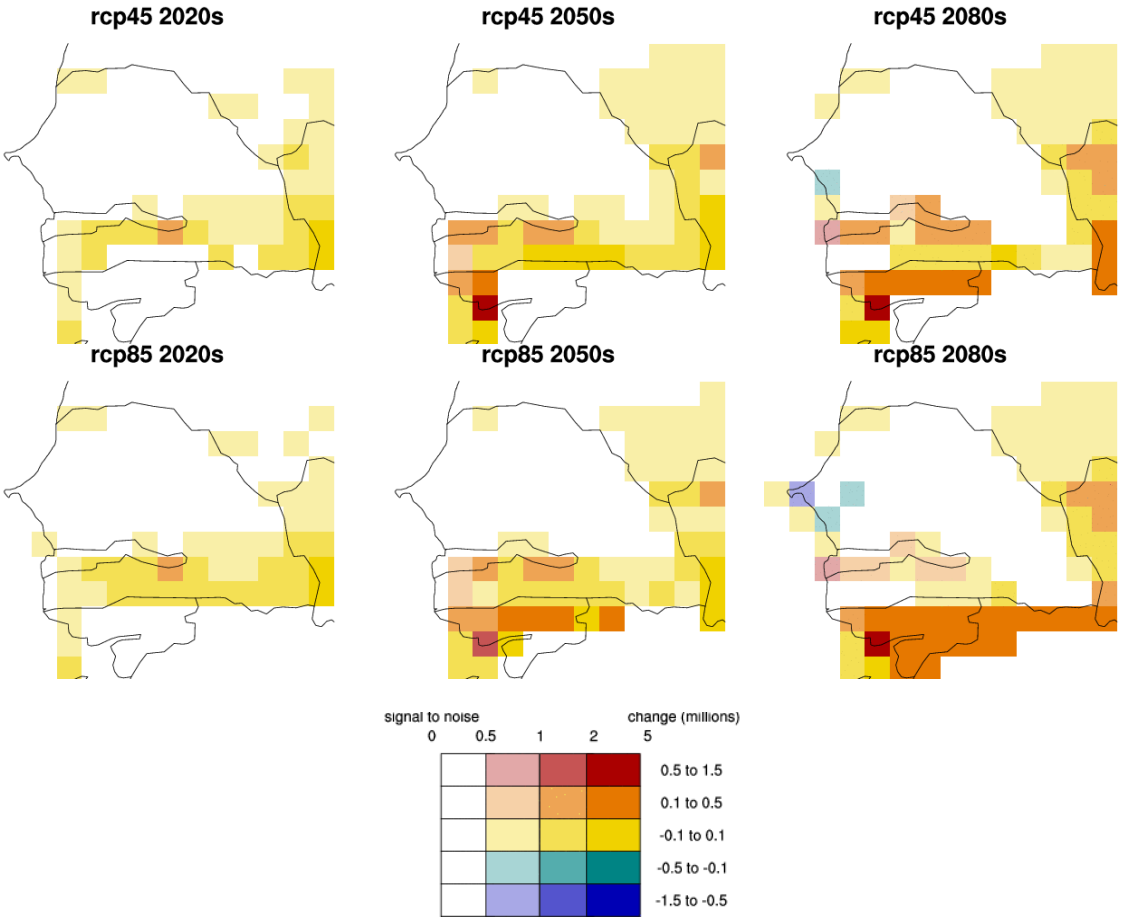

Fig. 63: The effect of climate scenarios on future population at risk of Malaria: changes in additional people at risk of malaria (CORDEX ensemble). Each map shows the results for a different emission scenario (RCP). The different hues represent change in the length of the transmission season for the mean of CMIP5 sub-ensemble (with respect to the 1980-2010 historical mean. The different saturations represent signal-to-noise (μ/Sigma) across the super ensemble (the noise is defined as one standard deviation within the multi-GCM and multi-malaria ensemble). The stippled area shows the multi-malaria multi GCM agreement (60% of the models agree on the sign of changes).

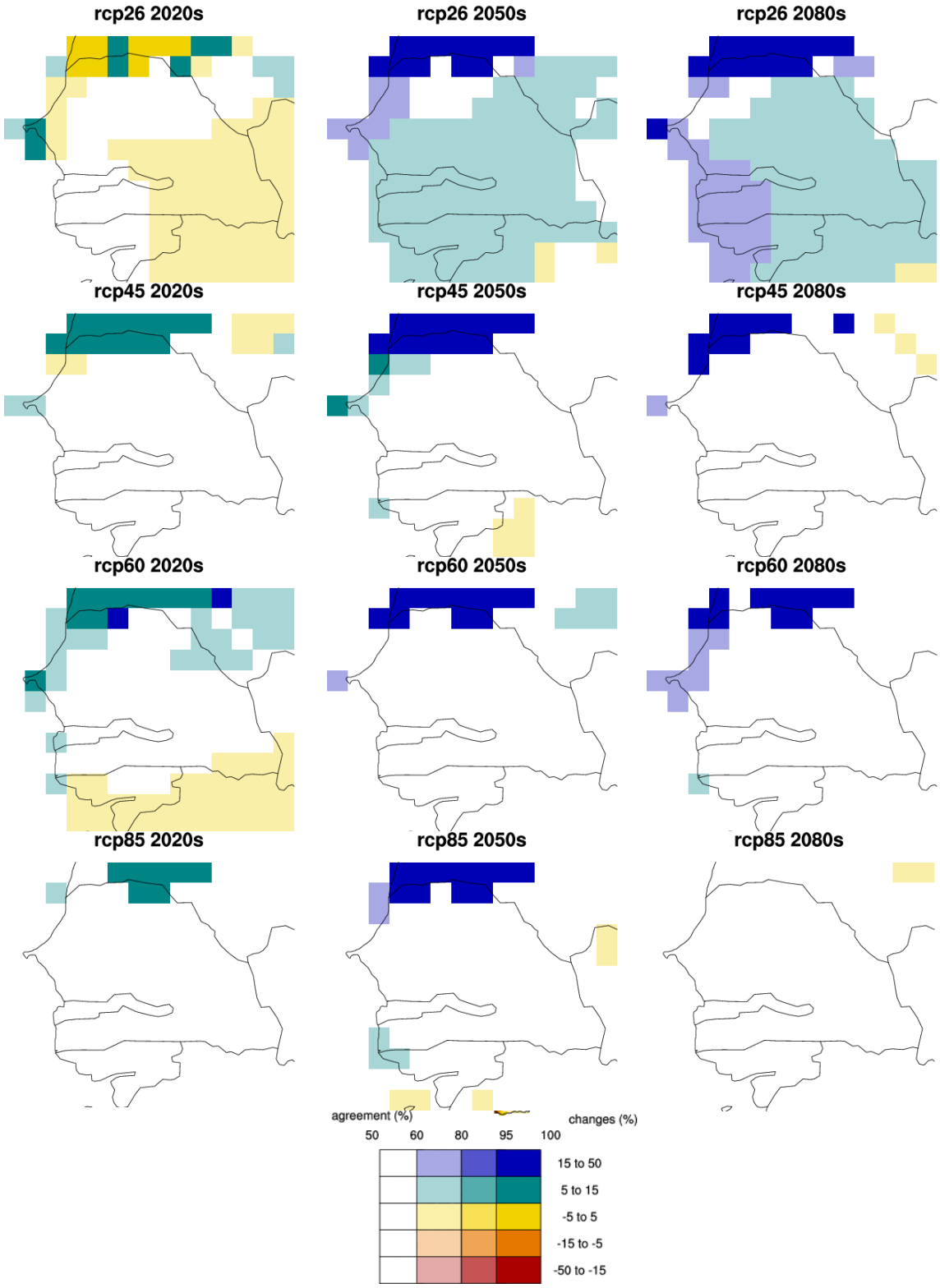

Fig. 64: The effect of climate scenarios on simulated rainfall changes (ISI-MIP GCMs). Each map shows the results for a different emission scenario (RCP) and a different time period. The different hues represent change in rainfall (%) for the mean of CMIP5 sub-ensemble with respect to the 1980-2010 historical mean. The different saturations represent sign agreement (%) across the GCM ensemble.

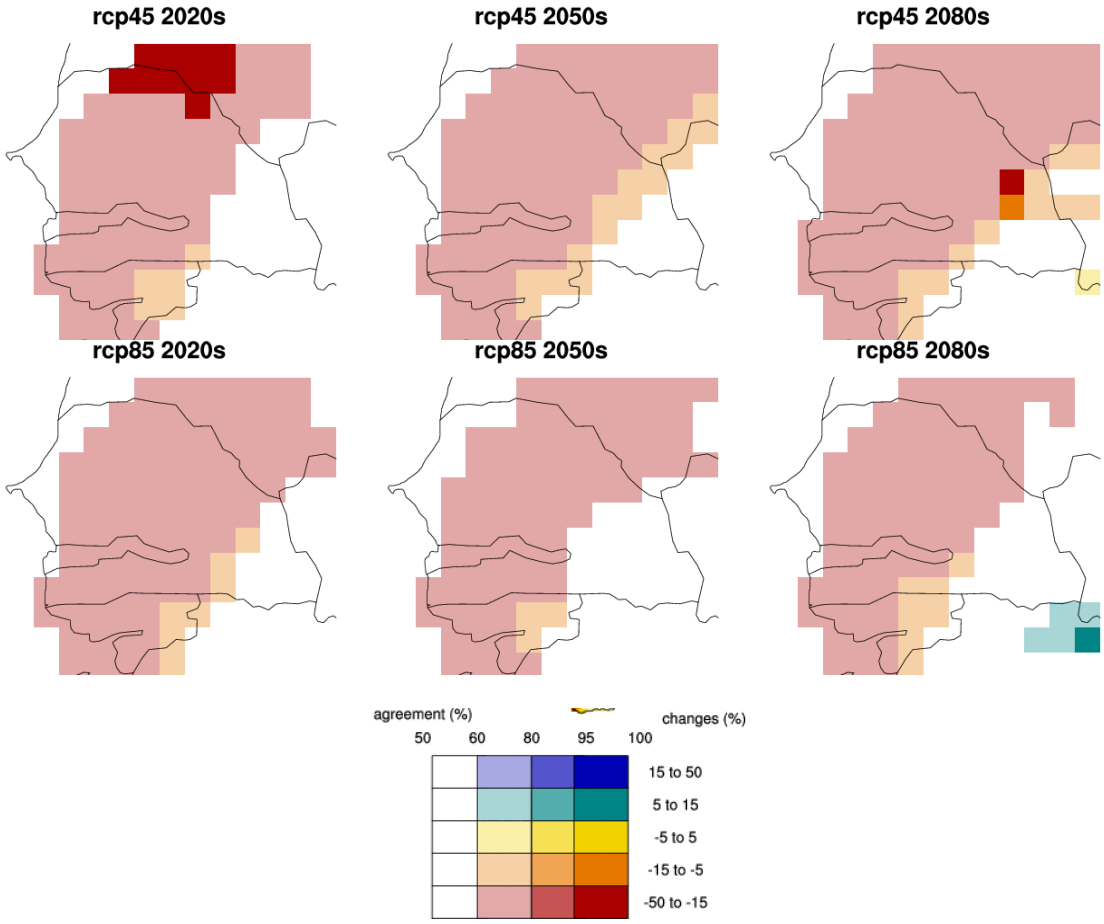

Fig. 65: The effect of climate scenarios on simulated rainfall changes (CORDEX RCMs). Each map shows the results for a different emission scenario (RCP) and a different time period. The different hues represent change in rainfall (%) for the mean of the CORDEX RCM ensemble with respect to the 1980-2010 historical mean. The different saturations represent sign agreement (%) across the RCM ensemble.

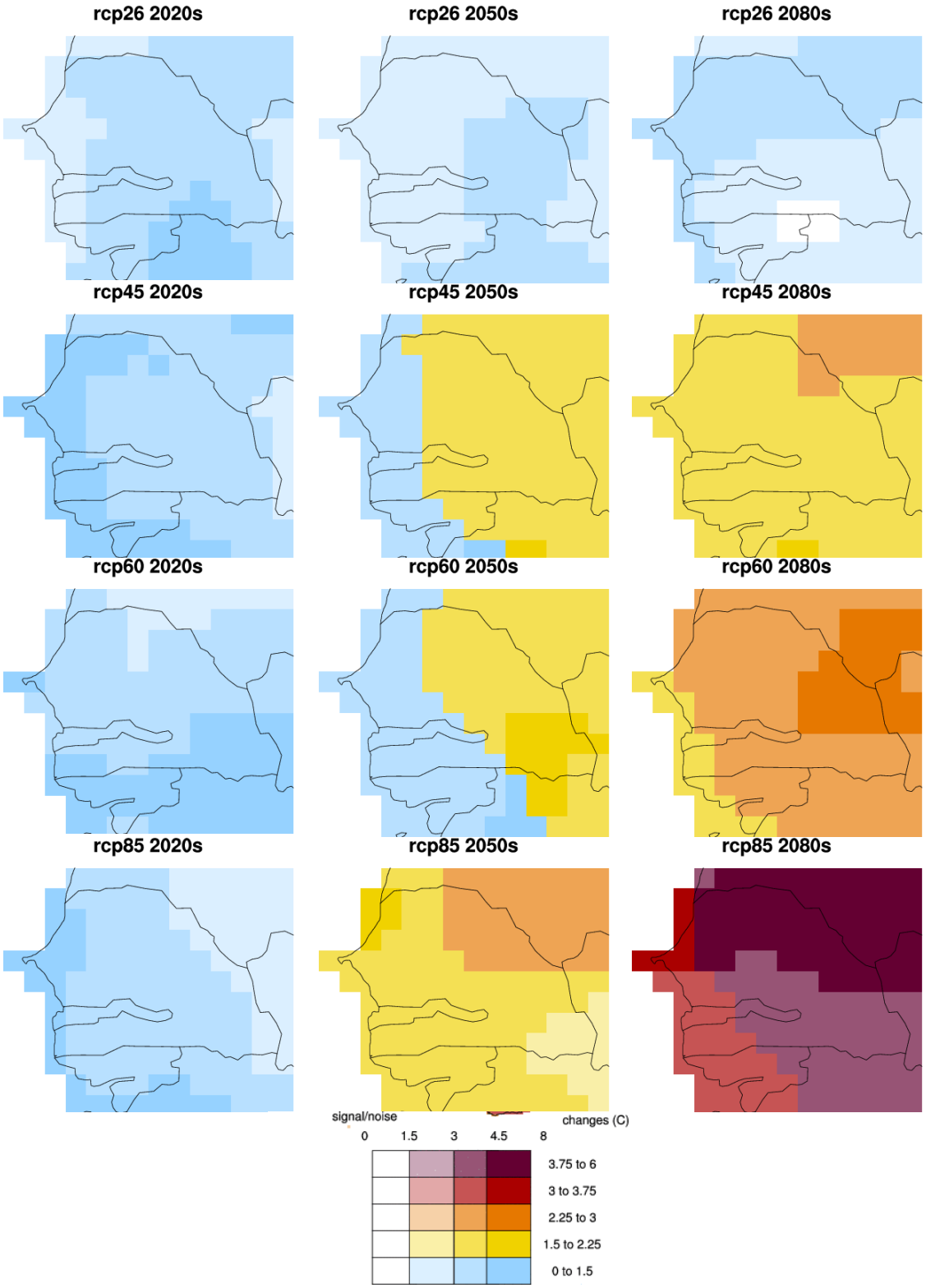

Fig. 66: The effect of climate scenarios on simulated temperature changes (ISI-MIP GCMs). Each map shows the results for a different emission scenario (RCP) and a different time period. The different hues represent change in temperature (°C) for the mean of CMIP5 sub-ensemble with respect to the 1980-2010 historical mean. The different saturations represent signal-to-noise (μ/Sigma) across the super ensemble (the noise is defined as one standard deviation within the multi-GCM and multi-malaria ensemble).

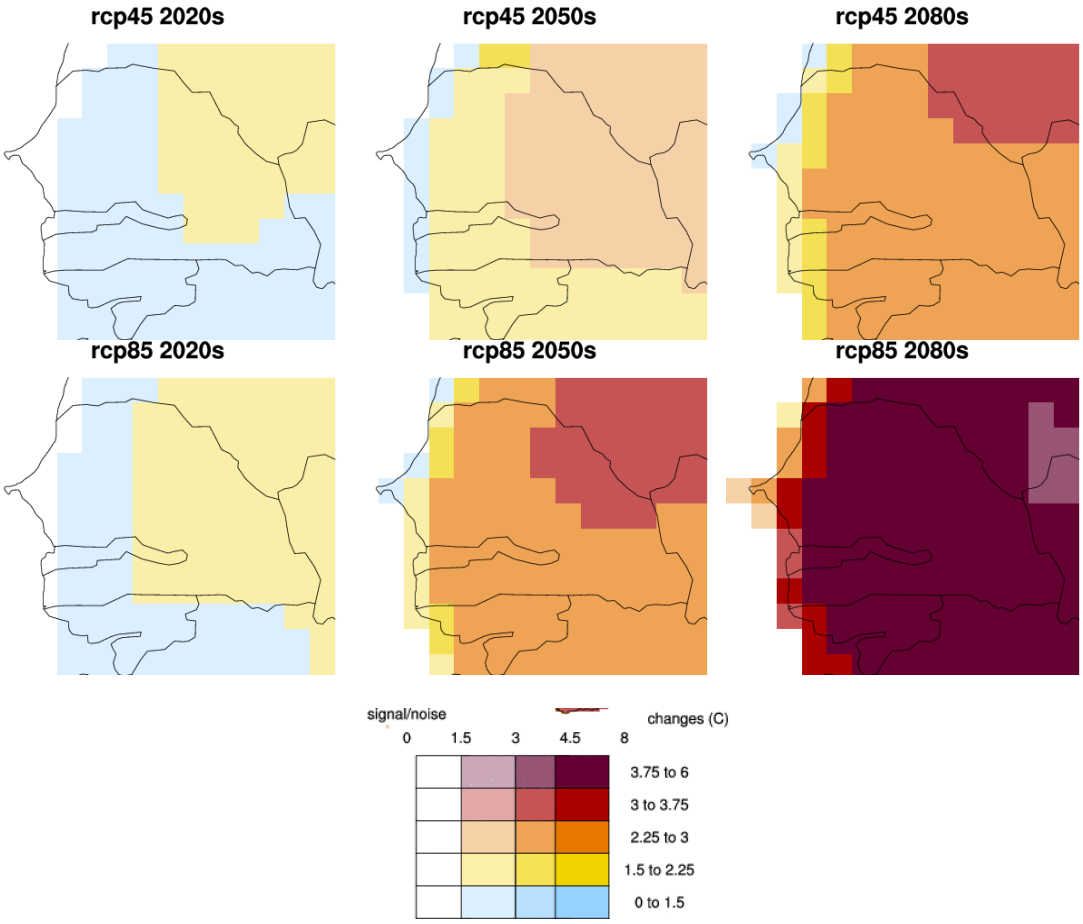

Fig. 67: The effect of climate scenarios on simulated temperature changes (CORDEX RCMs). Each map shows the results for a different emission scenario (RCP) and a different time period. The different hues represent change in temperature (°C) for the mean of the CORDEX RCM ensemble with respect to the 1980-2010 historical mean. The different saturations represent signal-to-noise (μ/Sigma) across the RCM ensemble (the noise is defined as one standard deviation within the RCM ensemble).